M-PM-Sym1   CONFORMATIONAL FLEXIBILITY IN PROTEINS Barry Honig, Department of Biochemistry and
Molecular Biophysics, Columbia University, 630 W. 168 St., New York, NY 10032

The concept of a "conformational change" is frequently invoked to account for a variety of phenomena associated with the functioning of proteins. The use of this term is often viewed as revealing ignorance as to what is actually going on and indeed, there has been, until recently, only limited information regarding the detailed nature of the conformational changes that proteins can undergo. In the past few years, major progress has been made in elucidating the internal dynamics of globular proteins. A large number of experimental and theoretical approaches have been brought to bear on the problem and motions ranging in time between less than a picosecond to greater than a second have been identified. These motions may correspond to small fluctuations involving only a few atoms or to the collective "rigid body" movements of entire structural subunits such as helices or domains. The purpose of this symposium is to highlight a number of recent developments in our understanding of the conformational flexibility of proteins and to consider the relationship of specific classes of fluctuations to their possible functional significance. The types of motions to be considered will range from the major conformational changes involved in protein folding as revealed by the NMR studies of Christopher Dobson to the smaller fluctuations discussed in Martin Karplus' theoretical treatment of active site dynamics. Benno Schoenborn will discuss his work on hydrogen-deuterium exchange which has identified specific and highly localized regions of the protein that are rigid or flexible while Hans Fraunfelder's studies of the binding of ligands to heme proteins will be used in an attempt to classify "functionally important motions". It is anticipated that these different approaches and points of view will make it possible to evaluate the current state of knowledge as to the nature and role of conformational flexibility in proteins.

M-PM-Sym2 PROTON NMR STUDIES OF DYNAMICAL EVENTS IN PROTEINS.   Christopher M. Dobson, Inorganic
Chemistry Laboratory, South Parks Road, Oxford OX1 3QR, England.

Many resonances in the ^{1}H NMR spectra of small proteins can now be assigned, and this permits studies of the dynamical behaviour of individual residues in these proteins. In experiments with hen lysozyme, a variety of local fluctuations within the native state of the protein have been characterized. Recently, it has been possible to approach the study of cooperative dynamical events such as the folding and unfolding of the protein. Magnetization transfer techniques have enabled the kinetics of the reversible folding and unfolding reactions to be determined. Assignments of resonances in the spectrum of the denatured protein have also been possible using this approach by correlating them with resonances in the spectrum of the native protein. In conjunction with other measurements, for example of hydrogen exchange rates, the conformational state of the denatured as well as the native protein has been explored. This approach has been extended to other proteins including staphyloccal nuclease where it has been possible to study the kinetics of interconversion between the denatured state and different states of the native protein.

M-PM-Sym3 HYDROGEN–DEUTERIUM EXCHANGE STUDIES BY NEUTRON DIFFRACTION REVEAL LOCALIZED STABLE
REGIONS IN PROTEINS.   B. P. Schoenborn, N. V. Raghavan and R. M. Fine, Biology
Department, Brookhaven National Laboratory, Upton, NY 11973.

The unique ability of neutron diffraction to measure the degree of H/D exchange of the labile protons in proteins has led to new insights into the flexibility of protein chains. Analyses of the H/D exchange ratios for the main chain amide peptides reveal regions within proteins that are not accessible for hydrogen exchange. While the data sets of such exchange studies are still small, evidence emerges that structure with β sheets are more stable than α helical structures. In neutron studies of myoglobin derivatives, two regions were found that are not accessible for hydrogen exchange and that can be considered as hinge regions for molecular deformations. The occupancy factors of exchangeable hydrogens at amide peptide positions were determined by restraint least square procedures.   These reciprocal space refinement techniques (Hendrikson, W. A. and Konnert, J. A. 1980.   In: Biomolecular Structure, Vol. 1, pp. 43–57, R. Srinivason, ed. Pergamon, Oxford) were preceded by an analysis of the solvent contribution to the low order reflections.   In the solvent refinement, data from crystals soaked in H_2O and D_2O were used.   In order to limit errors in Fourier maps derived from data with often weak intensities with large σ, particular attention to data reduction was given (Schoenborn, B. P.   1983.   Acta Cryst. A39: 315– 321). The observed change of H/D exchange ratios as a function of soaking time was correlated and compared to local temperature factors.   The accessibility of water to the stable regions was studied by simple model calculations evaluating the energy of deformation needed that would allow H exchange. (Research carried out under auspices of U. S. Department of Energy)

M-PM-Sym4 PROTEIN DYNAMICS: APPLICATION TO ACTIVE SITES OF ENZYMES, M. Karplus, A. Brünger, and C. Brooks, III.

New results in protein dynamics will be briefly reviewed. A method for molecular dynamics simulations of localized chemical events in solvated proteins will be presented. Only the significant protein atoms and solvent molecules are included in the simulation; the effect of the remainder of the protein atoms and the surrounding solvent is treated implicitly by the introduction of boundary forces and by the presence of a stochastic heat bath region. Illustrative applications to the active site dynamics of ribonuclease and lysozyme will be given.

M-PM-Sym5 PROTEIN STATES AND MOTIONS. Hans Frauenfelder, Departments of Physics and Biophysics, University of Illinois at Urbana-Champaign, 1110 West Green Street, Urbana, IL 61801.

Proteins are capable of assuming a large number of states and performing a great variety of motions. Selecting myoglobin as a prototype, and using data from many different experiments, the following picture emerges. In a given state, for instance deoxymyoglobin (Mb), the protein molecule can assume a large number of $\underline{\text{conformational substates}}$ (CS). Each substate contains a large number of sub-substates (CS^2) and each of these again can assume different sub-sub-substates (CS^3). The energy barriers between CS are of the order of 100 kJ/mol, those between CS^2 of the order of 30 kJ/mol, those between CS^3 of the order of a few kJ/mol. We denote the $\underline{\text{equilibrium}}$ $\underline{\text{fluctuations}}$ among CS^1 by EF i. At 300 K, all classes, EF1, EF2, and EF3, occur. $\overline{\text{Below 210 K}}$, the EF1 are frozen out, below about 60 K, only the EF3 are still active. In a $\underline{\text{protein reaction}}$, the protein will move from one state to another. A simple example is the binding or dissociation of a small ligand from Mb, Mb + CO $\updownarrow$ MbCO. During such a reaction, the protein will undergo $\underline{\text{functionally important motions}}$ (fims). We have studied fims in Mb by observing changes in protein-structure markers after photodissociation. Experiments so far provide evidence for three different fims, with characteristically different activation energies. Each fim can be associated with a corresponding set of CS and EF. Ef and fim are linked by the $\underline{\text{fluctuation-dissipation theorem}}$. The hierarchical model of the protein sketched here suggests similarities with glasses and spin-glasses and opens the possibility of applying concepts and theories of amorphous solids to proteins.

M-PM-A1 MECHANISMS OF cGMP SENSITIVE Ca^{2+} TRANSPORT BY ROS DISKS

John S. George and Mark W. Bitensky, Life Sciences Division,
Los Alamos National Laboratory, Los Alamos, New Mexico 87545 USA

Cytoplasmic Ca^{2+} activity (Aca) appears to control the Na^+ dark current of the vertebrate rod, but mechanisms regulating Aca are not well understood. We have studied Ca^{2+} metabolism in preparations of isolated, concentrated rod outer segments (ROS) with leaky plasma membranes, using Ca^{2+} and pH electrodes to monitor ion activities and measuring ^{45}Ca partition between particles and suspending aqueous medium. Mitochondrial Ca^{2+} transport was inhibited with ruthenium red and tested by addition of antimycin and oligomycin. In the dark, ROS disks take up Ca^{2+} by an ATP dependent process that is effective to submicromolar Aca. Ca^{2+} uptake is associated with, but does not require a rise in suspension pH. Both Ca^{2+} uptake and alkalinization are stimulated by cGMP in the presence of ATP; 8-Br-cGMP and cAMP also stimulate, though less vigorously. Creatine phosphate (CrP) facilitates ATP dependent Ca^{2+} uptake and alkalinization apparently because ATP hydrolysis and regeneration from CrP causes net binding of protons in the medium. Dinitrophenol inhibits ATP dependent Ca^{2+} uptake by disks and releases sequestered Ca^{2+}. ATPase activity thus appears to establish a proton gradient across the disk membrane which drives a separate Ca^{2+} uptake process. Light released Ca^{2+} from preloaded, dark-adapted disks - thousands of ions per second per bleached rhodopsin for bleaches < 1 photon per disk. Continuous light (<.5% bleach per second) rapidly released much larger total quantities of Ca^{2+}, producing changes of several micromolar. This Ca^{2+} release depended on the hydrolysis of cGMP. Activation of cGMP hydrolysis by a variety of biochemical strategies also provoked Ca^{2+} release from disks. Since cGMP hydrolysis produces protons in the extradisk space, we suggest that both Ca^{2+} uptake and release may operate by exchange of Ca^{2+} for H^+ across the disk membrane. (Supported by NIH grant R01 AM 31610-02).
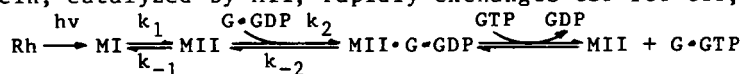
M-PM-A2 EXOGENOUS cGMP INCREASES DARK CURRENT AND LIGHT SENSITIVITY OF RETINAL RODS WITHOUT CAUSING DELAY OF EXCITATION.

W. H. Cobbs & E. N. Pugh, Jr., Departments of Neurology and Psychology,
University of Pennsylvania, Philadelphia, PA 19104

Membrane currents of isolated tiger salamander rods were recorded with combined suction pipette and tight-seal whole cell voltage-clamp electrodes. Rods in Ringers containing 1 mM calcium were held by either the outer or inner segment in the suction electrode, presenting the other segment to a patch electrode of 10-20 megohm resistance containing KAc 100, Hepes 10, $MgCl_2$ 1, EGTA 0.05, and cGMP 5 mM. Upon rupture of attached patch of 1-5 gigohm the following occurred: (1) dark current rapidly (5-10 secs) increased from 25-50 pA to 80-500 pA, with mean ratio 9 (n=16); (2) the duration of saturation of bright flash (1000-isomerization) photocurrents increased 7-fold; (3) light sensitivity to dim flashes (10 isomerizations) increased > 10-fold; (4) the rising phase of bright-flash photocurrents (normalized by dark current) remained unchanged; (5) after successful withdrawal of cGMP electrode, dark current and photocurrent kinetics returned to baseline over 2 min. Observations (1), (2) and (4) are inconsistent with transduction schemes in which both light affects the light-sensitive conductance (g_{hv}) exclusively through modulation of the concentration, [cGMP], and in which the sole role of cGMP in excitation is to act upon g_{hv}, either directly through an instantaneous relation or indirectly through a delay step such as a protein kinase.

M-PM-A3 KINETIC ANALYSIS OF THE BINDING OF METARHODOPSIN II TO G-BINDING-PROTEIN ON THE ROD DISK MEMBRANE.

John H. Parkes and Paul A. Liebman, Departments of Anatomy and Ophthalmology, School of Medicine, University of Pennsylvania, Philadelphia, Pa.

Rhodopsin, upon bleaching, rapidly forms a reversible equilibrium between metarhodopsins I and II (MI and MII). MII binds to G-binding-protein (G) on the rod disk membrane, and while bound is apparently stabilized as MII. In the presence of physiologic amounts of GTP, the G-protein, catalyzed by MII, rapidly exchanges GDP for GTP, releasing the MII:

$$Rh \xrightarrow{h\nu} MI \underset{k_{-1}}{\overset{k_1}{\rightleftharpoons}} MII \underset{k_{-2}}{\overset{G \cdot GDP \quad k_2}{\rightleftharpoons}} MII \cdot G \cdot GDP \underset{}{\overset{GTP \quad GDP}{\rightleftharpoons}} MII + G \cdot GTP$$

In the absence of GTP, abnormally large amounts of MII (MII·G) are formed at low bleaches until the free G is exhausted. This enhanced MII formation permits the study of the binding of MII to G. Previous work (1) based on equilibrium analysis of the MII formed by a series of small bleaches argued for a relatively slow, weak binding of MII to G.

The formation of MII was measured spectrophotometrically at 390 nm. The theoretical rate of formation of MII and MII·G was calculated by numerical integration of the rate equations for a given set of rate constants and these parameters were then varied by a least squares (Simplex) method to give a best fit to the experimental data. The results confirm our earlier conclusions that MII is weakly bound to G, and that MII·G is formed from a partial equilibrium between MI and MII, so that the slow rate of formation of MII·G is due to the small value for k_2. Supported by USPHS Grants EY00012 and EY01583.

(1) Parkes and Liebman (1984) Invest. Ophthal. and Visual Sci. <u>25</u> (ARVO Suppl.) p 156.

M-PM-A4 STUDY OF THE LIGHT-INDUCED CYCLIC NUCLEOTIDE CASCADE IN RETINAL RODS BY FAST NEUTRON
DIFFRACTION. T.M. Vuong (Dept. of Cell Biology, Stanford), D.L. Worcester (ILL Grenoble),
C. Pfister (CEN Grenoble), M. Chabre (CEN-Grenoble).

The light-activated cyclic nucleotide cascade in retinal rod cells has been extensively studied by
near IR light-scattering techniques (Kühn et al., PNAS 78:6873-6877, Vuong et al., Nature 311,
659-661 (1984). While these studies have provided much information on the kinetics and stochiometry
of the reactions, they contribute little in describing the structural events involved. We have
performed analogous studies by fast neutron diffraction on oriented frog rods using the D11
instrument on the ILL high flux reactor (Grenoble). We investigated the dependence of the
structural changes on the amount of photoactivated rhodopsin and the presence of GTP. With 1 minute
time resolution, at 20°C, in the absence of GTP, light-induced changes in peak intensity are mainly
observed for orders 2 and 4. These changes saturate at 10 % bleaching : this corresponds to the
saturation of the R*-Transducin binding reaction. A small lattice compression (0.3 %) is also
observed. With GTP present, qualitatively similar light-induced changes also appear, but at very
low illumination, and saturate below 0.5 % bleaching. This corresponds to the "dissociation" signal
as defined by light-scattering, a signal that relates to the dissociation of the R*-T complex
following GDP/GTP exchange. Measurements with an improved time resolution of 4 sec, at 6°C
demonstrated that in the presence of GTP the diffraction peak intensity changes precede the lattice
changes : they thus correspond to different phenomena. Quantitative analysis is in progress and
further improvements in time resolution shall be implemented.

M-PM-A5 ARRESTIN: AN ATP/ADP EXCHANGE PROTEIN THAT REGULATES cGMP PHOSPHODIESTERASE ACTIVITY
IN RETINAL ROD DISK MEMBRANES (RDM). Ralph Zuckerman*†, Bruce Buzdygon*, Nancy Philp*,
Paul Liebman*†, Ari Sitaramayya*. Departments of Anatomy* and Ophthalmology†, University of
Pennsylvania, School of Medicine, Philadelphia, Pa 19104
Photolyzed rhodopsin triggers large, rapid reciprocal changes in free ATP and ADP content of
intact retinal rod outer segments (ROS).[1] 8-azido ATP was found to label RDM 48 Kd protein almost
exclusively.[2] We now show an ATP/ADP exchange to be mediated by 48 Kd protein (A-protein) when
reconstituted with bleached peripheral-protein-stripped RDM. We also find purified A-protein (A)
to significantly potentiate quenching of cGMP phosphodiesterase (PDE) activation in the presence
of ATP. Conversely, antibody to a retinal 48 Kd protein, S-antigen, can specifically abolish the
ATP-dependent quench. Amplified production of A·ATP's may arrest PDE activation by competing for
active rhodopsin, G-protein or PDE. Thus, we propose this regulatory protein be called arrestin.
Arrestin and S-antigen are probably the same protein based upon immuno-cross reactivity of purified
proteins on Western blots and their identical molecular weight.
1. Zuckerman, R. et al. (1982) Proc. Nat'l Acad. Sci. USA, 79: 6414-6418
2. Zuckerman, R., Buzdygon, B., and Liebman, P.A. (1984) Biophys. J., 45: 292A
Antibody against S-antigen was kindly provided by Dr. Igal Gery, NIH, NEI.
Supported by EY00012, EY05461 and EY01583.

M-PM-A6 MODULATION OF VERTEBRATE PHOTORECEPTOR POTENTIALS BY INJECTION OF INOSITOL TRISPHOSPHATE.
G. Waloga*, R.E. Anderson† and R.F. Irvine‡; *Boston University School of Medicine,
Boston, MA 02118, U.S.A., †Baylor College of Medicine, Houston, TX 77030, U.S.A., and ‡ ARC
Institute of Animal Physiology, Babraham, Cabridge CB24AT, U.K.
Light-induced hydrolysis of phosphatidylinositol 4,5-bisphosphate has been demonstrated in the
vertebrate retina (Ghalayini and Anderson, 1984, BBRC). One of the endproducts of this hydrolysis,
inositol 1,4,5-trisphosphate has been shown to cause the release of bound calcium in other tissue
(Streb et al., 1983, Nature). Since calcium ions have previously been implicated in the process of
vertebrate phototransduction, we have begun to study the effect of intracellular injection of
inositol trisphosphate upon rod membrane voltage.
The pressure-injection of inositol trisphosphate into the outer segment of a dark-adapted, soli-
tary, salamander rod induced a reversible hyperpolarization that was proportional to the strength
of the pressure injection, but sometimes outlasted the time period of the applied pressure. The
amplitude of receptor potentials induced by dim lights was diminished during the time that the rod
membrane was hyperpolarized by the injection of inositol trisphosphate. When membrane voltage re-
turned to the level preceding the injection of inositol trisphosphate, the amplitude of the recep-
tor potentials recovered. Repetitive injection of inositol trisphosphate into the outer segment of
a dark-adapted rod induced repetitive, reversible hyperpolarizations. The hyperpolarizing res-
ponses induced by repetitive injections of inositol trisphosphate were greatly diminished after a
bright light was used to stimulate the rod and slowly recovered as the rod dark-adapted. Thus, the
injection of inositol trisphosphate can decrease the size of receptor potentials induced by dim
light, and light can decrease the response of the rod to the injection of inositol trisphosphate.

M-PM-A7   INOSITOL-TRISPHOSPHATE INDUCES AN INCREASE IN INTRACELLULAR IONIZED CALCIUM IN INTACT AND FUNCTIONING <u>LIMULUS</u> PHOTORECEPTORS.   J.E. Brown and L.J. Rubin, Dept. of Ophthalmology, Washington University School of Medicine, St. Louis, MO. 63110.

Pressure injection of inositol-trisphosphate (IP_3) into <u>Limulus</u> ventral photoreceptor cells induced responses that mimicked several aspects of light responses (Brown, et al. and Fein, et al., Nature, <u>311</u>, 1984). Micropipettes were filled with IP_3 (0.075-1.0 mM) plus 200 mM KCl. Photoreceptor cells were bathed in EGTA-sea water (containing 10 mM EGTA, no Ca added) and repetitively illuminated until sensitivity became reduced; in this state, iontophoretic injection of Ca increased sensitivity. Also, in this state, injection of IP_3 increased sensitivity to the next flash; this indicates indirectly that Ca_i was increased after IP_3 injections.

Also, cells were injected with aequorin to detect changes of Ca_i. Both injection of IP_3 and stimulus flashes induced increases of aequorin luminescence, even after a prolonged bath in EGTA-sea water. Thus, injections of IP_3 induce increases of Ca_i in intact, functioning cells by release of Ca from intracellular stores.

M-PM-A8   INOSITOL 1,3,4-TRISPHOSPHATE CONCENTRATION IS CHANGED BY ILLUMINATION OF <u>LIMULUS</u> VENTRAL PHOTORECEPTORS.   R.F. Irvine[*], R.E. Anderson[+], L.J. Rubin[#] and J.E. Brown[#]. [*]Dept. of Biochemistry, ARC Institute of Animal Physiology, Babraham, Cambridge, UK; [+]The Cullen Eye Institute, Baylor College of Medicine, Houston, TX; [#]The Dept. of Ophthalmology, Washington University, St. Louis, MO.

Illumination of <u>Limulus</u> ventral photoreceptors induces a rise in the content of inositol-trisphosphate (Brown, <u>et al</u>., Nature <u>311</u>, 157-160, 1984). We have incubated <u>Limulus</u> ventral eyes in [^{3}H]-inositol in artificial sea water (ASW) for 5 hours and then washed in ASW without label for 1 hour, all in the dark. One eye from each animal was illuminated for 30 sec (40 mW/cm^2), the other kept for a dark control. All eyes were fixed and extracted in chloroform:methanol:HCl (2:1:0.025). The aqueous phase was analyzed by HPLC. This technique reveals that <u>Limulus</u> eyes contain an isomer of inositol-trisphosphate in addition to 1,4,5-IP_3. 1,4,5-IP_3 is the predominent isomer made by erythrocyte chosts. The previously unsuspected isomer is 1,3,4-IP_3 (Irvine, <u>et al</u>., Biochem. J. <u>223</u>, 237-243, 1984). Light induces a change in the content of the 1,3,4-IP_3 isomer, predominantly.

M-PM-A9   INTRACELLULAR INJECTION OF CALCIUM BUFFERS BLOCKS IP_3-INDUCED BUT NOT LIGHT-INDUCED ELECTRICAL RESPONSES OF <u>LIMULUS</u> VENTRAL PHOTORECEPTORS.   L.J. Rubin & J.E. Brown. Dept. of Ophthalmology, Washington Univs., St. Louis, MO.

Intracellular injection of inositol-trisphosphate (1,4,5-IP_3) into <u>Limulus</u> ventral photoreceptor cells mimics several aspects of stimulation with light. The electrical response induced by IP_3 injection is accompanied by an increase in Ca_i due to Ca released from intracellular sites. Cells were impaled with a single barrel micropipette that contained the calcium sequestering compound EGTA (0.5M, pH=7.8) or BAPTA 250 mM, pH=7.8) and was used to measure membrane voltage and also a double barrel micropipette. One barrel contained IP_3 (0.075-0.2 mM plus 200 mM KCl); the other barrel contained 2 M KCl and was used to pass voltage-clamp current. After EGTA or BAPTA was pressure-injected intracellularly, the IP_3-induced electrical response became strongly attenuated whereas the sensitivity of the cells to light most often increased. For these cells, we presume that the resting level of Ca_i was raised above normal after impalement with the pipette containing IP_3, as has been detected in cells filled with aequorin. Because injection of a calcium chelator into the cytosol of <u>Limulus</u> ventral photoreceptors tends to block the electrical responses induced by pressure-injection of IP_3, but does not block the light responses it is unlikely that a light-induced increase in 1,4,5-IP_3 is a step in a single-file, unique chain of reactions mediating excitation.

M-PM-A10 LIGHT - INDUCED LOSS OF CALCIUM FROM THE DISCS OF SUNFISH ROD OUTER SEGMENTS.
M. Poenie, A. Dearry, B. Burnside and R.Y. Tsien. Dept. of Physiology-Anatomy, University of California, Berkeley, CA 94720

We have examined the calcium content of intact rods of the sunfish, <u>Lepomis cyanellus</u>, using a new method for ultrastructural calcium localization based on <u>in situ</u> precipitation of calcium by fluoride ions. The procedure involves primary fixation in glutaraldehyde containing 150mM fluoride. During secondary fixation, either the fluoride precipitate is preserved by keeping excess fluoride present, or else the fluoride is exchanged for the more electron-dense antimonate ion. Using either procedure on dark adapted retinae, all the precipitate in the rod outer segments is seen by transmission EM to be inside the discs. The precipitate formed by antimonate replacement of fluoride is heavier, coarser and visually more striking, whereas the precipitate using only fluoride is fine grained and concentrated in the peripheral cisternae of the discs. By contrast, retinae fixed at the end of a 1 sec. exposure to moderate room illumination(50 ft.-candles, or about 10^7 photons$\cdot$rod^{-1}sec^{-1}), show much less or no intradiskal precipitate by either fixation method. In antimonate treated specimens, electron probe analysis is complicated by overlap of the antimony and calcium X-ray lines. However, in specimens fixed in fluoride only, the calcium peak is detectable in the X-ray spectrum of dark adapted rod outer segments but disappears after the light exposure.

These results from intact retina are consistent with the Hagins - Yoshikami hypothesis, in particular the idea that light induces the release of calcium stored <u>within the discs</u>.

M-PM-B1 Chemiosmotic Mechanism of Acetylcholine-Induced Ion Channels

Konrad Kaufmann
Department of Neurobiology
The Weizmann Institute of Science
Rehovot/Israel

The mechanism of acetylcholine-induced ion channels is described in detail. Based on thermodynamic phospholipid monolayer phase diagrams, permeability fluctuations in lipid bilayers are shown to appear as consequence of first principles of chemomechanical coupling and thermal fluctuations of area and thickness. The theory explains the observations of proton-induced ion channels in pure phospholipid bilayers. Local control of permeability and electromotive force across asymmetrically protonated phospholipid membranes is shown to allow a common physical interpretation of chemiosmotic and receptor functions of ATPases and AChesterase. Enzymatic hydrolysis thus induces ion channels in agreement with the requirement of a specific receptor mechanism.

M-PM-B2 BLOCK OF THE ACETYLCHOLINE-ACTIVATED CHANNEL IN CHICK MYOTUBE BY GUANIDINE. Terry M. Dwyer and Jerry M. Farley. Depts. of Physiology and Biophysics and Pharmacology and Toxicology. UMMC. Jackson, MS. 39216.

Small organic cations that are permeant by reversal potential criteria reduce the amplitude of ACh-activated channels. Inside-out gigohm seals were obtained from 21 day old chick myotubes. External solutions contained 2 mM barium and all solutions were buffered to pH of 7.4 with 5 mM HEPES. The IV curve in 360 Cs//80 Cs (external//internal, plotted as O) showed the same curvature as that in 80 Cs//360 Cs with the signs of the current and voltage negated. Internal 100 mM guanidine blocked outward currents by 20% without changing inward currents. External 100 guanidine (X) blocked ~50% of inward and outward currents 100 mV from the reversal potential; block of inward currents was relieved at more negative potentials. 20 mM external guanidine (+) blocked inward, but not outward, currents.
(Supported by NIH grants NS-16462 & NS-17789.)
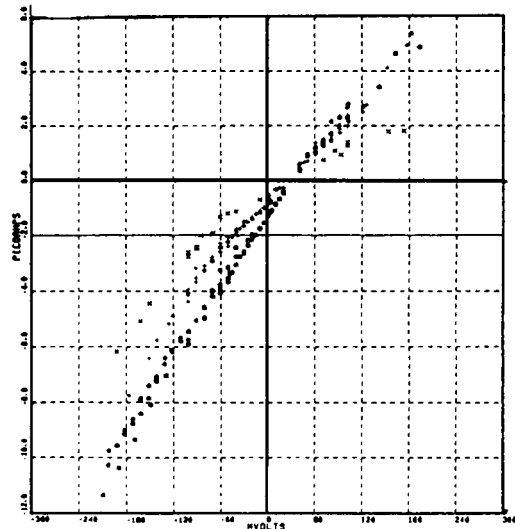
M-PM-B3 CHLORPROMAZINE ALTERS ACETYLCHOLINE-ACTIVATED CHANNEL KINETICS. A.Ribera[*], A.Trautmann[+], C.Pinset[*], J-P.Changeux[*](Intr. by R.T.Kado)[*]Biologie Moléculaire, Institut Pasteur and[+]Neurobiologie, Ecole Normale Supérieure, Paris, France.

Chlorpromazine(CPZ) decreases suberyldicholine-induced currents in E.electroplaques[1]. In order to determine which channel properties are affected by CPZ, we studied its effects on single acetylcholine(ACh)-activated channels in cell-attached patches from the mouse muscle cell line, C2, 1-4 days post fusion. In the presence of 200 nM ACh, the distribution of channel conductances had a major peak at 33 pS and a minor peak at 47 pS. The larger conductance channels will not be discussed here. Kinetic analysis of the 33 pS channels showed that a typical channel(at a potential 100 mV hyperpolarized from rest)opened for $32^{\pm}1$ ms(n=4). This value was obtained from the exponential fit to the main component of the channel open duration histogram(ignoring closures briefer than 3 ms). On the average, a channel presented $0.7^{\pm}0.3$ transient closures of $0.5^{\pm}0.1$ ms duration. The histograms showed a second component,τ=$0.4^{\pm}0.1$ ms. These rapid channels contributed to 1-2 % of the total open time. In the presence of both 50 nM CPZ and 200 nM ACh, the conductance of the ACh channels was not changed from control(33 pS). However, a channel opened for only $21^{\pm}3$ ms(n=4; 100 mV hyperpolarized). These channels presented an average of $0.8^{\pm}0.4$ transient closures of $0.49^{\pm}0.1$ ms duration. As above, the population of rapid channels(τ=$0.5^{\pm}0.04$ ms)contributed to 1-2 % of the total open time. Both in the presence and absence of CPZ, ACh-activated channel open times increased 1.3 times by a 50 mV hyperpolarization, suggesting that CPZ's effect is voltage-independent. Thus, CPZ alters the kinetics but not the conductance of ACh-activated channels. 1. Koblin and Lester(1979)Mol.Pharm.$\underline{15}$:559. A.R. was supported by an MDA postdoctoral fellowship.

M-PM-B4 ACTIVATION INDEPENDENCE AND AGONIST BINDING INDEPENDENCE OF THE ENDPLATE ACETYLCHOLINE RECEPTOR. V.E. Dionne, Dept. of Medicine, University of California, San Diego, La Jolla, CA 92093

The kinetics of single channel currents elicited by acetylcholine from endplate acetylcholine receptors (AChR) have been analysed for information on activation and agonist binding using the single channel ensemble method (Leibowitz and Dionne, Biophys. J. (1984) 45:153). This approach allows membrane patches containing many channels to be studied and single channel kinetic parameters to be estimated independent of the number of active channels. Data were recorded from junctional regions of garter snake twitch muscle fibers using conventional patch clamp techniques. The cells were treated with enzymes to remove the nerve terminal and prepare the surface for seal formation. Patch pipettes contained 500 nM ACh. 1) The activation interdependence of channels was tested by constructing a conditional opening rate histogram which plots the time at which channels open after any opening. If the opening of one channel alters the probability that its neighbors will open, such a histogram should show a non-uniform density. However, these histograms were flat between 300 "s and 25 ms independent of voltage, indicating that endplate AChR channels are functionally independent at low agonist concentrations. 2) The time course of the first latency histogram (a plot of all resolved closed intervals) is sensitive to the kinetics of agonist binding and to the rates of channel opening and closing. Present resolution is sufficient to distinguish between two alternative postulates about agonist binding. Data support the idea that the two agonist sites on each AChR are independent with equal affinities, but are not consistent with a model of two sites having equal affinities but which are necessarily occupied in sequence. Models somewhat intermediate between these extremes cannot be excluded. Supported by NS 15344.

M-PM-B5 KINETIC ANALYSIS OF SPONTANEOUS ACETYLCHOLINE RECEPTOR CHANNEL GATING. Meyer B. Jackson, Department of Biology, UCLA, Los Angeles, CA 90024.

Spontaneous openings of the acetylcholine receptor channel were recorded in cultured embryonic mouse muscle with a patch clamp. Recordings were made at patch electrode potentials of +50 and +100 mV with the cell at rest in physiological saline to see how the kinetic behavior varied with membrane potential. Likelihood maximization ascertained the number of exponential components needed to describe open time and closed time distributions. Fits to open times improved dramatically when two exponentials were used instead of one. At +50 mV a fast component comprised 84% of all openings. The fast component decay constant was 11000 s^{-1} and the slow component decay constant was 2200 s^{-1}. Increasing the patch electrode potential to +100 mV reduced the decay constants to 7700 s^{-1} and 1400 s^{-1} respectively, but did not significantly change the relative weights of the two components. Fits to closed times were improved significantly by using a sum of two exponentials. At +100 mV the fast component (decay constant = 3300 s^{-1}) usually comprised less than 20% of all closed times. The rate of opening of the channel increased as the membrane was hyperpolarized. Once a correction for possible differences in the number of missed openings at the two potentials was made, the rate of opening was found to increase by a factor of 1.6 from +50 to +100 mV. These studies provide information on the conformations available to the channel in the absence of ligand. Thus, there are two open states which cannot be accounted for by singly and doubly liganded receptors. The voltage dependence indicates that some of the charge movement associated with gating is independent of the charge on a cholinergic ligand.

M-PM-B6 HETEROGENEOUS BURST KINETICS OF *XENOPUS* ACETYLCHOLINE RECEPTOR CHANNELS AT HIGH AGONIST CONCENTRATIONS. Anthony Auerbach and Christopher Lingle, Dept. Biophys. Sci., SUNY, Buffalo, NY and Dept. Biol. Sci., FSU, Tallahassee, FA.

At high agonist concentrations ACh—activated channels in *Xenopus* myocytes open in clusters or bursts which last hundreds of milliseconds and which can contain hundreds of openings (stg. 19—22 embryos grown 1—2 days in culture, cell—attached patches, est. Vm=−120 mV, 23°C). For each conductance class of channel (40 and 60 pS), there are three classes of bursts which can be distinguished by the probability of a channel being open within a burst (p). At 20 μM ACh, the three classes of bursts have mean p values of >0.8, 0.1—0.5, and <0.05. In most records over 80% of 40 pS channel bursts belong to the high duty—cycle population (p=0.87+/−0.04; mean+/−SD, 7 patches) while >80% of 60 pS channel bursts belong to the intermediate duty—cycle population. The differences in p between burst classes appear to arise from differences in both open and shut periods within bursts. For all classes of bursts p increases with increasing [ACh]. For 40 pS, high duty—cycle bursts, p saturates at a value >0.98 (50—100μM ACh). The apparent channel closing rate (not corrected for missed gaps) for bursts with p values >0.8 is 200/sec, thus a lower limit on the channel opening rate is 10,000/sec. In addition to these general characteristics of bursts there are differences in kinetic parameters between bursts of the same conductance and p class which are greater than those expected from sampling errors alone. Also, on a few occasions we observed switching between p modes (but not conductance class) within an isolated burst. We suspect that the major features of the variety in ACh receptor burst kinetics arise from slow state transitions within a single population of channels. (MDA Research Grant to CL and NS—13194 to F. Sachs).

M-PM-B7   ACTIVATION OF ACETYLCHOLINE RECEPTORS BY LOW CONCENTRATIONS OF AGONIST. S.M.Sine and J.H.Steinbach, Departments of Anesthesiology and of Anatomy and Neurobiology, Washington University School of Medicine, St. Louis, MO.

We examined activation of acetylcholine receptors (AChRs) to estimate the rates of channel opening, β, and dissociation of agonist, $\underline{k}$. Currents were recorded through single open AChR channels in cell attached patches on BC3H-1 cells at low concentrations of acetylcholine (100 nM), carbamylcholine (2 μM) or suberyldicholine (50 nM)(11°C, -100mV). At low concentration, long duration openings occur as bursts of several openings separated by brief closed periods. Two short duration closed components are seen, brief and intermediate. The mean duration of brief closures is relatively constant for all agonists (50 μsec), whereas the duration of intermediate closures varies about two-fold(0.5 to 1.0 msec). All three agonists elicit brief closures at a similar rate (60 per sec of open time), while intermediate closures occur at a rate of 10 to 30 per sec, depending on the agonist. We applied the approach of Colquhoun and Hawkes to each component to estimate β and $\underline{k}$. The estimates for β from brief closings are similar for these three agonists (12000 to 16000 Hz), while those from intermediate closures differ several-fold (180 to 1300 Hz). Overall, these data suggest that brief closures reflect a process intrinsic to the open channel which is independent of the agonist used to activate the channel. Intermediate closures show more agonist specificity, suggesting that they reflect steps in agonist binding and receptor activation. Supported by NIH grant NS 13719. SMS supported by an NIH postdoctoral fellowship.

M-PM-B8   ACTIVATION OF ACETYLCHOLINE RECEPTORS BY HIGH CONCENTRATIONS OF AGONIST. S.M.Sine and J.H.Steinbach, Departments of Anesthesiology and of Anatomy and Neurobiology, Washington University School of Medicine, St. Louis, MO.

We studied the activation of acetylcholine receptors (AChRs) at high agonist concentrations to directly estimate the rate of channel opening, β. Currents were recorded through single open AChR channels in cell-attached patches on BC3H-1 cells using (ACh: 20 μM to 1 mM; Carb: 180 μM to 1 mM; 11°C, -70mV to -100mV). At these concentrations, long duration openings occur in groups of openings separated by brief closures. Closed duration histograms show three brief duration components (within groups) and two long duration components. The long duration components reflect desensitization processes. Brief duration closures reflect additional receptor processes including activation. A major brief closed component is seen whose decay constant, $\underline{b}$, depends on agonist and on agonist concentration. $\underline{b}$ increases with concentration, approaching limiting values of 480 Hz for ACh and 130 Hz with Carb, close to β estimated from intermediate closures at low agonist concentration (480 Hz and 180 Hz). $\underline{b}$ shows a sigmoid concentration dependence with half maximal values at about 50 μM for ACh and 300 μM for Carb. The measured fraction of time spent open in a group is 0.91 for ACh and 0.75 for Carb (1 mM), in good agreement with calculated probabilities of being open. These observations on AChR activation at high agonist concentration are consistent with our interpretation of data at low agonist concentrations. Supported by NIH grant NS 13719. SMS supported by an NIH postdoctoral fellowship.

M-PM-B9   PATCH-RECORDED SINGLE-CHANNEL CURRENTS OF THE PURIFIED AND RECONSTITUTED ACETYLCHOLINE RECEPTOR FROM DENERVATED GUINEA PIG SKELETAL MUSCLE. [+]P. Gardner and [*]E.A. Barnard. Intr. by [+]W. Clusin. [+]Dept. of Medicine, Stanford University Medical Center, Stanford, CA 94305 and [*]Biochemistry Dept., Imperial College, London SW7, U.K.

Acetylcholine receptors from guinea pig skeletal muscle two weeks post denervation were solubilized, purified by affinity chromatography on an α-Naja n. siamensis toxin affinity gel, and reconstituted in multilamellar soybean lipid vesicles. Single channel currents from the reconstituted receptors were assayed by the gigaseal patch-recording technique. High resistance seals were obtained by suction of vesicles onto the pipette or after formation of lipid bilayers from monolayers at the tip of the pipette. The single channel conductance of the channels activated by 1 uM ACh was 25.7 $\pm$ .2 pS (n=8) in symmetrical 0.15M NaCl solutions. Channel conductance was voltage-independent. Infrequently multiples of single channel current amplitudes (two to nine times unit value) were seen, suggesting that channels may aggregate and behave as synchronous multimers. The distributions of channel open times at room temperature were fitted by the sum of two exponentials with mean time constants of 3.62 msec and 12.89 msec at -70mV, with a minimum resolvable open duration of .15 msec. These results suggest that solubilization, purification and reconstitution of low density ACh receptors from mammalian muscle can be achieved. Future studies will compare properties of extra-synaptic ACh receptors from denervated muscle to synaptic ACh receptors from innervated muscle. This may determine if the functional differences between synaptic and extrasynaptic ACh receptors noted in the in situ membrane are intrinsic to the receptors or are related to differences in local environment.

M-PM-B10 MODEL FOR THE ION CHANNEL IN THE ACETYLCHOLINE RECEPTOR. Paul A. Bash, Robert Langridge, Robert M. Stroud. Departments of Biochemistry and Pharmaceutical Chemistry, University of California, San Francisco.

An atomic model for the ion channel in the acetylcholine receptor is proposed based on the now established topology of the peptide chains. This topology suggests that one homologous hydrophilic sequence from each of the five similar subunits could form the ion channel. These sequences, which consist of residues 425-460 from each subunit, have the characteristics of an amphipathic α-helix. Structural studies show the entire complex to be quasi five-fold symmetric in the stoichiometry $\alpha_2\beta\gamma\delta$. In the model, the axis of each helix is separated by 10 Å from the adjacent helices of the other subunits, twisted 17° with respect to the vertical and positioned to form a quasi five-fold symmetric channel. The helices are rotated about their axis such that the 21 positive and 19 negatively charged amino acids, 425-451, are oriented toward the center of the channel. The side chains of these residues are positioned to maximize inter- and intrasubunit ion pairing. To ask if this structure could provide for ion transport, the side chains of the residues in the channel are moved to the space between adjacent helices without any change in the inter-helix separation. This results in a channel 6-7 Å in diameter, close to the diameter found by electrophysiology. Electrostatic energy calculations show that this proposed structure could provide the necessary characteristics to explain ion conductivity. It indicates a strong preference for cations over anions, and provides a test bed for mechanistic correlates of the structure.

M-PM-B11 ACETYLCHOLINE RECEPTOR CHANNEL PERMEABILITY PROPERTIES FOR MONO- AND DIVALENT CATIONS. John Dani and George Eisenman, Dept. of Physiology, UCLA School of Med., L.A., CA 90024.

Single nicotinic AChR channels in rat myotubes were studied using giga-ohm seal patch clamp techniques. I-V relations for a wide concentration range of pure Na and Cs were found to have qualitatively similar shapes, with Cs having a higher maximum conductance and greater binding affinity than Na. The single channel zero-voltage conductance at low concentrations (7 mM Cs) is higher than predicted by a simple, single-site binding curve fitted to the high concentration data. Millimolar concentrations of Mg or Ba added to the external solution block inward current. At -100 mV the chord conductance in pure symmetrical 45 mM Cs is 55 pS. With 1 mM Mg or Ba added externally, it is reduced to 26 and 35 pS, respectively. As more divalent cation is added, the block increases until Cs is displaced from the channel by the divalent cation, which then carries the inward current. The inward current for 110 Mg + 45 Cs outside is about the same as for pure 110 Mg outside. Various single occupancy Eyring transport models, including a 2-state fluctuating barrier model, can describe the data. However, only fluctuating barrier or multiple occupancy models can describe the higher than predicted conductance at low concentrations of pure Cs mentioned above. Alternatively, negatively charged amino acids lining the channel and near the vestibules could explain this, as well as the greater affinity of divalent- than monovalent cations. The permeability and relatively high affinity of divalents may have important functional implications. For example, at neuromuscular endplates, where the AChR density is high, physiological concentrations of divalents may decrease monovalent permeability and the divalents may be transported into the muscle cell. This could influence neuromuscular transmission as well as alter the local concentration of internal divalents near the endplate. Supported by NSF (PCM 81-09702 and USPHS (GM 24749).

M-PM-C1   CHOLESTEROL STABILIZES THE CRYSTAL-LIQUID INTERFACE IN PHOSPHOLIPID MONOLAYERS
Robert M. Weis and Harden M. McConnell, Department of Chemistry, Stanford University, Stanford CA. 94305.

Recent Epifluorescence studies of fluorescent probe doped dipalmitoylphosphatidylcholine (DPPC) monolayers at the air/water interface have revealed the pressure-induced formation of 2-dimensional crystal domains from the fluid lipid(1,2 & references therin). These domains exhibit an unbelieveably rich variety of shapes and spatial patterns. The central question in understanding these geometrical features is the extent to which domain size and shape is determined by kinetic and/or equilibrium properties of the system. We have discovered that small mole fractions of cholesterol have dramatic effects on domain geometry. Our data are best interpreted in terms of an equilibrium binding of cholesterol to the line interface between liquid and crystal regions. A typical crystal form of DPPC is illustrated. The crystal length/crystal width ratio is approximately proportional to cholesterol concentration in tne fluid phase. Crystals become thinner on compression due to the increased cho-lesterol concentrations in the fluid phase, a change that is reversible on decompression. The marked effect of cholesterol on domain shape is thought to be due to a preferential binding of cholesterol to different crystal faces. The high affinity of cholesterol for certain crystal faces may be related to the existence of 'roughening transitions' that provide a high multiplicity of surface bind-ing sites for cholesterol. This research was supported by NSF Grant PCM-8313770. RMW acknowledges the Hertz Foundation for support.

1) Weis & McConnell, Nature 310 (1984) 47-51.
2) Fischer et al., J. Physique Lett. 45 (1984) L785-L791.

L-α-DPPC, 2% cholesterol

|← 100 μm →|
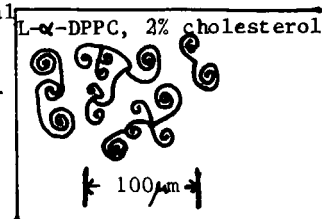
M-PM-C2   STRUCTURE OF HYDRATED N-STEAROYL SPHINGOMYELIN (18:0-SM) AND ITS INTERACTION WITH
CHOLESTEROL. P.R. Maulik, P.K. Sripada, and G.G. Shipley. Biophysics Institute, Boston University School of Medicine, Boston, MA 02118.

Differential scanning calorimetry (DSC) and x-ray diffraction have been used to investigate the structure and properties of 18:0-SM and its interactions with cholesterol. Hydrated multibilayers of 18:0-SM exhibit a reversible order-disorder transition (T_c) at 45°C ($\Delta H = 6.7$ Kcal/mol). X-ray diffraction studies at temperatures below (22°C) T_c show a bilayer gel structure (periodicity, d = 74.8Å; sharp 4.26Å reflection). Above T_c, at 58°C, a bilayer liquid crystal structure (d = 66.6Å, diffuse 4.6Å) is present. Thus, the reversible transition corresponds to a bilayer gel → liquid crystal transition. Addition of cholesterol results in a progressive decrease in the enthalpy of the transition at 45°C and the appearance of a broad transition at ∿ 47°C; this latter transition progressively broadens and is not detectable at cholesterol contents > 40 mol%. By x-ray diffrac-tion, at 22°C a decrease in the bilayer periodicity occurs (74.8 to 63.6Å) with increasing choles-terol content and the sharp 4.26Å reflection is progressively broadened and shifted, reaching a limiting value of 4.8Å at ∿ 50 mol% cholesterol. At 58°C the bilayer periodicity decreases slightly (66.6 to 62.7Å) and the broad reflection at 4.6Å shifts progressively to 4.8Å. Thus, cholesterol inserts into 18:0-SM bilayers, progressively removing the chain melting transition and changing the structural characteristics of the bilayer. The mode of interaction appears to be similar to that of phosphatidylcholine-cholesterol bilayers.

M-PM-C3 ^{13}C NMR STUDIES OF CHOLESTERYL ESTERS AND THEIR ANALOGUES: STEROID RING DYNAMICS NEAR THE ONSET OF THERMOTROPIC MESOPHASE FORMATION. David H. Croll, Donald M. Small and James A. Hamil-ton, Biophysics Institute, Boston University School of Medicine, Boston, MA 02118

^{13}C NMR spectroscopy has been used to characterize steroid ring dynamics of two cholesteryl esters (myristate and oleate) and their ether or carbonate analogues in the liquid phase near the onset (Tm) of thermotropic cholesteric mesophase formation. Linewidths of the C3 and C6 resonances were used to calculate correlation times for steroid ring reorientation about the long molecular axis of symmetry (τ_{rz}) and the short non-unique axis (τ_{rx}). For myristate (14:0) compounds at the same relative temperature, Tm+1°C, both the ester (Tm=85°C) and the corresponding ether (Tm=67°C) have nearly identical steroid ring dynamics (ester; $\tau_{rx}=6.0 \times 10^{-8}$ s, $\tau_{rz}=8.5 \times 10^{-10}$ s, ether: $\tau_{rx}=5.5 \times 10^{-8}$ s, $\tau_{rz}=8.5 \times 10^{-10}$ s). These results indicate the motions near Tm, particularly the anisotropy ($\tau_{rx}/\tau_{rz} \sim 70$), are not affected by the nature of the steroid-acyl linkage. The anisotropies of ole-ate (18:1) compounds are higher than for the 14:0 compounds. However, the anisotropies of cholest-eryl oleoyl carbonate (Tm=30°C) ($\tau_{rx}=1.5 \times 10^{-6}$ s, $\tau_{rz}=9.0 \times 10^{-9}$ s) and cholesteryl oleate (Tm=46°C) ($\tau_{rx}=2.9 \times 10^{-7}$ s, $\tau_{rz}=2.8 \times 10^{-9}$ s) (Ginsburg et al., (1982) Biochemistry 21:6857), are similar within experimental error (i.e., $\tau_{rx}/\tau_{rz} > 100$) showing that alteration of the steroid-acyl linkage in the case of the unsaturated (18:1) acyl chain did not drastically affect the anisotropy of motions near Tm. Thus, although for a given acyl chain, the acyl-steroid linkage affects the Tm of mesophase formation (and hence intermolecular interactions), it did not result in significant differences in ring motional anisotropy in the isotropic phase near Tm.

M-PM-C4 ^{13}C-AND ^{2}H-NMR STUDIES OF GALACTOCEREBROSIDE, SPHINGOMYELIN AND GALACTOCEREBROSIDE/ CHOLESTEROL BILAYER MEMBRANES.
M.J. Ruocco, D.J. Siminovitch, S.K. Das Gupta, P. Sripada, G.G. Shipley and R.G. Griffin. Intr. by W. Curatolo. Massachusetts Institute of Technology, Cambridge, MA and Biophysics Institute, Boston University School of Medicine, Boston, MA.

Saturated acyl-containing N-(^{13}C=O)palmitoylgalactosylsphingosine (^{13}C-NPGS) (cerebroside) and N-(^{13}C=O)oleoylgalactosylsphingosine gel bilayers all exhibit axially asymmetric lineshapes characteristic of slow ($\leq 10^{2}$s^{-1}) axial diffusion of the amide carbonyl, thereby demonstrating the minor influence of chain unsaturation upon cerebroside dynamics in the gel bilayer phase. N-(^{13}C=O)palmitoylsphingomyelin gel bilayers similarly exhibit rigid lattice spectra which suggests that galactose and phosphocholine headgroups have a much weaker influence on the amide carbonyl motion at the bilayer interface in comparison to the much stronger local intramolecular interactions of the amide moiety. ^{2}H- and ^{13}C-spectra of [7,7-^{2}H$_2$]-NPGS/Cholesterol (CHOL) and ^{13}C-NPGS/CHOL dispersions, respectively, indicate that cholesterol has little influence on the spectra of gel NPGS bilayers at low temperatures. At T $\leq$ 50°C, a single rigid lattice ^{13}C-lineshape is observed. At 50°C $\leq$ T $\leq$ 70°C, two component ^{2}H-spectral lineshapes are observed which exchange slowly on the deuterium time scale. From ^{2}H quadrupolar splittings as a function of temperature and CHOL concentration, the two bilayer phases, cerebroside/CHOL (1:1) liquid crystal and cerebroside gel bilayer phases, are defined. The slow exchange between the two phases contrasts with the fast exchange observed for phospholipid/cholesterol bilayers and is explained in terms of a strong preferential association between gel cerebroside molecules. The two-component ^{2}H-spectra of NPGS/CHOL bilayers permit the quantitation of disordered versus unmelted ordered cerebroside fractions by lineshape simulation.

M-PM-C5 PROPERTIES OF BILE SALT-LECITHIN MIXED MICELLES. Charles Spink, Frank Reda and Thomas Walton. Chemistry Department, SUNY-Cortland, Cortland, NY 13045.

Bile salts and synthetic lecithins form a variety of aggregate structures whose properties depend on the relative lipid composition and on solution conditions. This paper will summarize recent work on differential scanning calorimetry (DSC) and fluorescence probe studies of the micelles formed when bile salts and dipalmitoylphosphatidylcholine (DPPC) are mixed. Correlations of DSC results on the cooperativity of the thermal transitions with the size and shapes of the micelles as composition is changed will be presented. The data suggest that the behavior of the micelles with specific bile salts is different because of compositional variations caused by changes in the equilibria involved in their formation. Cholesterol incorporation in the micelles (at about 2 mole %) causes significant changes in the thermal transitions, particularly in micelles containing higher amounts of bile salts.

To aid in interpretation of the thermal behavior, studies of the fluorescence transitions of β,β-dinaphthylpropane (DNP), a molecule that forms an intramolecular excimer, are presented. The ratio of excimer to monomer band intensities reflects the microviscosity of the environment of the probe. The spectral changes indicate variations in microviscosity within the micelles which are consistent with some of the observed changes in the thermal transitions from the DSC work. The temperature dependence of the fluorescence microviscosity shows that marked ordering occurs within the micelles as temperature decreases. The implications of these results will be discussed in terms of current models for the micellar size and shape.

M-PM-C6 THE PHASE BEHAVIOR AND BILAYER PROPERTIES OF FATTY ACIDS: HYDRATED 1:1 ACID-SOAPS. David P. Cistola, David Atkinson, and James A. Hamilton. Biophysics Institute, Boston University School of Medicine, Boston, Massachusetts 02118 (Intr. by Donald M. Small)

Titration of an aqueous potassium soap solution with hydrochloric acid results in the formation of either crystals or liquid crystals of a 1:1 fatty acid-potassium soap compound ("acid-soap"). We present a phase diagram for an acid-soap (1:1 potassium hydrogen dioleate) as a function of water concentration and temperature based on differential scanning calorimetry, x-ray diffraction, and polarized light microscopy results.

Anhydrous 1:1 potassium hydrogen dioleate forms crystals with a 47Å lamellar periodicity. This compound is stable up to 47°C, at which point it decomposes into crystalline potassium oleate and an isotropic liquid. Upon hydration, the decomposition temperature falls to 11°C at 30% water content and then remains constant at higher water content. Above this temperature, two one-phase liquid crystalline regions are present: a hexagonal type II liquid crystalline phase at low hydration, and a lamellar liquid crystalline phase at >60% water. The former shows angular, striated, and nongeometrical textures by polarizing microscopy; x-ray small-angle reflections index into a 2D hexagonal lattice. The lamellar phase shows oily-streak and mosaic textures by microscopy; x-ray small-angle reflections index into a one-dimensional lamellar pattern. At >90% water, one-dimensional order is lost and the sample contains two phases: bilayers in excess aqueous phase.

Since soaps form micelles, acid-soaps form bilayers, and acids form oils above the chain melting transition, we conclude that surface charge density (and hence, ionization state) largely determines the type of aggregates formed by long-chain fatty acids in water.

M-PM-C7   NEUTRAL GLYCOSPHINGOLIPID ORGANIZATION IN BILAYERS AS DEDUCED FROM SPONTANEOUS INTERBILAYER TRANSFER KINETICS. R.E. Brown, I.P. Sugar and T.E. Thompson (Introduced by R.P. Taylor) Department of Biochemistry, University of Virginia, Charlottesville, VA 22908.

Spontaneous transfer kinetics were investigated by monitoring tritiated glycosphingolipid movement from donor to acceptor vesicles. At desired time intervals, donors were separated from acceptors by either ion exchange or molecular sieve chromatography. Asialo-GM_1 net transfer was calculated relative to that of [^{14}C]-cholesteryl oleate which served as a non-transferable marker in the donor vesicles. Treatment of the [^3H] asialo-GM_1 transfer data as a reversible first order kinetic process resulted in a biphasic half logarithmic plot suggesting the existence of two asialo-GM_1 pools departing from donor vesicles at different rates. A mathematical model was developed to evaluate the two pool glycolipid model. The mathematical model allows determination of the glycolipid pool sizes and their respective rate constants. A molecular interpretation identifies the faster transferring pool as glycolipid monomers and the slower transferring pool as glycolipid-enriched domains within the phospholipid matrix. Control experiments eliminate an alternative model that associates the rate from the slower transferring pool with the asialo-GM_1 flip-flop rate from the inner to the outer bilayer surface before departure from the donor. (Supported by USPHS Grants GM-23573 and GM-14628).

M-PM-C8   INTERACTIONS OF TRIACYLGLYCEROLS WITH PHOSPHOLIPID BILAYERS. James A. Hamilton & Howard S. Lilly, Biophysics Institute, Boston University School of Medicine, Boston, MA 02118 (Intr. by Eugene Serrallach)

Interactions of triacylglycerols (TG) with dipalmitoylphosphatidylcholine (DPPC) bilayers in both the gel and liquid-crystalline phases have been studied using carbonyl ^{13}C-enriched TG and ^{13}C NMR spectroscopy. Up to ∿3 wt% triolein (TO) or tripalmitin (TP) can be incorporated into DPPC vesicles by cosonication of the TG and DPPC at 50-55°C. In the temperature range of the NMR studies (25-55°C) pure TO is a liquid and pure TP is a solid. In spectra at 40-55° of vesicles with TG, both TG have narrow (<10 Hz) carbonyl resonances, indicative of rapid motions, and similar chemical shifts: 173.2 ppm (sn-1,3) and 172.5 ppm (sn-2). These chemical shifts are downfield from those of TG in an oil phase and show that the TG carbonyls are H-bonded with solvent (H_2O) at the aqueous interfaces of the vesicle bilayer. Below the phase transition temperature of the vesicles (∿37°C), several phospholipid peaks broaden beyond detection. These include the carbonyl, glyceryl backbone, and certain aliphatic resonances. In vesicles with TO, the TO carbonyl peaks are only slightly broader (∿2-fold) below the transition; however, in vesicles with TP, the TP carbonyl peaks are broadened beyond detection. Moreover, there is no change in the integrated intensity of the TO carbonyl peaks but a gradual intensity decrease for the TP carbonyl peaks on cooling from ∿40° to 25°C. Thus, TP solidifies with DPPC in the gel phase of the phospholipid whereas TO remains liquid. The chemical shifts of the TO carbonyl peaks are invariant with temperature. Thus, TO does not partition into the hydrocarbon interior but may exhibit lateral phase separation into liquid domains in the gel phase of DPPC.

M-PM-C9   THE pH AND TEMPERATURE DEPENDENCE OF DIBUCAINE BINDING TO PHOSPHATIDYLCHOLINE VESICLES. M. R. Eftink and R. K. Puri, Dept. of Chemistry, U. of Mississippi, University, MS 38677

The interaction of the local anesthetic dibucaine with the liquid-crystalline phase state of unilamellar vesicles of dimyristoylphosphatidylcholine (DMPC) was studied by equilibrium dialysis. Saturating binding profiles, as a function of dibucaine concentration, were found at pH 5.0, 7.0 and 7.5 (ionic strength, 0.05 M, 35°C). The binding data were analyzed using the Stern relationship, which takes into account the electrostatic effect on binding the cationic drug due to the build up of a surface potential (McLaughlin and Haray, Biochemistry 15, 1941 (1976); Rooney and Lee, BBA 732, 428 (1983)). In this analysis, a Langmuir adsorption isotherm is assumed for both the cationic and neutral drug forms, the surface cationic drug concentration is described by a Boltzman relationship, and the surface potential is related to the amount of bound cationic drug by the Grahame equation. A fit is obtained for the data at the three pHs with K_D^+ (the intrinsic association constant for the cationic drug) = 1.25 x 10^3 M^{-1}, σ_m (the maximum possible number of drug molecules adsorbed per unit area of vesicle surface) = 1/320 $Å^{-2}$, γ_L (the surface area per lipid molecule) = 70 $Å^2$, a pK_a = 8.85 for free dibucaine (independently determined value), and a ΔpK (difference in the pK_a of bound and free drug) = -1.35. According to this fit, a maximum of 1 dibucaine molecule is bound per c.a. 5 DMPC molecules at saturation and the neutral drug binds 22 times better than the cationic drug. We have also studied the binding of dibucaine to the gel state of DMPC vesicles at 15°C. The value of K_D^+ is found to remain about the same for the gel state, but the value of σ_m is found to decrease to about 1/550 $Å^{-2}$. In other words, the size of the drug binding site is found to increase from c.a. 5 DMPC molecules in the liquid-crystalline state to about 14 in the gel state. Supported by NSF grant PCM-82-06073.

M-PM-C10 DIACYLGLYCEROL, A PRODUCT OF PHOSPHATIDYLINOSITOL METABOLISM, CAUSES MAJOR STRUCTURAL PERTURBATIONS IN LIPID BILAYERS. Sudipto Das and R.P. Rand, Department of Biological Sciences, Brock University, St. Catharines, Ontario, Canada L2S 3A1.

Phosphoinositides and diacylglycerol (DAG), the products of phosphatidylinositol (PI) metabolism, have attained the role of secondary messengers in transmembrane signalling in a host of cellular processes. However the exact mechanism of action of these substances is not yet clear. DAG is a specific activator of protein kinase C and various phospholipases. DAG production is closely correlated with membrane fusion of myoblasts and in synaptic transmission. We have demonstrated by x-ray diffraction and freeze-fracture electron microscopy that DAG causes major structural changes in phospholipid bilayer systems. At 5 mole%., DAG induces a lamellar-to-hexagonal (H_{II}) transition in egg phosphatidylethanolamine (PE) bilayers at 25°C which is complete by 10 mole%.. At 25°C, 30 mole%. DAG causes the same transition in egg phosphatidylcholine (PC) bilayers and forms a primitive cubic phase around 75 mole%.. The amount of DAG needed to induce the transition is reduced as temperature is increased from 4°C to 60°C. DAG disorders the bovine brain phosphatidylserine lamellar phase. DAG by itself floats on water. We have constructed phase diagrams to elaborate the lyotropic-thermotropic nature of these transitions at selected lipid compositions. We interpret the induction of non-bilayer structures by DAG as diagnostic of its potential to destabilize planar membrane structures, at least in its immediate vicinity. In order to assess this we are measuring the effect of DAG on interbilayer forces and bilayer compressibility.

M-PM-C11 STRUCTURE AND METASTABILITY OF N-LIGNOCERYL GALACTOCEREBROSIDE BILAYERS.
R.A. Reed and G.G. Shipley. Biophysics Institute, Boston Univ. Schl. Med., Boston, MA.
Differential scanning calorimetry (DSC) and X-ray diffraction have been used to study hydrated N-lignoceryl galactocerebroside (NLGC) bilayers. DSC of hydrated (70 wt.% H_2O) NLGC shows an endothermic transition at 69°C, immediately followed by an exothermic transition at 72°C; further heating shows a high temperature (T_c = 82°C), high enthalpy (ΔH = 15.0 Kcal/mol NLGC) transition. Heating to 75°C, cooling to 20°C and subsequent reheating shows no transitions at 69-72°C; only the high temperature (82°C), high enthalpy (15.0 Kcal/mol) transition is observed. Two exothermic transitions are observed on cooling; for the upper transition its temperature ($\sim$ 65°C) and enthalpy ($\sim$ 6 Kcal/mol NLGC) are essentially independent of cooling rate, whereas the lower transition exhibits marked changes in both temperature (30 $\rightarrow$ 60°C) and enthalpy (3 $\rightarrow$ 9.5 Kcal/mol NLGC) as the cooling rate decreases from 40 to 0.625°C/min. On heating, the enthalpy of the 69°C transition is dependent on the previous cooling rate. The DSC data provide clear evidence of conversions between metastable and stable forms. X-ray diffraction data recorded at 22, 75 and 93°C show clearly that NPGS bilayer phases are present. The X-ray diffraction pattern at 75°C shows a bilayer periodicity d = 65Å, and a number of sharp reflections in the wide angle region indicative of a crystalline chain packing mode. This stable bilayer form converts to a liquid crystal bilayer phase; at 93°C, d = 63Å, diffuse reflection at $1/4.6\text{Å}^{-1}$. The diffraction pattern at 22°C represents a combination of the stable and metastable low temperature bilayer forms. Thus, NLGC exhibits a complex pattern of thermotropic changes related to conversions between metastable (gel), stable (crystalline) and liquid-crystalline bilayers.

M-PM-C12 ELECTROKINETIC AND ELECTROSTATIC PROPERTIES OF BILAYERS CONTAINING GANGLIOSIDES G_{M1}, G_{D1a} and G_{T1b}. Kim Sharp(1), Robert V. McDaniel(2), Alan C. McLaughlin(3), Anthony P. Winiski(2), Donald Brooks(1) and Stuart McLaughlin(2).1 Department of Pathology, University of British Columbia, Vancouver, B.C., 2 Department of Physiology, Health Sciences Centre, State University of New York at Stony Brook, Stony Brook, NY 11790 and 3 Department of Physiology, University of Pennsylvania, Philadelphia, PA.

To model the electrokinetic behaviour of erythrocytes we formed vesicles from mixtures of egg phosphatidylcholine (PC) and ganglioside G_{M1}, G_{D1a}, or G_{T1}. We observed similar electrophoretic mobilities in NaCl, CsCl, and TMACl solutions, which suggests that monovalent cations do not bind significantly to these gangliosides. We described the mobility data in 1, 10 and 100 mM monovalent salt solutions with a combination of the nonlinear Poisson-Boltzmann and Navier-Stokes equations by assuming that the sugar moieties (modeled as Stokes spheres) exert hydrodynamic drag and that the sialic acid groups are located at some distance from the vesicle surface. The theoretical results depend strongly on the head group thickness and charge placement, but are relatively independent of the Stokes radius of each sugar and the placement of the hydrodynamic shear plane. We obtained a reasonable fit to the mobility data by assuming that all ganglioside head groups are about 2.5 nm thick, and that fixed charges are about 1 nm from the bilayer surface. We tested the latter assumption by measuring the surface potentials on PC:ganglioside bilayers, using three techniques: 1) conductance measurements on planar bilayers 2) ^{31}P NMR measurements on sonicated vesicles 3) TNS fluorescence measurements on sonicated vesicles. The results were consistent with our assumption.

M-PM-D1   THREE DIMENSIONAL RECONSTRUCTION OF THE CENTRAL APPARATUS IN THE PIGMENT CELLS OF HOLOCENTRUS. N.D. Gershon, K.R. Porter and M.A. McNiven, LTPB/NICHD, NIH, Bethesda, MD 20205 and Dept. of Biol. Sciences, Univ. of Maryland, Catonsville, MD 21228.

The central apparatus of this and other pigment-bearing chromatophores comprises two centrioles and a complex of so called dense bodies (DB). These function as initiating sites for the assembly of microtubules and thus influence their disposition and radial organization. The central apparatus seems therefore to be involved in form determination.
We have sought in this study to use the technics of computer graphics to reconstruct in three dimensions the basic form of the apparatus and to document any changes it may undergo as the cell aggregates its pigment along tracks provided by the microtubules. Electron micrographs of serial sections cut vertically through single chromatophores (erythrophore) provided the data. The images of the dense bodies in these micrographs were digitized and made available for the reconstruction of the entire complex. Thus it was found that the dense bodies are arranged in six planes separated by about 100 nm. The complex exists as a stack of these planar units with the centrioles central to the axis of the stack but in a depression. In other series of micrographs, changes in the disposition of dense bodies was followed in cells induced to aggregate their pigment and thus change their form. A shift in the position of dense bodies peripheral to the complex was noted and is being examined in repeated series. Whether these changes anticipate the other phenomena of pigment aggregation is a question that can be answered by a study of cells in different states of aggregation.

M-PM-D2   STRUCTURAL STUDIES OF THE BASAL BODY OF BACTERIAL FLAGELLA. M.J.B. Stallmeyer, D.J. DeRosier[+], S.-I. Aizawa[*], R.M. Macnab[*], K. Hahnenberger[#], and L. Shapiro[#]. Graduate Program in Biophysics and [+]Dept. of Biology, Brandeis University, Waltham, MA 02254; [*]Dept. of Molecular Biophysics and Biochemistry, Yale University, New Haven, CT 06511; and [#]Dept. of Molecular Biology, Albert Einstein College of Medicine, Bronx, NY 10461.

We have used cross-correlation averaging methods to analyze negatively stained electron micro-graphs of complete and partial basal body structures from Caulobacter crescentus and Salmonella typhimurium. From averaged images we have computed 3-D maps of the cylindrically averaged structure (CAS). The basal bodies from Caulobacter and Salmonella are very similar. In averaged images, the hook-proximal L and P rings appear to be discrete flat rings but in CAS are connected at their outer radii. The primary differences are at the hook-distal end. Both Caulobacter and Salmonella have a disc-like S ring, but additionally a thin fifth ring lying between the S and P rings, designated the E ring, is present in half of native Caulobacter basal bodies. The M ring of Caulo-bacter basal bodies appears thicker on the axis than the corresponding structure from Salmonella due to the presence of a cap-like structure on top of the M ring which we have designated the "button." In some Caulobacter basal bodies the button is missing and the M ring resembles that of Salmonella and appears much like a "wing nut" as viewed from the side. The distance between the L-P rings and the M-S-(E) rings is variable both in Salmonella and in Caulobacter, as determined from measurement of individual images and from analysis of computed variance maps. This is what would be expected if the L and P rings act as bushings and are not connected to the rod. Difference images suggest that the rod is at most long enough to reach to the S ring. Supported by NIH GM 21189.

M-PM-D3   THREE-DIMENSIONAL ORGANIZATION OF ENDOPLASMIC RETICULUM-LIKE STRUCTURES IN HYPOTHALAMIC NEURONS. N.D. Gershon[a], F. Naftolin[c], H. Sakamoto[c], M. Garcia-Segura[d], and B.L. Trus[b], [a]LTPB, NICHD & [b]CSL, DCRT, The National Institutes of Health, Bethesda, MD 20205, [c]Dept. of OB-GYN, Yale Univ. School of Medicine, New Haven, CT 06510, and [d]Inst. of Histology & Embryology, Univ. of Geneva Medical School, Geneva, Switzerland.

In some sex-steroid regulated hypothalamic neurons, the endoplasmic reticulum (ER) seems to fold into a spiral looking complex designated "whorl body" (WB). These complexes change in size and number per cell in response to estrogens during the normal estrus cycle and as a function of age and endocrine conditions. Neurons which contain whorl bodies also have more ER and more synapses (F. Naftolin et al, Brain Res., in press) than profiles without WB. 3-D Reconstruction, by computer graphics technique, shows that WB has an elongated form. An associated Golgi complex follows along the outer surface of the WB. The internal structure of the whorl body shows that it composed of cisternae which are equally spaced from each other. Image analysis coupled to microdensitometry demonstrates that the cisternal plates are separated by 200A or more. On the other hand, the cisternal membranes are around 150A thick. The constant and relatively wide distance between cisternal plates may indicate the presence of intervening (glycocalyx-like?) material. The presence of layers of glue-like material surrounding the cisternal plates could explain the flattened appearance and their close packing density.

M-PM-D4   COLLAGEN CRYOSECTIONS: X-RAY MONITORING AND FIBRIL STUCTURE. Michael Chew and John Squire. Biophysics Section, Department of Physics, Imperial College, London SW7 2BZ.

Longitudinal cryosections of rat-tail tendon collagen are seen to have a lateral periodicity with long range order over several D-periods in its auto-correlated image (Squire and Freundlich, Nature 288, 410-413, 1980). The technique for obtaining these cryosections for electron microscopy has been further developed using X-ray diffraction to monitor the structural integrity of a specimen at each stage of the preparative protocol. The important first row-line spacing of about $(1/39)A^{-1}$ and the 'triplet' around the $(1/13.6)A^{-1}$ and $(1/12.9)A^{-1}$ positions at the equator are not significantly altered throughout the schedule. The second row-line $(1/26)A^{-1}$ reflection on the equator remains through all but the last stage; here the introduction of stain may have decreased the contrast of this reflection. Electron micrographs of negatively stained collagen fibrils prepared under closely similar conditions show the familiar D-periods of 'gap' and 'overlap' regions. A lateral periodicity is clearly observed in the 'gap' regions where there is sufficient retention of negative stain to enhance contrast. Optical diffraction of individual 'gap' regions along single fibrils yielded clear peaks that correspond to 61.9A - 117.6A with an average of 88.3 $\pm$ 14.8A (n=55). The optical transform of a continuous series of D-periods suggests a smallest structural component of diameter 36.5A - 44.6A. These results reveal a higher level of organisation than the single molecule in the widely accepted quasi-hexagonal molecular crystal model for Type I collagen (Hulmes and Miller, Nature 282, 878-880, 1979). It remains unclear if the regular lateral arrangement in negatively stained cryosections can be explained by a 'superlattice' of molecules within the quasi-hexagonal structure. (Supported by the Arthritis & Rheumatism Council, UK.)

M-PM-D5   STRUCTURE OF DOUBLE-STRANDED DNA BACTERIOPHAGES. Gary A. Griess, Philip Serwer, and Paul M. Horowitz, Dept. of Biochemistry, The Univ. of Texas Health Science Center, San Antonio, TX 78284.

To help determine the structure of the double-stranded bacteriophages, T7 and P22, the following experiments have been performed: a) measurement of the equilibrium binding of ethidium bromide (EB) to packaged DNA, b) measurement of the binding kinetics of EB to packaged DNA, and c) characterization of degradation products of P22 after inactivation by elevated temperature. Scatchard plots of the equilibrium binding of EB to T7 and P22 revealed two classes of binding site: most sites for T7 had a negative ΔH°, equal to that of DNA released from the bacteriophage capsid (free DNA); 1-2% of the binding sites had a ΔH° 2X higher and appear to be kinks in the packaged DNA. The initial entry rate of EB into T7 and T7 deletion mutants was a decreasing function of the amount of DNA per volume. These and other data suggest that the density of packaged DNA limits the rate of entry for T7. Although P22 has the same density of packaged DNA as T7, the entry rate of EB was 10-20X slower for P22 than it was for T7. After inactivation of P22 at 75°C, at least two types of empty P22 capsid, distinguished by size and surface charge, were found. Together with previous data, this latter observation indicates at least four stable, distinguishable states of the P22 capsid.

M-PM-D6   A GENERAL THEORY OF THE STRUCTURES OF THE FILAMENTOUS BACTERIOPHAGES
C.J. Marzec and L.A. Day. The Public Health Research Institute, 455 First Ave., New York, NY 10016

Mathematical models of the filamentous bacteriophages are developed for the purpose of explaining observed structural features in terms of elementary geometrical constraints. The constraints entail the close packing of protein subunits made of nearly rigid alpha helices in two layers coaxial with the DNA. The most significant observations explained by the modeling are the linear density of the filamentous bacteriophages, constant for viruses of types I and II, and the subunit rotation angle, constant among type II viruses. fd has coat proteins packed with rotational symmetry and a classical bases-in DNA structure; Pf1 has helically packed coat proteins and is believed to have an inverted bases-out DNA structure. However, close packing models of both virions show the same overall morphology. The procedure shows that there exists a small set of geometrically feasible models, two of which correspond to the type I and type II virions. The others may represent viruses yet undiscovered.

fd   Pf1
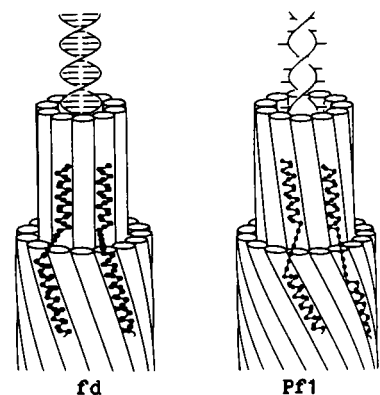
M-PM-D7   RADIAL ELECTRON DENSITY PROFILES OF CURVED FILAMENTOUS PARTICLES FROM STEM MICROGRAPHS
S.A. Reisberg and L.A. Day. The Public Health Research Institute, 455 First Ave., NY, NY 10016

A technique has been developed for analyzing data from the scanning transmission electron microscope (STEM) to yield radial mass distributions of gently curved filamentous particles. Low dose electron scattering intensities, closely proportional to mass, are recorded and digitized by the STEM so that a micrograph is a 512 x 512 array of 8-bit pixel values. We have developed an algorithm that assigns a centerline with subpixel accuracy to the digital image of a naturally curved particle by taking advantage of local straightness. A second algorithm then sorts relevant pixels and bins them according to their perpendicular distance from the centerline. Finally, radial density profiles are obtained by transformation of the binned intensity data. Absolute radial densities can be obtained through calibrations with known mass standards. By averaging data from a large number of particles, radial resolution significantly below the 10 A pixel size is achieved. This technique is especially useful in comparing the radial density profiles of heavy atom modified and unmodified structures in order to determine the radial site of modification. Preliminary results on fd (M13, f1) bacteriophage show a central core of high density out to about 10 A, which is assigned to the DNA, and a lower density region extending out to the particle radius, which is assigned to the protein.

The experimental data have been obtained in collaboration with Joseph S. Wall and his colleagues at the Brookhaven National Laboratory. A.C. Steven et al. have recently carried out transforms of STEM data for straight TMV particles (PNAS, 1984, in press).

M-PM-D8   ENTROPY-DRIVEN POLYMERIZATION OF RIB GRASS VIRUS PROTEIN. Ragaa A. Shalaby[*] and
Max A. Lauffer, Biophysical Laboratory, Dept. of Biological Sciences, University of Pittsburgh, Pittsburgh, PA 15260.

The coat protein of Holmes rib grass virus (HRV), a distantly related strain of tobacco mosaic virus (TMV), differs substantially in amino acids composition and sequence from TMV protein, especially in that it contains one histidine residue and three methionine residues compared to none of either for TMV protein. As in the case of TMV protein, the early stage polymerization of HRV protein is entropy-driven, and the first major polymerized product is a 20S component, presumably a double disk or two-turn helix. In contrast, unpolymerized HRV protein, A protein, sediments at 3S rather than at 4S as in the case of TMV; it is probably a dimer of the polypeptide chain. Ultracentrifugation studies show that the enthalpy of polymerization per mole of A protein, ΔH^*, is 18,400 cal compared to about 30,000 for TMV A protein. One mole of H^+ ion per mole of HRV A protein, compared to 1.5 for TMV, is bound during polymerization to the 20S state. Very little if any electrical work contribution was detected for the polymerization of HRV A protein. Hydrogen ion titration experiments show that HRV protein binds hydrogen ions significantly in the unpolymerized A protein state, unlike TMV A protein.

* Present address: Dept. of Natural Sciences, Point Park College, Pittsburgh, PA 15222

M-PM-D9   THE STRUCTURE OF SV40 VIRUS BY ELECTRON MICROSCOPY OF UNSTAINED FROZEN HYDRATED SUSPEN-
SIONS AND NEGATIVELY STAINED CRYSTALLINE ARRAYS. T. S. Baker[*], J. Drak[+], and M. Bina[+].
Departments of [*]Biological Sciences and [+]Chemistry, Purdue University, W. Lafayette, Indiana 47907.

Simian Virus 40 and polyoma virus are closely related members of the papovavirus family, sharing remarkable similarity in many genetic, chemical, and physical characteristics. The recent structural studies of polyoma by X-ray crystallography[1], electron microscopy, and image analysis[2], revealing the unexpected all pentamer capsomere arrangement in the T=7 icosahedral protein coat, have stimulated interest in the question of whether all papovaviruses have similar capsid structures. A resolution of ∿2-3 nm should be sufficient to distinguish a pentameric capsomere shape, consequently we have initiated a study of the structure of SV40 by electron microscopy. Large hexagonal and small square arrays of the virus have been prepared by the Negative-Stain Carbon-Film Technique and are being examined for suitability for image reconstruction methods. Concentrated virus solutions have been frozen and images of particles suspended in thin layers of vitreous ice over holes have been recorded with minimal electron dose (∿500 e^-/nm^2) to provide enough independent views for a three-dimensional reconstruction of the unstained hydrated virus. Supported by start-up funds from the American Cancer Society and the Indiana Elks to TSB and a grant from the National Science Foundation to MB.

[1]Rayment, I., Baker, T. S., Caspar, D. L. D., and Murakami, W. T. (1982) *Nature* 295:110-115.
[2]Baker, T. S., Caspar, D. L. D., and Murakami, W. T. (1983) *Nature* 303:446-448.

M-PM-D10 HETEROGENEITY OF BACTERIOPHAGE PROCAPSIDS. Philip Serwer and Robert H. Watson, Dept. of Biochemistry., The University of Texas Health Science Center, San Antonio, TX 78284.

Double-stranded DNA bacteriophages assemble DNA-free procapsids that package DNA. These procapsids contain a major internal protein absolutely required for assembly of the procapsid's outer shell and smaller amounts of internal proteins attached to a specialized vertex of the procapsid [details for the related bacteriophages, T7 and T3, are summarized in (1)]. The specialized vertex proteins of T7 appear to correct errors in procapsid outer shell assembly (2), and are not absolutely required for this assembly. Thus, bacteriophage procapsids appear to have control mechanisms for assembly more highly evolved than the control mechanisms of the T=3 plant viruses (3). To analyze these control mechanisms, it is desirable to determine the structure of procapsids. By agarose gel electrophoresis, we have found variability of the electrophoretic mobility (μ) of bacteriophage T7, T3 and P22 procapsids. In the case of T3, it has been found that the negative μ of procapsids increases in magnitude by up to 3% with increasing time after assembly of a procapsid. This increase is: a) caused by an increase in the magnitude of the solid support-free μ (μ_o), not by a decrease in radius, and b) independent of DNA packaging by the procapsid. The increase in the magnitude of μ_o is accompanied by addition of an unidentified T3 protein to the procapsid. The variability of procapsid structure may limit the resolution of structure determination by x-ray diffraction, unless this variability can be eliminated. 1. Serwer, P., et al. (1983) J. Mol. Biol. 170, 447; 2) Serwer, P. and Watson, R. H. (1982) J. Virol. 42, 595; 3. Harrison, S. C. (1983) Advances in Virus Research 28, 175.

M-PM-D11 CHARACTERIZATION OF TMV PROTEIN AGGREGATES IN SOLUTION: STACKS OF DISKS, SHORT AND LONG HELICES. K.Raghavendra, Mary L Adams and Todd M Schuster, Biological Sciences Group, Biochemistry and Biophysics Section, University of Connecticut, Storrs, CT 06268.

We present the results of sedimentation velocity and circular dichroism measurements of stacks of disks and short and long helical aggregates of TMV protein in solution in an attempt to characterize them. For this purpose, spectral markers arising from aromatic amino acid residues have been obtained from the near-UV CD spectra of the protein aggregates. A method has been developed to obtain by computer the CD spectra of the pure aggregating species such as 20s and 24s. CD spectra of stacks of disks of different sizes (present in solution conditions similar to those used for the crystallization of disk aggregates) are indistinguishable from one another. In contrast, there are remarkable spectral (and hence, structural) differences between the stacks of disks and 20s aggregates, the nucleating species in the virus assembly (both measured under conditions used for virus assembly). We propose an open helical structure for the 20s species in solution contrary to the existing notion of closed disk-like structure for them. Preliminary results of reconstitution involving stacks of disks, 20s species and viral RNA will be discussed. Equilibrium short helical aggregates, 20s (presumably 2-turn) and 24s (corresponding to 3-turns) exhibit similar CD spectra. Long helical aggregates present in two different solution conditions exhibit similar spectra but differ from the spectra of the short helices. The differences will be discussed in terms of the end effects dominating the short helical aggregates and the length dependance of CD spectra exhibited by the long helices. (Supported by NIH grant AI 11573).

M-PM-D12 MEASUREMENT OF THE ELASTIC PROPERTIES OF A MICROTUBULAR STRUCTURE: DEFORMATION OF MARGINAL BANDS ISOLATED FROM NUCLEATED ERYTHROCYTES. Richard Waugh, Gary Erwin and Ahmed Bouzid, University of Rochester Medical Center, Rochester, NY 14642

A novel technique has been developed for measuring the mechanical properties of marginal bands isolated from nucleated erythrocytes. These structures are composed primarily of microtubules (Cohen et al., 1982, J. Cell Biol. 93:828-838). The technique consists of manipulating the isolated band with a glass micro-hook and looping it over the end of a thin glass fiber. The hoop is elongated by displacing the glass hook with a micromanipulator and stretching the band between the hook and the beam. The deflection of the hoop can be observed under the microscope. The magnitude of the force on the band is calculated from the deflection of the glass fiber. The fibers are calibrated according to the method of Evans et al. (Cell Biophys. 2:99-112, 1980). Measurement of deflections on the order of 1.0 μm allows us to resolve forces on the order of 10^{-6} dyn.

The force vs. deformation curves for the marginal bands are analyzed according to a method adapted from the analysis of Libai and Simmonds (Int. J. Nonlinear Mechanics 18:181-197, 1983). Preliminary measurements of the elastic modulus of marginal bands of the dogfish have been completed. These results indicate an elastic modulus for small deformations of approximately 3 x 10^8 dyn/cm^2, which is similar to the modulus of a soft plastic, e.g., low density polyethylene.

The authors wish to thank Dr. William Cohen, who provided the isolated marginal band samples for our measurements.

M-PM-E1   MONOCLONAL ANTIBODY BLOCKS THE POST BURST HYPERPOLARIZATION IN R15 AND BAG CELL NEURONS.
F. Strumwasser, D. P. Viele, and K. D. Lovely, Dept. of Physiology, Boston University School of Medicine, Boston, MA 02118 and Marine Biological Laboratory, Woods Hole, MA 02543.

We have generated monoclonal antibodies (MAbs) to neural and glial membranes in the mollusc <u>Aplysia</u> in the hope of finding MAbs that will recognize pacemaker neurons specifically. One strategy, in this study, is to concentrate on MAbs that are able to interfere with pacemaker function in some specific way. Once such MAbs are obtained they should help us identify and isolate the sets of proteins involved in pacemaker function. There are three pacemaker systems of particular interest to us in <u>Aplysia</u>: 1) Relatively constant bursting pacemakers such as R15 in the abdominal ganglion (AG). 2) Transient pacemakers such as the peptidergic bag cells. 3) Circadian pacemakers such as in the eye. In the present study 70 MAbs were generated from three fusions involving mice, separately immunized to crude membranes of bag cells, abdominal ganglia (minus bag cells) and eyes. These MAbs have been screened against a variety of tissue membrane antigens using immunodots, fixed frozen sections of ganglia and eyes, primary cell cultures and by two physiological assays involving intracellular injection into R15 in the isolated AG and bag cells in primary culture. Our findings include: A MAb (2BC4) which on intracellular injection blocks the post-burst hyperpolarization in R15 and in bag cells. The MAb 2BC4 (Ascites fluid 1:1000 dilution) binds to 4 protein bands (major band at 38kd, minor bands at 43, 44, 50kd) extracted from the AG. A MAb (4AG4) which specifically recognizes glia in sections of ganglia and binds to a different set of protein bands than MAb 2BC4. A MAb (4AG11) which binds to the R3-8, R14 neurons in the AG. Neither MAbs 4AG4 or 4AG11 interfere with bursting pacemaker activity when injected intracellularly into R15.

M-PM-E2   LOCATION ON ALPHA MOTONEURONS OF SYNAPSES RESPONSIBLE FOR SPONTANEOUS IPSPs OCCURRING DURING ACTIVE SLEEP OR CARBACHOL-INDUCED ATONIA.   J.K. Engelhardt, F.R. Morales, P.J. Soja and M.H. Chase.   Depts. of Physiology and Anatomy and the Brain Research Institute, School of Medicine, University of California, Los Angeles, CA 90024.

Alpha motoneurons of behaving cats are bombarded by spontaneous inhibitory postsynaptic potentials (IPSPs) during the atonia of active sleep (Morales and Chase, <u>Exp</u>. <u>Neurol</u>. 78:471, 1982). We have recently observed that carbachol, microinjected into the pontine reticular formation of acute decerebrate cats, also markedly increases IPSP frequency in alpha motoneurons. These discrete IPSPs were detected and analyzed by a microcomputer from digitized intracellular records. IPSPs exhibited large variability in their amplitude and rise-time with a positive correlation between amplitude and rise-time (i.e., larger amplitude IPSPs had longer rise-times). In both the chronic behaving and the acute decerebrate preparations, injections of either polarizing current or chloride ions altered the amplitude of the larger-amplitude, longer-rise-time IPSPs more readily than that of the smaller-amplitude, shorter-rise-time IPSPs. These observations support the following conclusions: (1) the larger-amplitude, longer-rise-time IPSPs are produced by synapses close to the recording electrode; and (2) the synapses responsible for both the carbachol-induced IPSPs and active sleep-dependent IPSPs appear to be widely distributed on the soma-dendritic tree of alpha motoneurons. The question then arises as to how proximally located synapses could produce IPSPs with longer rise-times than those produced by synapses located more distally. Supported by NSF grant 84-12308.

M-PM-E3   Computer Simulation of the Effects of the Corpus Callosum, P. Anninos and N.D. Cook

Based upon the "neural net" simulation model, developed by Anninos and colleagues (Kybernetik 11,5,1972; Biol. Cyber. 36,187, 1980; etc.), a related simulation has been undertaken in which the effects of an associational tract between two neural nets have been studied. The neurons within each neural net are randomly interconnected and such nets have previously been shown to exhibit alpha rhythm-like cycles, epileptiform-like activity and hysteresis. Two such nets, representing small patches of cortex in the left and right cerebral hemispheres, were connected via an associational tract, the corpus callosum, and the inhibitory/excitatory and homotopic/heterotopic nature of this tract was specified prior to simulation. The effects of these physiological and anatomical parameters on the spontaneous cyclic activity of the two nets was then examined. In contrast to a previous simulation in which the two "hemispheres" were randomly interconnected,(Biol. Cyber. 50, 1984), the degree of point-to-point, mirror-image homotopicity was specified and found to have effects on subsequent net activity. These effects were studied in relation to the "homotopic callosal inhibition" hypothesis (Brain & Language 23, 116, 1984).

The results of the simulation were analyzed in terms of the "learning" capabilities of each hemisphere, i.e., the time required to acquire cyclic activity, and in terms of power spectral symmetries (using autoregressive model fitting) and the spectral coherence between the two "cerebral hemispheres".

M-PM-E4 NEURONAL CIRCUITRY IN THE TURTLE RETINA. Leo E. Lipetz, Dept. of Zoology and Institute for Research in Vision, The Ohio State University, Columbus, Ohio 43212.

New data on the visual pigments and oil droplets in the retinal photoreceptors of freshwater turtles (Biol. Bull. 163:396) reveal that there are one rod and six cone types. The rod is green-sensitive (g). The double cone consists of a red-sensitive (r) chief cone (O-cone)with an orange droplet and a dropletless (r) accessory cone (A-cone). Single cones in order of decreasing size are: red droplet R-cone (r); yellow droplet Y-cone (g); large clear droplet C-cone, blue-sensitive (b); and small clear droplet N-cone (r).

This data allows interpretation of published studies of responses (esp. spectral) of photoreceptors and horizontal cells (HCs) in the turtle retina, leading to a model of their circuitry. The model describes flows of graded potential signals and specifies polarity, spectral sensitivity, and transmission delays of each (in press, 1984), "Human Visual Function", Vol. 1, Alan R. Liss).

The model predicts both the receptive field organization and the spectral sensitivities of an as yet unmeasured HC, the H4 of Leeper (1978a). For the linear response range the model gives a close fit to the measured spectral sensitivity curves of the HCs by a calculation based on: (1) signal flow paths of the model, (2) calculated spectral sensitivities of the photoreceptors, (3) the assumption that the HC feedback subtracts linearly from the cone's output at each cone, and (4) assumed relative weighting factors for the amplitude of each cone's output versus the HC feedback for that cone.

The model provides a neuronal basis for edge discrimination and spectral (color) discrimination. The model provides a basis for tetrachromatic vision in freshwater turtles.

M-PM-E5 DYNAMIC ELECTROTONIC COUPLING IN MAMMALIAN INFERIOR OLIVE AS DETERMINED BY SIMULTANEOUS MULTIPLE PURKINJE CELL RECORDING. K. Sasaki and R. Llinás, Dept. Physiol. & Biophys., New York Univ. Med. Ctr., 550 First Ave., New York 10016.

Simultaneous extracellular recordings from 32 Purkinje cells (PCs) in Crus IIA of the cerebellar cortex of pentobarbitalized rat were implemented using an improvement of the technique of Bower & Llinás (Soc. Neurosci. Abst., 1983). The 200 μm spacing between electrodes demarcated a rectangular matrix 800 x 1600 μm. Degree of electrotonic coupling between neurons of origin of the climbing fiber (CF) in the inferior olive (I.O.) was indirectly determined by the degree of cross-correlation of PC complex spikes. Although the spontaneous 10/s oscillation of CF responses was poor in this lobule before injection of the alkaloid, harmaline, spontaneous CF firing did occur in a synchronous manner over the lobule. Trigeminal tactile stimulation produced responses in 3 bands with 200-400 μm in the mediolateral direction and 800 μm rostro-caudally, separated from each other by a "corridor" of nonresponsive bands of 400 x 800 μm. Following harmaline injection, the oscillatory property of I.O. neurons (8-10 Hz) became obvious and prominent oscillation was found in the activity of CFs through the tactile responsive bands. Cross-correlograms revealed that the degree of coupling was most prominent with each of the trigeminal bands, but was also present between cells in the corridor. Injection of both harmaline and picrotoxin produced total correlation between band and corridor cells and the tactile stimulation elicited responses even in the previously nonresponsive corridor. Results suggest that the patterns of electrical coupling are governed by a GABAergic inhibitory decoupling of neurons otherwise coupled in a close to isotropic manner over the I.O. nucleus. (Grant NS13742)

M-PM-E6 EFFECT OF MET ENKEPHALIN ON A PROTOZOON'S LIGHT AVOIDANCE. J. K. Randolph, Physics Department, University of Tulsa, Tulsa, Ok. 74104 (Intr. by H. J. Harmon).

The effect of met enkephalin on the light avoiding reaction of the protozoon, Stentor Coeruleus, has been studied further.[1] The avoiding reaction is a stop in swimming. This is usually followed by swimming to the side or backwards. The stop is known to involve a (graded) action potential with Ca^{2+}, K^+ and perhaps Cl^- currents.[2]

The probability of avoidance was measured from stops in swimming produced by flashes of a filtered strobe light. (Attempts to directly measure the action potential in stationary protozoa gave a highly variable, small receptor potential.) With the brief strobe flash, ambiguous responses were only 6% and were excluded. Unexposed protozoa from the same culture were used as controls in a double blind procedure. Results from 1800 flashes are expressed in terms of Δ, the difference in avoidance probabilities (positive corresponds to enhancement).

Concentration	Control Probability	Δ	Standard Error of Mean
0.2 μM	.76	+.122	.100
0.6 μM	.75	+.037	.075
2.0 μM	.78	-.123	.045
6.0 μM	.75	+.025	.045

(Supported in part by the Research Office of The University of Tulsa.)
1. J. K. Randolph, Biophys. J. 45, 396A (1984).
2. D. C. Wood, J. Comp. Physiol. 146, 537-550 (1982).

M-PM-E7   ELECTRICAL RESPONSE OF PARTIALLY PURIFIED OPIOID RECEPTOR.
John W. Smuda and Robert de Levie, Department of Chemistry,
Georgetown University, Washington D.C. 20057.

The existence of specific receptors for opium-related drugs in the vertebrate
central nervous system was established by Pert & Snyder (Science 179 (1973) 1011;
P.N.A.S. 70 (1973) 2243). Shortly afterwards, Hughes discovered the endogenous neuro-
transmittorsto which they respond (Brain Res. 88 (1975) 295) and elucidated their
structures (Nature 258 (1975) 577). There is now a body of evidence in the literature
that these opioid receptors can affect synaptic neurotransmittor release as well as
transmembrane fluxes of calcium and potassium. We here report direct evidence for
ionic membrane conduction caused by opioid receptors.

Ion exchange chromatography of a crude mitochondrial fraction of bovine brain
yielded a sample enriched in opioid receptors as assayed by ^{3}H-naloxone binding. This
fraction, when introduced into a Takagi-Montal lipid bilayer membrane, elicits a
stereospecific, agonist-dependent and antagonist-blocked electrical conductance.

M-PM-E8   CHARACTERIZATION OF MULTIPLE OPIOID RECEPTORS AND PEPTIDES IN RAT AND GUINEA PIG
SUBSTANTIA NIGRA. M.E. Lewis, M.S. Lewis*, R.M. Dores, J.W. Lewis, H. Khachaturian,
S.J. Watson and H. Akil. Mental Health Research Institute, University of Michigan, Ann Arbor,
MI. 48109 and *BEIB, DRS, National Institutes of Health, Bethesda, MD. 20205.

Although the existence of multiple subtypes of opioid receptors is well established, the rela-
tionship of these receptors to opioid neuronal systems remains unclear. We therefore characterized
opioid receptor subtypes and molecular forms of the opioid peptide, dynorphin A, in substantia
nigra (SN), the terminal area of a dynorphin pathway originating in striatum. Saturation analyses
of mu, delta, and kappa opioid binding sites (labelled, respectively, with ^{3}H-DAGO, ^{3}H-DSLET, and
^{3}H-bremazocine in the presence of 100 nM DAGO and DTLET) were carried out on membrane fractions
from rat and guinea pig (GP) SN. Data were analyzed by nonlinear least-squares curve fitting,
using MLAB on a DEC-10 computer to fit one- or two-site models. Using a one-site model, the number
and affinities of mu and delta sites were comparable between species, but the number of kappa sites
appeared three-fold higher in GP than rat SN. However, the GP kappa saturation data alone were
poorly fit using the one-site model. Instead, these data showed an excellent fit to the two-site
model, and the values of the fitting parameters showed that rat and GP have comparable numbers of
high affinity kappa sites in SN, but that GP has an additional large population of low affinity
kappa sites. Radioimmunoassay of acid extracts of rat and GP SN indicated that the conversion of
dynorphin A(1-17) to the lower affinity, less kappa-selective form, dynorphin A(1-8), is more
complete in rat than GP SN. The possible existence of a functional relationship between processing
of peptides and the characteristics of peptide receptors requires further study.

M-PM-E9   IMPROVED ESTIMATE OF SUB-MEMBRANE CA2+ CONCENTRATION FOLLOWING EXCITATION IN NERVE
CELLS. Enrico Nasi and Douglas Tillotson. Department of Physiology, Boston University
School of Medicine, Boston, MA 02118.

Careful examination of the Arsenazo III-Ca^{2+} absorbance change signal associated with a voltage
clamp pulse in a nerve cell body reveals a distinct time lag between the end of the pulse and the
peak of the signal. We have performed a series of experiments to determine the factors which may
contribute to this delay (e.g. Ca^{2+} tail currents, Ca-AzIII reaction equilibration) and conclude
that local (i.e. near the plasma membrane) saturation of AzIII accounts for a significant part of
the observed phenomenon. In simplified form the notion here is that a sizable fraction of the
total Ca, which exists as an extremely steep spatial gradient at early times following entry, is
not "seen" by the AzIII in that cytoplasmic region. As the gradient relaxes, more of the total Ca
falls within the measurable range and hence the signal continues to rise. Only when the Ca^{2+}
concentration at all points is below the saturating level does the signal peak. At that time, the
Ca^{2+} concentration at the membrane is the saturating concentration.
The relationship between absorbance and free Ca^{2+} (and hence AzIII saturation) can be
empirically determined in vitro. After consideration of irreversible Ca^{2+} removal processes and
Ca-AzIII reaction equilibration we estimate that the sub-membrane Ca^{2+} associated with a 50 msec
voltage clamp step to +30 mV in an Aplysia R-15 neuron is likely to be in the range of 100-500 μM
approximately 20 msec following the termination of the pulse. Supported by NIH Grant NS11429.

M-PM-E10   DECLINE IN CALCIUM COOPERATIVITY AS THE BASIS OF FACILITATION AT THE SQUID GIANT SYNAPSE. E.F. Stanley, NINCDS, MBL, MA. (Intr. by H. Lecar).

Depolarization of the nerve terminal is known to be linked to transmitter release by an influx of Ca^{2+} ions. On the basis of a fourth power relation between external Ca^{2+} and release at the frog neuromuscular junction, it has been suggested that four Ca^{2+} ions cooperate to release each transmitter quantum (Dodge and Rahamimoff, 1967). In contrast, at the squid giant synapse, power functions of 1 to 3.5 have been reported, due, at least in part, to the technical difficulty imposed by a marked diffusion barrier from the bathing medium to the synapse itself. The use of a newly described arterial perfusion technique eliminates this barrier, reduces equilibration times from over an hour to less than 2 minutes and allows a detailed examination of this relation.

Stellate ganglia were perfused with artificial sea water containing 0.5 to 10 mM Ca^{2+} while stimulating the presynaptic giant axon and recording excitatory postsynaptic potentials (EPSPs) from the postsynaptic axon. At low stimulus frequencies (<0.3Hz) and low, non-saturating Ca^{2+} levels, the EPSP was found to be related to the external Ca^{2+} raised to a power of $3.9^{\pm}0.1$ (n=19). At higher frequencies there was a decline in the Ca^{2+} power: 10Hz, 2.3; 50Hz, 1.7; and 80Hz, 1.0. The results are consistant with a model of four Ca^{2+} binding sites on the quantal release site, all of which must be bound for release to occur. Facilitation may be due to the slow dissociation of the bound Ca^{2+}: at stimulus frequencies above 0.3Hz, the Ca^{2+} that remains bound to the release site after one impulse reduces the number of additional Ca^{2+} ions that need bind during a subsequent impulse to activate the transmitter release site. Thus, maximum facilitation occurred at a stimulus frequency of 80Hz, when three sites were saturated.

M-PM-E11   A 3-DIMENSIONAL CALCIUM DIFFUSION MODEL SIMULATES PHASIC TRANSMITTER RELEASE, FACILITATION, AND RELEASE DEPENDENCE ON CALCIUM CURRENT. <u>Aaron L. Fogelson and Robert S. Zucker.</u> Depts. of Mathematics and Physiology-Anatomy, Univ. of Calif., Berkeley, CA 94720.

Transmitter release is triggered by calcium ions entering the presynaptic terminal during an action potential. A 1-dimensional model with uniform calcium influx across the membrane and radial diffusion can account for release and facilitation elicited by one spike. However, such a model predicts too great a post-tetanic accumulation of submembrane calcium, failing to preserve the time course of transmitter release (Zucker, Biophys. J. 45:264a, 1984).

We have developed a new model of presynaptic calcium movements at frog neuromuscular junction and squid giant synapse. Calcium enters through discrete channels, diffuses with binding away from channel mouths in 3 dimensions into a closed terminal, and is extruded at the surface. The location of calcium channels and transmitter release sites was based on anatomical observations. We assumed a power-law relation between calcium at release sites and transmitter release. We obtained an exact analytic solution which was evaluated numerically.

Confining calcium entry to discrete domains leads to larger calcium peaks near points of entry, sharper spatial gradients, and more rapid diffusion of calcium than in a 1-dimensional model. Channels are spaced sufficiently closely that residual calcium accumulates at release sites during a tetanus and decays slowly afterwards. Transmitter release grows during a tetanus, and post-tetanic as well as post-spike facilitation decline with magnitudes and time constants similar to those observed experimentally. Furthermore, the decline of phasic transmitter release is similar following spikes early and late in the tetanus.

This model also predicts the relationship between presynaptic calcium current and transmitter release for variable depolarizations. We found that calcium-release stoichiometries of 4-6 yield release vs. current power relations of about 3, as observed experimentally. We also found that large depolarizations will evoke more release for a given total calcium current, due to the greater overlap of calcium domains surrounding more closely apposed open channels.

M-PM-E12   PRESYNAPTIC DEPOLARIZATION DOES NOT APPEAR TO EVOKE TRANSMITTER RELEASE DIRECTLY AT CRAYFISH MOTOR NERVE TERMINALS. <u>Luca Landó and Robert S. Zucker.</u> Dept. of Physiology-Anatomy, Univ. of Calif., Berkeley, CA 94720.

It is generally believed that presynaptic depolarization evokes transmitter release by admitting Ca through voltage-dependent channels, and the Ca accelerates the rate of exocytosis. Recently, Dudel et al. (Pflügers Arch. 399:1, 1983) have proposed that presynaptic depolarization acts directly, in concert with elevated intracellular Ca, to evoke transmitter release. This conclusion was based in part on the result that a small depolarization of the terminals evoked much more release when it followed a brief tetanus than if presented alone. When we replicated this experiment, we found that the pulse, which was subthreshold in isolation, elicited a spike after the train. The hugh post-tetanic facilitation was blocked in tetrodotoxin, when a train of depolarizing pulses was substituted for action potentials. Other results suggesting that presynaptic potential directly evokes release are also subject to alternative interpretations.

We further tested the hypothesis of voltage-dependent release with two experiments. In the first, hyperosmotic suscrose solutions were used to elevate MEJP frequency, probably by raising presynaptic Ca. Terminals were depolarized by exposure to high (25 mM) K. Ca was omitted, and EGTA added, to all solutions to prevent Ca influx through Ca channels. K did not increase transmitter release, as it does in a normal Ca medium or as predicted if depolarization directly accelerates release. Rather, depolarization reduced MEJP frequency, probably due to Ca efflux through Ca channels opened by depolarization.

In the second experiment, we used CCCP to uncouple mitochondrial oxidative phosphorylation from electron transport and release mitochondrial Ca. We used an external suction electrode on a motor nerve branch to depolarize presynaptic terminals. Spikes were blocked with tetrodotoxin, and a 2 ms pulse adjusted until EJPs were recorded from an adjacent muscle fiber. When EGTA was substituted for Ca, transmission was blocked. Addition of 10 μM CCCP accelerated MEJP frequency 100 fold. Still, depolarization of nerve terminals failed to evoke phasic transmitter release. Thus, results of both experiments were inconsistent with a direct effect of presynaptic potential on neurosecretion.

M-PM-F1 PHOTOLABELING OF THE PHENOTHIAZINE RECEPTOR OF THE Ca^{2+}-INDUCED Ca^{2+} RELEASE CHANNEL FROM CARDIAC SARCOPLASMIC RETICULUM WITH [^{3}H]TRIFLUOPERAZINE. Kevin P. Campbell, Molly Strom and Craig Davidson, Dept. of Physiology and Biophysics, The University of Iowa, Iowa City, IA 52242.

A variety of compounds such as ryanodine, ruthenium red and phenothiazines have been demonstrated to inhibit the Ca^{2+}-induced Ca^{2+} release from cardiac sarcoplasmic reticulum vesicles (Chamberlain et al.J. Biol. Chem. 259, 7547-7553, 1984). We have used direct photolabeling with [^{3}H]trifluoperazine in an attempt to identify the phenothiazine receptor of the Ca^{2+}-induced Ca^{2+} channel in isolated cardiac sarcoplasmic reticulum vesicles. High intensity UV irradiation of these vesicles in the presence of 0.05 - 1.0 uM [^{3}H]trifluoperazine resulted in the specific covalent labeling of one major component with apparent molecular weight 82,000 Da and one minor component of 55,000 Da. The minor [^{3}H]trifluoperazine labeled protein was identified as cardiac calsequestrin, and purified cardiac calsequestrin was also shown to be photolabeled with [^{3}H]trifluoperazine. The 82,000 Da [^{3}H]trifluoperazine labeled protein was found to be concentrated in a ryanodine-sensitive fraction of cardiac sarcoplasmic reticulum which is enriched with Ca^{2+}-induced Ca^{2+} release and absent from ryanodine-insensitive vesicles which lack Ca^{2+}-induced Ca^{2+} release. Endo H digests of [^{3}H]trifluoperazine labeled membranes have shown that the 82,000 Da protein is a glycoprotein. Finally, 2 mM procaine, another inhibitor of Ca^{2+}-induced Ca^{2+} release, was shown to reduce the incorporation of [^{3}H]trifluoperazine into the 82,000 Da protein by 65% thus supporting our current hypothesis that the 82,000 Da glycoprotein is the phenothiazine receptor of the Ca^{2+}-induced Ca^{2+} release channel in cardiac sarcoplasmic reticulum. (Supported by NIH (NS 18814) and AHA)

M-PM-F2 RAPID FLOW CHEMICAL QUENCH STUDIES OF CA^{2+} RELEASE FROM SARCOPLASMIC RETICULUM IN VITRO Noriaki Ikemoto and Bozena Antoniu Dept. Muscle Res., Boston Biomed. Res. Inst.; and Dept. Neurol., Harvard Med. Sch., Boston, Mass. 02114

Some aspects of Ca^{2+} release, such as dependence on the EGTA-buffered extravesicular Ca^{2+} ($[Ca_0^{2+}]$) and high [ATP], which were difficult by spectroscopical measurements with Ca^{2+} indicators, are now possible with a chemical quench technique. Both the Ca^{2+} uptake and Ca^{2+} release reactions were quenched instanteneously by addition of a mixture of 10 mM EGTA and 5 uM ruthenium red. The time courses of rapid $^{45}Ca^{2+}$ release induced by chemical depolarization (replacement of 0.15 M K gluconate with 0.15 M choline Cl) or addition of Ca^{2+} and caffeine were investigated with a multi-mixing chemical quench apparatus (Froehlich and Berger model CQF-105). Studies at various $[Ca_0^{2+}]$ have revealed two components of depolarization-induced Ca^{2+} release. In agreement with the previous report (E.W. Stephenson, Biophys. J. 45, 400a, 1984), one is virtually independent of $[Ca_0^{2+}]$ in the range of 0-0.1 mM; the other is activated upon increase of $[Ca_0^{2+}]$ from 0.5 to 4.0 uM and inactivated upon further increase of $[Ca_0^{2+}]$ in a similar fashion to $(Ca^{2+}+caffeine)$-induced Ca^{2+} release. In the presence of several mM ATP or AMPPNP, the rate constant of $(Ca^{2+}+caffeine)$-induced Ca^{2+} release but not of depolarization-induced Ca^{2+} release increased considerably, the rate constants of both types of Ca^{2+} release being of the same order of magnitude (40-140 s^{-1}). These results suggest that both types of Ca^{2+} release have some steps in common, though they are distinguishable in terms of the triggering mechanism. Supported by grants from NIH (AM 16922) and MDA.

M-PM-F3 CALMODULIN-DEPENDENT PHOSPHORYLATION AND DEPHOSPHORYLATION REGULATE SARCOPLASMIC RETICULUM (SR) CALCIUM RELEASE. Do Han Kim and Noriaki Ikemoto. Dept. of Muscle Res., Boston Biomed. Res. Inst.; Dept. of Neurol., Harvard Med. School, Boston, MA 02114

The possibility that phosphorylation of SR components (e.g. 60K dalton protein) by calmodulin (CaM)-dependent protein kinase might be involved in the regulation of Ca^{2+} release has been suggested (e.g. Campbell and MacLennan, J.B.C., 257,1238-1246, 1982) from indirect evidence. Several proteins (Mr= 100K, 60K, 45K and 32K) were phosphorylated by the addition of 0.5 mM [r-^{32}P] ATP to the SR vesicles loaded with 5 mM Ca^{2+}. Phosphorylation of the 60K dalton protein, but not the others, was increased considerably by 1 uM CaM. The maximal degree of phosphorylation was reached within 3 min in the absence of CaM compared with within 30 sec in the presence of CaM. Efflux of passively loaded $^{45}Ca^{2+}$ was measured by the dilution of the loaded SR with 2 uM Ca^{2+} with or without phosphorylation. The amount of Ca^{2+} release decreased in parallel with the increased extent of phosphorylation of the 60K dalton protein by CaM. Inhibition of Ca^{2+} release was reversed by dephosphorylation with phosphatase. Depletion of ATP with the glucose-hexokinase system did not abolish the phosphorylation effect on the inhibition of Ca^{2+} release indicating that the inhibition is not Ca^{2+} pump-mediated. CaM-inhibitors (e.g. TFP) reduced the extent of inhibition of Ca^{2+} release. These results suggest that the CaM-dependent phosphorylation and dephosphorylation of the SR protein (60K) is involved in the regulation of Ca^{2+} release. Supported by grants from NIH (AM16922) and MDA. D.H.K. was supported by an NIH postdoctoral fellowship.

M-PM-F4   MEMBRANE POTENTIAL MEASUREMENTS DURING ATP-DEPENDENT Ca^{2+} UPTAKE BY SARCOPLASMIC
RETICULUM VESICLES (SR) USING VOLTAGE-SENSITIVE DYES AND RADIOLABELLED LIPOPHILIC
IONS. Guy Salama, University of Pittsburgh, Department of Physiology, Pittsburgh, PA 15261.
    SR (0.2 to 1 mg prot./ml) isolated from rabbit white skeletal muscle were incubated for 10
min at 23°C in various media containing 5-10 uM dis-C_3-(5). With the dye in equilibrium
between the lipid and aqueous phases, Ca^{2+} then ATP were added to initiate Ca^{2+} transport.
Differential absorption changes of diS-C_3-(5) at 655 minus 685 nm avoided a specific absorption
changes of the suspension and indicated a transient membrane potential, positive inside: (1) Dye
absorption increased at 670 nm (membrane bound) vs 650 nm (free-dye) as previously shown for
positive potentials in chromaffin granules and red blood cell ghosts. 2) The kinetics of the
voltage-dependent signals was dependent on the membrane permeability of ions in the medium. (3)
Stimulation of rate and total Ca^{2+} uptake by SR similarly increased the diS-C_3-(5) response.
(4) In the presence of thiacyenate (25 mM), any existing potential differences should collapse,
and indeed Ca^{2+} uptake was normal whereas the diS-C_3-(5) response was abolished. To
calibrate and further validate the optical signals, membrane potential was measured under
identical conditions through the ionic distribution of [^{14}C] SCN$^-$, in and out of the vesicles
passively diffused accross the SR membrane with a half-time of 15 s. During Ca^{2+} uptake by SR,
^{14}(C)SCN concentration in the lumen of the SR increased with a time course similar to the
diS-C_3-(5) signals. The voltage calculated from the concentration of SCN$^-$ in and out of the
vesicles ranged from 30 to 70 mV at its peak value. Supported by NIH: NS 18590 and K04 NS 00909.

M-PM-F5   CALCIUM CHANNELS IN SARCOPLASMIC RETICULUM (SR) MEMBRANES. C.B. Orozco,B.A. Suarez-Isla,
J.P. Froehlich and P.F. Heller. LNS and LMA_2,NIA, NIH, Bethesda and Baltimore, MD.
    Several mechanisms have been proposed to explain Ca^{2+} release from SR (Endo,Physiol.Rev.57,1977).
One of them considers the presence of Ca^{2+} channels in the SR membrane. In agreement with this sugges
tion we have observed small conductance channels in fragmented SR from rabbit white skeletal muscle.
Single channel fluctuations were recorded with the patch-clamp technique(EPC-7,List Electronic,10
kHz). Gigaseals(10-20 GΩ)were obtained with the "double dip" method(Coronado & Latorre,Biophys.J.43,
1983;Suarez-Isla et al.,Biochem.22,1983)from suspensions of SR membrane fragments that had been ex-
tensively washed to reduce total [K$^+$] below 50 μM. Fluctuations of 1 pA were detected at +200 mV in
symmetrical solutions(in mM:200 $CaCl_2$,10 Hepes,1-2 SITS;pH 7.0;22-24 °C). The slope conductance was
5 pS for Ca^{2+} and was linear between +50 and +200 mV(positive inside pipet). The events appeared in
bursts and, at more positive potentials, 2 or more equal current levels were detected. The channels
remained up to several seconds in the open state(1-8 s)and showed rapid closures(5-50 ms)within a
burst. The current amplitude increased with [Ca^{2+}] and
in the presence of Ca^{2+} gradients, the extrapolated re-
versal potential was close to the calculated Ca^{2+} equi-
librium potential. In addition, Ba^{2+} could substitute
for Ca^{2+} as current carrier species (Fig.:100 mM $BaCl_2$,
+100 mV). Cd^{2+},La^{3+}(0.1-1 mM)and ryanodine(1 mM)blocked **1 pA**
the channel. These results indicate the presence of a   **1.0 s**
spontaneously active Ca^{2+} channel in skeletal SR that is   **0.1 s**   **$BaCl_2$**
modulated by voltage.
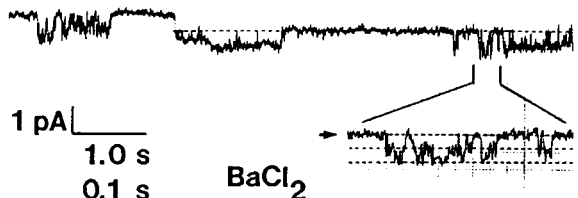
M-PM-F6   ISOLATION AND RECONSTITUTION OF THE CALCIUM RELEASE CHANNEL FROM THE
SKELETAL SARCOPLASMIC RETICULUM.   S. Tsuyoshi Ohnishi*, Kurumi Y. Horiuchi*,
Kazumi Horiuchi** and Emanuel Rubin**. *Dept. of Hematology/Oncology, and
**Dept. of Pathology and Laboratory Medicine, Hahnemann Universitty School of
Medicine, Phila. PA 19102
    Based upon kinetic studies, we have proposed that a gated calcium channel is
located in the heavy sarcoplasmic reticulum(HSR) (1 - 3). We have recently
succeeded in isolating such a channel from the HSR prepared from rabbit skeletal
muscle. The HSR was solubilized by cholate, and proteins were subsequently
fractionated by DEAE cellulose column chromatography. A fraction was collected in
which proteins with molecular weights of 31,000 and 41,000 were major components.
This fraction was incorporated into liposomes which had been loaded with Ca^{2+} and
tetramethyl murexide. Then, the liposomes were diluted with a Ca-EGTA buffer
solution (the Ca^{2+} concentration: 0.1 μM - 200 μM). The rate of Ca^{2+} efflux was
measured from the absorbance changes of tetramethyl murexide entrapped inside the
lumen (1). The efflux rate was small at both low and high Ca^{2+} concentrations,but
had a maximum at 3 μM Ca^{2+} concentration, suggesting that this protein fraction
has the characteristics of the gated calcium channel (1).
References: (1)The Mechanism of Gated Calcium Transport across Biological
Membranes(1981, Academic Press); (2)FEBS Letters 161:103(1983); (3)Archiv.
Biochim. Biophys.233:588(1984).   (Supported by NIH Grants AA05662 and GM30703)

M-PM-F7 THE DISORDERING OF SARCOPLASMIC RETICULUM MEMBRANE OF RAT SKELETAL
MUSCLE WITH CHRONIC ALCOHOL INGESTION. Alan J. Waring*($), S. Tsuyoshi
Ohnishi***, Kazumi Horiuchi**, Shyh-Rong G. Fang**, Tomoko Ohnishi* and Emanuel
Rubin**. *Dept. of Biochemistry and Biophysics, University of Pennsylvania,
Phila. PA, **Dept. of Pathology and Laboratory Medicine, ***Dept. of Biological
Chemistry, Hahnemann University School of Medicine, Phila. PA.

Using chronic alcoholic rats, we have studied the effects of chronic and acute
alcohol on the skeletal sarcoplasmic reticulum(SR). The calcium permeability (as
determined from the absorbance changes of entrapped indicator; 1) of alcoholic
rat SR was higher than that of normal rat SR. The membrane fluidity (as measured
by the order parameter of doxylstearic acid spin-probes) of alcoholic rat SR was
higher than that of normal rat SR. These observations suggest that chronic
alcohol ingestion disorderd the SR membrane, thereby causing a calcium leakage,
and subsequently a decrease in the calcium content of the SR. This may account
for the negative inotropism observed in alcoholism (2). The in vitro (acute)
addition of ethanol to the SR suspension increased both calcium permeability and
fluidity. However, increases of both quantities in alcoholic rat SR were smaller
than those in normal rat SR, suggesting that alcoholic rat SR has acquired some
kind of resistance against acute alcohol effects. (Supported by AA05662 & GM30703)
($)Present address:Dept. of Biochem. & Biophys, UCSF School of Medicine.
References:(1) Membrane Biochemistry(in press);(2) Amer.J.Pathol.83:499(1982)

M-PM-F8   CHRONIC AND ACUTE EFFECTS OF ETHANOL ON THE SARCOPLASMIC RETICULUM
MEMBRANE AS MEASURED BY THE FLUORESCENCE DEPOLARIZATION. Kazumi Horiuchi*,
S. Tsuyoshi Ohnishi** and Emanuel Rubin*. (Intr. by A.C. McLaughlin) *Dept. of
Pathology and Laboratory Medicine, and **Dept. of Hematology/Oncology, Hahnemann
University School of Medicine, Phila. PA.

Using the EPR spin-probe technique, it was demonstrated that chronic alcohol
ingestion disorders the membranes of mitochondria(1) and sarcoplasmic reticulum
(SR;2). We have studied the relationship between the Ca^{2+} permeability and the
membrane fluidity of the skeletal SR by measuring the fluorescence depolarization
of 1,6-Diphenyl-1,3,5-hexatriene (DPH). Kinoshita et al. demonstrated that this
technique is very useful to investigate not only the membrane lipid fluidity, but
also the conformational change of proteins as well as the interaction between
proteins and lipids(3). From the steady-state measurements, it was found that the
SR membrane of chronic alcohol rats was more disordered than that of normal rats.
This result is in good agreement with that of EPR measurement(2). However, in
contrast to EPR results, the fluorescence depolarization of DPH in alcoholic rat
SR increased in a greater degree than that of normal rat SR upon in vitro addition
of ethanol. It is possible that the EPR spin-probe technique and the fluorescence
depolarization technique measure slightly different physical properties.(Supported
by AA05662 and GM30703)   References:(1)Archiv. Biochem. Biophys. 216:51 (1982);
(2)Another abstract of ours in this meeting;(3)Biochim. Biophys. Acta 647:7(1981).

M-PM-F9   PROPERTIES OF TRANSVERSE TUBULE MEMBRANES ISOLATED FROM FROG MUSCLE. C. Hidalgo[a], P.
Donoso, J. L. Liberona, C. Parra, G. Riquelme and E. Jaimovich. Dept. Physiol. Biophys., Fac. Med.
U. of Chile, Santiago, Chile, and [a]Dept. of Muscle Res., Boston Biomed. Res. Inst. and Dept. of
Neurol., Harvard Med. Sch., Boston MA 02114.

Transverse tubule (T-tubule) membrane vesicles were isolated from frog skeletal muscle. 60-70%
of the vesicles were sealed with an inside-out orientation, as judged by the effect of detergents
on the activity of acetylcholinesterase, ouabain-sensitive Na^+-K^+-ATPase and ATP-dependent ouabain
binding. The T-tubules isolated from frog muscle have high contents of cholesterol and phospho-
lipid, with similar molar ratios of cholesterol to phospholipid and protein composition to those
described for T-tubules isolated from rabbit muscle (Rosemblatt et al. J. Biol. Chem. 256, 8140 -
1981). Only two ATPase activities were demonstrable in the T-tubule preparation: an ATPase that
utilizes either Ca-ATP or Mg-ATP as substrate, and the Na^+-K^+-ATPase.

The isolated T-tubules have a high density of nitrendipine binding sites (80-130 pmol/mg), with
a Kd of $1 \times 10^{-9}M$, and a low density of a single class of tetrodotoxin binding sites (4-6 pmol/mg)
with a Kd of $0.3 \times 10^{-9}M$.

Supported by NIH Grant HL23007 and by DIB Grant, U. of Chile, B912.

M-PM-F10   PURIFICATION AND CHARACTERIZATION OF CANINE CARDIAC PHOSPHOLAMBAN (PLB). Larry R. Jones, Heather K. Simmerman, Bill Wilson, and Adam D. Wegener. From the Krannert Institute of Cardiology and Indiana University School of Medicine, Indianapolis, Indiana 46202.

PLB, the putative protein regulator of the Ca pump of cardiac sarcoplasmic reticulum (SR), was purified from canine cardiac SR vesicles by selective extraction with sodium cholate, followed by adsorption to calcium oxalate, solubilization in Zwittergent-14, and sulfhydryl group affinity chromatography. PLB, isolated in the dephosphorylated state, was purified 80-fold in 15% yield ($\sim$ 2 mg PLB/g SR protein). The nondissociated holoprotein exhibited an apparent M_r=25,000 in SDS polyacrylamide gels. Five electrophoretic mobility forms of PLB were identified by SDS-PAGE and Coomassie blue staining when the protein was partially dissociated by boiling in SDS prior to electrophoresis. Complete dissociation of the oligomeric protein converted all mobility forms into a single low M_r mobility form, suggesting that native PLB is a pentamer of five identical monomers. In support of this, pure PLB was phosphorylated to a level of 189 nmol Pi/mg protein by catalytic subunit of cAMP-dependent protein kinase, consistent with a minimal M_r=5,300 for the monomeric subunits. Pure PLB was cysteine rich, containing 5.94 residues per 100 amino acid residues. Dephosphorylated PLB was strongly basic with a pI=10; phosphorylation decreased the pI to 6.7. Pure PLB (and PLB present in SR vesicles) was not readily extracted into acidified chloroform/methanol. Our results do not support the contention that cardiac PLB is an acidic proteolipid lacking cysteine, as has been reported previously by others. Reassessment of the functions and properties of cardiac PLB, and its relationship to the SR Ca pump, is currently in progress.

M-PM-F11   Immunolocalization of phospholamban in adult canine myocardium. A.O. Jorgensen[#] & L.R. Jones[*]. [#]Dept. of Anatomy, (Histology), University of Toronto, Toronto, Canada, M5S 1A8 and [*]Dept. of Med. & Pharm., Krannert Institute of Cardiology, Indianapolis, Indiana, 46202.

Phospholamban has been localized in cryostat and ultracryotomy sections of fixed canine ventricular muscle by immunofluorescence and immuno-colloidal gold labeling respectively. The specificity of the affinity purified rabbit antibodies to phospholamban was demonstrated by immunoblotting. When tested against boiled or untreated cardiac sarcoplasmic reticulum (SR) the antibodies bound to a single band of 11,000 dalton and 23,000 dalton corresponding to the electrophoretic motility of the monomeric and the oligomeric form of phospholamban respectively. The immunofluorescence studies showed that the myocardial cells were strongly and specifically labeled, while endothelial cells and fibroblasts as well as skeletal muscle fibers from rat gracilis muscle were labeled at the level of the background. Ultrastructural localization of phospholamban in canine ventricular muscle showed dense labeling over the SR while the sarcolemma, the transverse tubular and the mitochondrial membranes were labeled at the level of the background. Within the SR, the labeling was fairly evenly distributed in the network SR but absent from the region of the junctional SR which is closely apposed to either the sarcolemma or the transverse tubules. In conclusion, the results presented show that phospholamban is confined to the SR in myocardial cells where it like the Ca^{2+} + Mg^{2+} dependent ATPase is evenly distributed in the network SR. Although phospholamban was detected in cardiac sarcolemmal vesicle preparations by immunoblotting, the lack of immunocytochemical labeling of the cardiac sarcolemma with phospholamban antibodies renders it unlikely that phospholamban/calceduction is a component of the slow Ca^{2+} channel in the sarcolemma of intact myocardial tissue. Supported by [#]OHSF T.1-21 & [*] NIH grant 28556

M-PM-F12   PROTEOLYTIC ANALYSIS OF PHOSPHOLAMBAN (PLB) STRUCTURE - GENERATION OF A LOW RESOLUTION MODEL. Adam Wegener, Juris Liepnieks, Heather Simmerman and Larry Jones. From the Krannert Institute of Cardiology, IU School of Medicine, Indianapolis, IN 46202

Pure PLB, isolated from cardiac SR, was subjected to proteolysis after phosphorylation by different protein kinase (PK) activities. Trypsin, papain, chymotrypsin and elastase (in order of decreasing potency) each hydrolyzed only a small portion of the PLB molecule, comprising less than 15 amino acids per monomer and containing all of the phosphorylated residues. The proteolyzed PLB polymer was only slightly reduced in apparent M_r (21-23 kDa) from that of the 25-kDa nonproteolyzed protein. Boiling it in SDS prior to PAGE gave a homogeneous population of "clipped" monomers. Three hydrophilic tryptic phosphopeptides, not retained in SDS gels, were resolved by high voltage electrophoresis. cAMP-PK phosphorylated only serine in one peptide and Ca-calmodulin-PK phosphorylated threonine in another. PK-C phosphorylated these peptides, as well as a third unique peptide. The protease sensitive, phosphorylated region on PLB probably contained the major epitopes since polyclonal antibodies raised to intact PLB were nonreactive against proteolyzed PLB, even though the protease resistant domain contributed most of the protein mass. We propose that PLB consists of a hydrophobic, protease resistant domain and a smaller protease sensitive region, which contains all phosphorylated residues and is not required for association of PLB monomers. The protease sensitive region appears to possess a high positive charge density in the dephosphorylated state; native, dephospho-PLB has a pI=10, while the protease resistant domain has a pI around neutrality. Effective charge neutralization by phosphorylation may become relevant as the molecular structure and function of PLB are better defined.

M-PM-G1   THE PHOSPHATE BURST IN RABBIT SKINNED MUSCLE FIBRES.

M.A. Ferenczi, National Institute for Medical Research, Mill Hill, London NW7 1AA
Single muscle fibres or bundles of 2 to 4 fibres were studied by flash photolysis of tritiated caged-ATP (P^3-1-(2-nitro)phenylethyl-[2-^{3}H]adenosine 5'-triphosphate) followed by rapid freezing of the muscle fibre and analysis of the nucleotide contents by HPLC. Muscle fibres are held under isometric conditions and placed in a solution containing caged-ATP but no nucleotides. For fibres at a sarcomere length of 2.2-2.6 μm rigor tension develops, and the release of 1 mM ATP induced by photolysis of caged-ATP results in the fibres relaxing, or developing active contraction, depending on the absence, or presence of calcium respectively. In both cases two phases of ATP hydrolysis were measured: an initial rapid burst complete in 50 ms, followed by a much slower steady state rate. These two phases were also observed for fibres stretched to sarcomere lengths greater than 3.8 μm. By modifying the optical path of the pulse of laser light used for photolysing caged-ATP, the method described by Ferenczi, Homsher and Trentham (J. Physiol. 352, 575-599, 1984) was improved so that the time resolution of the measurement was increased ten-fold. The time course of the initial phases of ATP hydrolysis can now be resolved. The first results show that for fibres studied at 18°C, pH 7.1, I=200 mM in the absence of calcium ions ($<10^{-8}$M), the initial burst of ATP hydrolysis was 50% complete in about 35 ms.

M-PM-G2   OXYGEN EXCHANGE BETWEEN WATER AND MEDIUM P_i ACCOMPANIES ATP HYDROLYSIS IN
CA^{2+}-ACTIVATED, GLYCEROL-EXTRACTED RABBIT PSOAS FIBERS
M.R. Webb[*], M.G. Hibberd[+], Y.E. Goldman[+] and D.R. Trentham[*], National Institute
for Medical Research[*],Mill Hill, London NW7 1AA, U.K. and Department of Physio-
logy[+], University of Pennsylvania, Philadelphia, PA 19104, U.S.A.

Fibers, mounted between a force transducer and a rigid support, were immersed in a 35μl trough of activating solution including 15mM ATP and 10mM [$^{18}O_4$]P_i, pH 7.1, 22°C. After 2h, 20% of the ATP was hydrolyzed. The P_i was isolated, converted to triethyl phosphate and analyzed for ^{18}O by mass spectrometry. 2-3% of the [$^{18}O_4$]P_i had undergone oxygen exchange. P_i presumably binds to an ADP complex in the ATPase site and then condenses with the ADP to form protein-bound ATP, with con-comitant loss of one ^{18}O. If this ATP then is hydrolyzed, the product is [$^{18}O_3$]P_i. ∿50% of the exchanged P_i had lost more than one ^{18}O, indicating multiple reversals of the condensation-hydroly-sis step, with the value of the rate constant for the condensation approximately equal to that con-trolling P_i release. These experiments give a lower limit for the rate constant of P_i binding to the bound ADP state : 130 $M^{-1}s^{-1}$. This explanation of the oxygen exchange is consistent with the observations of Sleep and Hutton (Biochemistry (1980) 19, 1276-1283), that phosphate exchange occurs between medium P_i and ATP during ATP hydrolysis by actosubfragment 1. The bound ADP state formed during ATP hydrolysis differs from that obtained by adding ADP to the proteins or fiber, because the latter state is unable to bind P_i. Support: NIH grant HL 15835 and MRC, U.K.

M-PM-G3   CORRELATION BETWEEN CONTRACTILE FORCE AND STRUCTURAL CHANGES WITHIN THE S-2 REGION OF
MYOSIN IN GLYCERINATED MUSCLE FIBERS. Hitoshi Ueno and William F. Harrington. Department of
Biology, The Johns Hopkins Univ., Balto., MD 21218.
We have investigated the relationship between contractile force and structural changes in the LMM/HMM hinge domain of the S-2 region of myosin upon activation of glycerinated rabbit skeletal muscle. A quantitative enzyme-probe method (Ueno and Harrington, J. Mol. Biol. (1984) 173, 35-61) was employed to detect the structural changes. Activated glycerinated fibers (10-20 single fibers) were digested by chymotrypsin in various solutions (pH 7.3, μ = 0.10) in the presence of an ATP-regenerating system (5 mM creatine phosphate, 0.1 mg/ml CPK). The kinetics of proteolytic digestion and the sites of enzymatic cleavage in the polypeptide chains at various temperatures (5-37°C) were determined by following the time-course of fragmentation on SDS-gels. Cleavage rate constants were normalized at each temperature by comparison with the intrinsic hydrolysis rate of the enzyme for a model substrate. Four major cleavage sites in myosin were observed spanning the entire HMM/LMM hinge domain of about 20 nm as reported previously (Ueno and Harrington, PNAS (1981) 78, 6101-6105). The cleavage rate constant for activated muscle was two orders of magnitude higher than that observed for rigor or relaxed (rigor plus ADP-V_i) muscle. At each temperature, the rates of proteolytic cleavage increased sharply with increasing MgATP concentration and exhibited maxima at 0.2 mM (15°C), 0.3 mM (23°C) and 1.5 mM (35°C) [MgATP], respectively, above which the cleavage rate constants gradually decreased. The temperature-dependence of the (maximum) cleavage rate constants showed a good correlation with the isometric force vs. temperature curve as well as the rate constant vs. temperature profile of ATP cleavage in activated myofibrils. Thus there seems to be a close linkage between the force generation and a structural transition in the hinge domain.

M-PM-G4 THE STRUCTURE OF THE ACTIN-MYOSIN COMPLEX IN THE PRESENCE OF ATP. Roger Craig*, Lois E. Greene[+] and Evan Eisenberg[+]. *Anatomy Department, University of Massachusetts Medical School, Worcester, MA and [+]Laboratory of Cell Biology, NHLBI, NIH, Bethesda, MD. Intr. by P. Vibert.

The structure of the acto-S1 complex in the presence of ATP was examined by electron microscopy. This was accomplished using negative staining to study S1 which was covalently crosslinked to actin by the zero-length crosslinker, 1-ethyl-3-[3-(dimethylamino)propyl]-carbodiimide. Two levels of crosslinking were studied, with a molar ratio of crosslinked S1 to total actin of either 20% or 50%. In the absence of ATP, the appearances of both the 20% and 50% crosslinked filaments closely resembled the rigor appearances obtained using non-crosslinked proteins. The arrowheads observed (in the 50% preparations) had the conventional structure, and individual S1 molecules (in the 20% preparations) were elongated, curved and appeared to make an angle of ~45° with the thin filament. Addition of ATP to the crosslinked acto-S1 complex caused a radical change in the structure of the crossbridges. At both 10mM and 150mM ionic strengths, individual S1 molecules appeared to be attached at variable angles centered on ~90° and often appeared shorter and fatter than in rigor. The 50% crosslinked acto-S1 preparation appeared disordered with little obvious arrowhead polarity. Control experiments with ADP suggest that these effects were not due simply to a weakening of the binding of S1 to actin in the presence of nucleotide, but were most likely ATP-specific. The crosslinked acto-S1 complex, which hydrolyzes ATP at V_{max}, is composed of a mixture of A.M.ATP and A.M.ADP.P_i states, whose distribution changes with ionic strength. It therefore appears that these two states may bind to actin with a similar conformation, which in turn is very different from the classic arrowhead conformation of the A.M state.

M-PM-G5 THE THIN FILAMENT OF SKELETAL MUSCLE CO-OPERATIVELY ACTIVATES AS A UNIT.

Diamond MS, Brandt PW, Rutchik JS, and FH Schachat*, Department of Anatomy and Cell Biology, Columbia U. and *Department of Anatomy, Duke U.

Troponin C (TnC) is rapidly and specifically extracted from skinned single of rabbit psoas fibers exposed to 5 mM EDTA, 10 mM MOPS at pH 7.2, 30 C. The half time for extraction is between 4 and 8 minutes, depending on fiber diameter. The slope and maximum tension of the pCa/tension relationship diminishes with extraction and by 50% extraction, the Hill coeficient has fallen from about 6 to 2, the lowest value it assumes. The maximum calcium induced tension falls roughly in proportion to the loss of TnC. The pSubstrate/tension curve is relatively unaffected by extraction. Incubation of extracted fibers in pCa 8 relaxing media and 1.5 mg/ml of purified TnC restores both the tension and the slope of the pCa/tension curve to the normal range. Because replacement of the extracted TnC with purified TnC fully reverses the effect of extraction, TnC must be the only essential protein extracted and the only calcium binding protein responsible for the steep slope of the pCa/tension relation. We have determined that loss of as little as 5% of the TnC, ie. one troponin C per troponin-tropomyosin strand on a thin filament reduces the slope of the pCa/tension relation. We interpret this to mean that the regulatory units along a thin filament of rabbit psoas fibers are linked co-operatively so that a thin filament activates as a unit. The presence of extended co-operativity explains why the pCa/tension relation in skinned fibers has a slope much higher than predicted by binding of calcium to one regulatory unit (Brandt et al, 1980, 1982).

M-PM-G6 CRAYFISH TROPONIN C CAN SUBSTITUTE FOR THE ENDOGENOUS TROPONIN C OF SKINNED RABBIT SKELETAL MUSCLE FIBERS. P.E. Hoar[+], W. Wnuk[#], & W.G.L. Kerrick[+]; [+]Dept. of Physiology & Biophysics, Univ. of Miami, Miami, FL; [#]Dept. of Biochemistry, Univ. of Geneva, Geneva, Switzerland.

Crayfish troponin C (TnC) has one Ca^{2+} specific binding site believed to be responsible for the regulation of muscle contraction (Wnuk, W., Schoechlin, M., & Stein, E.A., J. Biol. Chem. 259:9017-9023, 1984). Endogenous TnC was extracted from skinned rabbit adductor (fast-twitch) fibers with a low ionic strength EDTA solution at 4°C (Cox, J.A. Conte, M., & Stein, E.A., Biochem. J. 195:205-211, 1981). In the presence of high Ca^{2+}, exogenous crayfish TnC restores Ca^{2+} sensitivity to the fibers. However, the fibers do not retain the incorporated crayfish TnC when they are removed from the TnC bathing solution, in contrast to the case with reincorporated rabbit skeletal or cardiac TnC. This is consistent with the hypothesis that the high affinity Ca/Mg sites are responsible for the attachment of rabbit TnC since these sites are missing in crayfish TnC. In contrast to rabbit skeletal TnC or calmodulin, which have no effect on the submaximal or maximal Ca^{2+} activation of control (non-extracted) skinned rabbit skeletal muscle fibers, crayfish TnC will cause these fibers to contract further. Moreover, crayfish TnC is similar to calmodulin in that it will further activate skinned smooth muscle cell bundles in submaximal or maximal Ca^{2+}, but differs from rabbit TnC which will not do so. In summary crayfish TnC is a Ca^{2+}-binding protein which can activate both skeletal and smooth muscle skinned cells in contrast to skeletal muscle TnC and calmodulin which can only activate skeletal or smooth muscle respectively. This is an interesting Ca^{2+}-binding protein which may provide further insight into the physiological importance of the various metal binding sites involved in muscle contraction. Supported by Amer. Heart Assn. & M.D.A.

M-PM-G7   THE EFFECT OF TROPOMYOSIN ON ACTO·S-1 ATPase ACTIVITY. David L. Williams, Jr. and Evan Eisenberg, NHLBI, NIH, Bethesda, MD 20205.

The steady-state kinetic properties of the actin-activated S1 ATPase activity were investigated with both the fully inhibited and fully potentiated actin-tropomyosin complex. Inhibition in the presence of tropomyosin occurs at very low S1 to actin ratios. Potentiation was achieved by adding large ratios of NEM-modified S1 to the normally inhibited system. This NEM S-1 exhibits a very low ATPase activity and is not dissociated from actin by ATP. As tropomyosin-actin is shifted from the inhibited to the potentiated state by increasing the amount of NEM-S1, the maximal ATPase rate, V_{max}, is increased about 4-fold; the actin concentration required to reach half-maximal activity, K_{ATPase}, is reduced about 12-fold; and the binding constant of S1 to actin in the presence of ATP, $K_{binding}$, appears to be strengthened about 2-fold. The small effect of tropomyosin on $K_{binding}$ compared to its large effect on K_{ATPase} means that with fully potentiated tropomyosin-actin there is a 15-fold difference between K_{ATPase} and $K_{binding}$. In addition, these data show that at low actin concentrations there can be up to a 48-fold difference in ATPase activity depending on whether the tropomyosin-actin complex is fully inhibited or potentiated. Since our previous work shows that tropomyosin may act like troponin-tropomyosin in the presence of Ca^{2+} (Williams and Greene (1983) Biochemistry 22, 2770), these results suggest that even after Ca^{2+} activation of muscle, the number of force-producing bridges present may modulate the force, velocity or ATP turnover rate exhibited by a muscle fiber.

M-PM-G8   EFFECT OF CA++ ON AMP-PNP BINDING TO SKELETAL MYOFIBRILS IN 50% ETHYLENE GLYCOL. Robert E. Johnson, Department of Biochemistry, University of Arizona, Tucson, AZ 85721

It has been shown by Marston and Tregear (1984, Biochem.J.,217,169-177) that the effect on myosin of substituting 50%(v/v) ethylene glycol for water is to weaken its affinity for actin by a factor of 100 without effecting its affinity for nucleotides. I have used a centrifuge method to measure the binding of nucleotides to rabbit back muscle myofibrils in both solvents at $0°C$. The affinity of Mg++ADP differs by less than a factor of two between solvents, but there is a dramatic increase in the binding of Mg++AMP-PNP in 50% ethylene glycol, reflecting its ability to dissociate actin and myosin under these conditions. Since the binding of Mg++AMP-PNP is directly coupled to dissociation, the apparent binding constant will reflect the strength of the actin-myosin interaction. I have found a 3-fold increase in the affinity of Mg++AMP-PNP for myofibrils in the absence of Ca++ compared to that in its presence. This correlates well with the 3-fold weakening of the regulated actin-S1 interaction seen by Williams and Greene (1983, Biochem.,22,2770-2774) with excess Mg++AMP-PNP. No evidence was found, however, of positive cooperativity of binding analogous to the cooperativity in S-1 binding seen by these authors in the absence of Ca++. Binding of Mg++AMP-PNP is more complex than Mg++ADP. There is clear evidence for either two classes of sites of equal size or negative cooperativity. This is especially clear cut in the absence of Ca++.
This work was supported by NSF Grant #PCM-8211794.

M-PM-G9   IS IT POSSIBLE FOR A SINGLE MODIFIER TO EXERT BOTH A POSITIVE AND A NEGATIVE EFFECT ON THE SKELETAL ACTOMYOSIN MgATPASE? S.M. Pemrick and P. Martinez, Dept. Biochemistry, SUNY Downstate Medical Center, Brooklyn NY 11203.

Yes, depending on the conditions. To explain the source of considerable controversy, we undertook a comparison of the modifying capabilities of Mg2+ at 2 extremes of ionic strength. At 55 mM, an apparent 2-3-fold activation was observed at low Mg2+, the absolute increase in rate was $2 s^{-1}$. Because MgATP was constant, as Mg2+ increased (20 μM to 1 mM), ATP free decreased (4 mM to 20 μM). When the [Mg2+] profiles of the actomyosin (AM) MgATPase were compared at 0.6,1,& 2 mM MgATP, the data could not be superimposed. The data were superimposable when replotted versus the [ATP free] proving that free ATP, a polyanion, was an activator at low salt. Kinetically, this translated into a 2-fold increase in Kapp (actin) and Vmax. At 95 mM, [Mg2+] had the opposite effect at Kapp. Since the basal rate was lower than at 55 mM activation by Mg2+ was 7-fold, but the absolute change was the same. A similar distinction between Mg2+ and ATP free existed in the data proving that free ATP could be a "-" modifier at high salt. Interestingly, between 71-75 mM, at Kapp, ATP free had no effect. Although in our laboratory, phosphorylation, the covalent attachment of a polyanion to L2 is usually a "+" modifier at low and high salt, we were able to generate a situation where at low salt, L2P was a "+" modifier, at high salt a "-" modifier, and without effect between 71-75 mM. We believe these results demonstrate a general kinetic effect of modifiers of the AM MgATPase, and explain the long controversy concerning the role of L2P. (Sup. by NIH grant HL22401).

M-PM-G10 THE MECHANISM OF REGULATION BY CARDIAC TROPONIN OF CARDIAC SUBFRAGMENT-1 ATPase ACTIVITY. Larry S. Tobacman and Robert S. Adelstein, Laboratory of Molecular Cardiology, NHLBI, NIH, Bethesda, MD 20205.

We have evaluated the effect of Ca^{2+} on the interaction of bovine cardiac S-1 with actin regulated by bovine cardiac troponin-tropomyosin. At low S-1: actin ratios and ionic strength 15 mM, chelation of Ca^{2+} with EGTA increases the acto-S-1 K_D in the presence of ATP from 15 μM to 36 μM. Therefore, in the absence of Ca^{2+}, cardiac troponin-tropomyosin weakens acto-S-1 binding but does not cause the cessation of binding predicted by the steric blocking model of muscle contraction. On the other hand, the same regulatory proteins have a profound effect on the steady-state acto-S-1 ATPase rate at saturating actin concentrations. The extrapolated values for V_{max} are 6.8 s^{-1} in the presence of Ca^{2+} and 0.41 s^{-1} in the absence of Ca^{2+}. Half saturation of the ATPase rates occurs at 12 μM actin in the presence of Ca^{2+} and 26 μM actin in the absence of Ca^{2+}. These results are similar to those previously reported with fast skeletal acto-S-1 regulated by fast skeletal troponin-tropomyosin (Chalovich, J.M. et al., J. Biol. Chem. 256: 575-578, 1981). They suggest that in the heart, as well as in skeletal muscle, troponin cannot inhibit cross-bridge binding sufficiently to explain muscle relaxation in the absence of Ca^{2+}. Rather, relaxation must also depend upon marked inhibition of other parts of the cross-bridge cycle, evidenced here by 94% inhibition of the acto-S-1 ATPase rate. We are also studying the effect of troponin I phosphorylation on acto-S-1.

M-PM-G11 THE EFFECT OF MYOSIN PHOSPHORYLATION ON THE CONTRACTION OF GLYCERINATED MUSCLE FIBERS. R. Cooke, K. Franks, and J.T. Stull. (Introd. by A. Waring) Dept. of Biochemistry and Biophysics, and the CVRI, University of California, San Francisco, CA 94143 and Dept. of Pharmacology, University of Texas, Dallas, TX 75235.

Rabbit psoas muscle was glycerinated in conditions that produced high levels of myosin phosphorylation (80%), or low levels (5-10%). In agreement with our previous work the ATPase activities of the phosphorylated fibers (0.77 s^{-1}) were approximately one half those of unphosphorylated fibers (1.3 s^{-1}) when assayed in 4 mM ATP at 35 C. The recent work of Barsotti and Butler (J. Mus. Res. Cell Mot. 1984), showing no correlation between myosin phosphorylation and ATPase activity in living fibers prompted a reinvestigation of this effect. To determine whether the decreased activity of phosphorylated fibers was due to phosphorylation or to other causes we used a phosphatase to remove the phosphate on the myosin. As measured by IEF gel electrophoresis the phosphatase reduced myosin phosphorylation levels to 5-15% with no other bands changing position, and the ATPase activity of the dephosphorylated fibers returned to 1.4 s^{-1}, close to control values. Thus the modulation of ATPase activity observed previously appears to be due to myosin phosphorylation. Measurements of the mechanics of fiber contraction suggest that the effect of phosphorylation on cross-bridge cycling occurs only when ATP regenerating systems are absent, as was the case in the measurement of ATPase activities. In the absence of a regenerating system the conditions inside the fiber resemble those seen during fatigue with levels of ATP depressed and levels of ADP and other metabolites elevated. Supported by grants from the USPHS AM32145 to RC and HL23990 to JTS.

M-PM-G12 THE EFFECT OF MYOSIN PHOSPHORYLATION ON THE CONTRACTILE PROPERTIES OF SKINNED SKELETAL MUSCLE FIBERS. A. Persechini, J.T. Stull, and R. Cooke. Dept. Pharmacol., Univ. Tx. Hlth. Sci. Ctr., Dallas, TX 75235, and Dept. Biochem./Biophys., Univ. Calif., San Francisco, CA 94143

We have studied the effect of myosin P-light chain phosphorylation on the isometric tension generated by skinned fibers from rabbit psoas muscle in the presence of an ATP-regenerating system at 0.6 μM or 10 μM Ca^{2+}. At the lower Ca^{2+} concentration, addition of purified calmodulin·myosin light chain kinase resulted in a 50% increase in isometric tension and an increase in P-light chain phosphorylation from 0.10 to 0.80 mol phosphate/mol P-light chain. Addition of phosphoprotein phosphatase C dephosphorylated P-light chain and reversed the isometric tension response. At 10 μM Ca^{2+}, P-light chain phosphorylation had little effect on isometric tension. Fibers stored in MgATP, KF, and potassium phosphate had 0.80 mol phosphate/mol P-light chain. At 0.6 μM Ca^{2+}, addition of phosphoprotein phosphatase C caused dephosphorylation of P-light chain and a reduction in isometric tension. The normalized force-velocity relationship for fibers showed no differences before and after phosphorylation of P-light chain. The extrapolated maximum shortening velocity was 2.2 fiber lengths/sec. Phosphorylation of heavy meromyosin caused a reduction in the apparent K_m for actin from 90 to 60 μM with no effect on V_{max} (22 sec^{-1} per myosin head). Thus, the maximum cross bridge cycling rate, either in situ or in vitro, does not change with phosphorylation. Our results suggest that in vertebrate skeletal muscle, P-light chain phosphorylation increases the level of activation at submaximal Ca^{2+} concentrations, perhaps by affecting the interaction between the myosin cross bridge and the thin filament. (Supported by HL23990, HL06296 and HL32145)

M-PM-H1   PATCH CLAMP DATA ANALYSIS: A NEW AND RAPID METHOD TO DETERMINE PORE KINETICS
WITHOUT MEASURING THE OPEN AND CLOSED TIMES.
Larry S. Liebovitch, Jorge Fischbarg, Julio A. Hernandez, and Jan P. Koniarek
Depts. Ophthalmology and Physiology, Columbia University, N.Y.

Consider a pore: closed $\underset{k_c}{\overset{k_o}{\rightleftharpoons}}$ open. The current $F(t)$ through such a pore can be measured by
the patch clamp technique. The distribution of open times is $P_o = k_o \exp(-k_o t)$ and closed times is
$P_c(t) = k_o \exp(-k_o t)$. Thus, frequency histograms of the open and closed times can be used to
determine the pore kinetics. However, because of noise, frequency response, and amplifier drift,
either manual or semi-automatic measurements of open and closed times are difficult and time
consuming. We present another, equally accurate, method to determine k_o and k_c that can be
50 times faster. Let $f(t) = F(t) - \langle F(t) \rangle$, where $\langle \rangle$ is the time average. In analogy to photon
correlation functions, let $g_1(\mathcal{T}) = \langle f(t) f(t+\mathcal{T}) \rangle / \langle f^2(t) \rangle$ and $g_2(\mathcal{T}) = \langle f^2(t) f^2(t+\mathcal{T}) \rangle / \langle f^2(t) \rangle^2$.
It is known that $g_1(\mathcal{T}) = \exp(-k\mathcal{T})$, and we were able to prove that $g_2(\mathcal{T}) = 1 + [(1-B)^2/B] \exp(-k\mathcal{T})$
where $k = k_o + k_c$ and $B = k_c/k_o$. Thus, the evaluation of these two functions, which requires
calculating only simple numerical integrals, can be used to solve for k_o and k_c. We tested
this procedure using both simulated and actual experimental data. It worked very satisfactorily,
as evidenced by the rapid and accurate determination of k_o and k_c.

M-PM-H2   VOLTAGE FLUCTUATIONS IN UNCLAMPED OR CURRENT-CLAMPED EXCITABLE CELLS. Izchak Z. Steinberg,
Chemical Physics Department, Weizmann Institute of Science, Rehovot 76100, Israel.
Fluctuations in the gating of channels in excitable cell membranes are usually considered under
voltage-clamp conditions. However, it may sometimes be advantageous to study voltage fluctuations in
unclamped or current-clamped cells or membranes patches. Moreover, voltage fluctuations in the unc-
lamped state are probably more directly relevant to excitable cells under physiological conditions
than current fluctuations under voltage-clamping. The statistical treatment of voltage fluctuations
in unclamped cells is complicated by the fact that the probabilities of opening and closing of a
given channel are not independent of the states of the other channels in the membrane. This is so
because the rates of opening and closing of the gates are a function of the membrane potential,
which depends on the number of channels already in the open state. A theoretical approach has been
developed for the statistical characterization of the noise properties of cells which contain such
interdependent channels in their membranes. We express, by appropriate differential equations, the
behavior of a large ensemble of cells, each of which has the same number and kind of channels on its
surface. By solving these differential equations, subject to prescribed initial conditions, one
obtains the whole spectrum of probabilities for a given cell, which has started out with a certain
membrane potential, to reach any other membrane potential in the range allowed by its ionic channels,
as a function of the time that has elapsed. With the information thus obtained for a variety of ini-
tial conditions we then evaluate the autocorrelation function of the fluctuating potential of the
cell membrane and hence can obtain the power spectrum of the voltage noise. This theoretical approach
is being applied to the evaluation of the voltage noise produced by the gating process of various ion
channels in unclamped or current-clamped membranes.

M-PM-H3   STATISTICAL DISCRIMINATION OF KINETIC MODELS FOR GATING AND PERMEATION OF IONIC CHANNELS.
Richard Horn, Department of Physiology, UCLA School of Medicine, Los Angeles, CA 90024.
Biophysicists typically quantify the gating and permeation mechanisms of ionic channels by choos-
ing kinetic schemes for the channel properties. But different schemes can produce nearly indistin-
guishable predictions. Most researchers pick a model or class of model which is either esthetically
pleasing, or else is supported by independent evidence. Here I discuss model selection by 3 pos-
sible statistical criteria. The first is the traditional method for comparison of "nested models".
In such cases a chi-squared variable can be obtained for comparison of any two models. Unfortunate-
ly, the models of most interest are usually not nested. The second option is to rank models in the
"information sense", using procedures developed in part by H.Akaike and G.Schwarz. In this option
maximum log-likelihoods (MLL's) or error sum-of-squares (ESS's) of two, possible non-nested, models
are compared, with a cost extracted from each model based on the number of free parameters. The
difficulty with this method is that the ranking of models does not guarantee differences from one
another at a known significance level: the ranking may be a chance consequence of the particular set
of random data examined. The third option uses a "parametric bootstrap" which allows significance
levels to be set in standard hypothesis tests between any two models. The idea derives from D.R.
Cox, who showed that in many cases the difference between the MLL's, or the ratio of ESS's, for two
models is asympotically normal. The parameters of this normal distribution can be obtained by simu-
lation, and used for the hypothesis tests. Examples of the use of these 3 options will be given for
single channel data and macroscopic currents from Na and endplate channels. Among other examples,
I will present tests for comparison of time-homogeneous and -inhomogeneous Markov chain models for
gating, and tests between fluctuating and stationary barrier models for ion permeation.

M-PM-H4 OPEN CHANNEL NOISE IN GRAMICIDIN-A AND SYNTHETIC ANALOGS INDICATES RAPID CONFORMATIONAL FLUCTUATIONS. F.J. Sigworth[1], D.W. Urry[2] and K.U. Prasad[2]. [1]Max Planck Institut für Biophys. Chemie, D-34 Göttingen, FRG and [2] Laboratory of Molecular Biophysics, Univ. of Alabama, Birmingham AL 35294.

We have adapted the pipette-bilayer technique of Andersen (Biophys. J. <u>41</u>, 119; 1983) to make high-resolution recordings of currents in decane-diphytanoyl PC bilayers. Recordings were made of channels from synthetic Gramicidin A (GA) and the following analogs: Ala[7], Leu[5], des-Val[7]-Val[8], and con-D-Leu[5]-L-Ala[5b] GA, obtained by solid-phase synthesis and purified by TLC and high- and low-pressure liquid chromatography. Difference power spectra showing the ion-transport noise through single channels in CsCl solutions were for the most part flat from <40 Hz to 20 kHz with an amplitude between 1.0 to 2.5 times the classical shot noise spectral density, $S=2iq$. Differing relative amplitudes were observed not only in the various analogs, but also among the different conductance states of individual channel types. The excess noise probably arises from rapid conformational fluctuations in the channel protein: analysis of the amplitude distribution of the current noise suggests a characteristic time scale shorter than 1 µs.

M-PM-H5 A COMPONENT ISOLATED FROM RATTLESNAKE VEMOM (CROTALUS ATROX) SPECIFICALLY ACTIVATES CA CHANNEL IN MAMMALIAN HEART. A. Yatani, S.L. Hamilton and A.M. Brown, Department of Physiology and Biophysics, University of Texas Medical Branch, Galveston, Texas 77550.

Toxins have proved to be useful probes for identifying membrane channel proteins such as the Na^+ and ACh channels. A component isolated from rattlesnake venom which we have designated "atrotoxin" specifically activated Ca^{++} channels in isolated heart cells. The active component was neither a protease nor a phospholipase. The effect of atrotoxin on Ca current (I_{Ca}) in isolated guinea pig and neonatal rat ventricular cells was examined by the whole-cell patch-clamp method. Atrotoxin ($10^{-9} \sim 10^{-5}$ g/ml) caused a dose-dependent increase in the action potential duration of isolated guinea pig ventricular cells. A similar dose-dependent increase of I_{Ca} was observed under voltage-clamp conditions. The activation was rapid and reversible. The enhancement of I_{Ca} by atrotoxin was not voltage sensitive and neither the current-voltage relation nor the steady-state inactivation curve was changed by this agent. Atrotoxin appeared to act selectively on Ca^{++} channels and in the doses used had no effect on Na or K currents. The effects on I_{Ca} were eliminated by Co^{++} (3 mM) or nitrendipine (10^{-5} M), but were not blocked by α- or β-adrenergic blockers. Atrotoxin also blocked the specific binding of [³H]-nitrendipine to sarcolemmal membranes prepared from guinea pig ventricles. These results suggest that atrotoxin may be a useful tool for characterization of the voltage-dependent Ca^{++} channel molecules.

M-PM-H6 FAST AND SLOW Ca CHANNELS IN TWITCH MUSCLE FIBRES OF THE FROG. G. Cota & E. Stefani. Dept. of Physiology and Biophysics, CINVESTAV-IPN, Apdo. Postal 14-740, 0700 México, D.F. México

Ca currents (I_{Ca}) were recorded at 18°C in intact fibres of cutaneous pectoris muscle from <u>R. montezume</u> by using the three microelectrode voltage-clamp technique. The saline contained 120mM-TEA-CH₃SO₃, 10mM-Ca, and 350mM-sucrose. Two components in the inward current were detected during the first 5 min of exposure to the saline. The well known, slow component (I_{Ca-s}) was detected at -35mV, reached a maximum peak value of -60 µA/cm² at about 0mV in 300 msec and had a time constant of decay of 1.5 sec during a maintained depolarization to 0mV. In addition, an early component of inward current (I_{i-f}) was detected at -60mV, reached a maximum peak value of -15 to -30 µA/cm² at -20 to -5mV, had a relatively fast time course of activation and practically did not decline during a maintained depolarization. The onset of this current was not resolved since it was masked by the capacity transients and remaining fast outward currents; an upper limit value of the peak time at 0mV was 12 msec. I_{i-f} was also carried by Ca since it was a net inward current, thus not due to a nonlinear resting conductance, was resistant to 0.6 µM TTX, disappeared after Ca replacement by Mg and was blocked by 2mM-Cd. Fast and slow Ca currents were not reduced by 5 µM-diltiazem. The amplitude of I_{Ca-f} decreased as a function of time to exposure to the recording saline while I_{Ca-s} remained practically unchanged; after 20 min the maximum peak value of I_{Ca-f} was -3 to -1 µA/cm². These results are consistent with the existence of two types of Ca Channels: fast and slow. Fast Ca channels have a low threshold and a fast time cours of activation, do not appear to inactivate and they tend to disappear in the hypertonic recording saline. If fast Ca channels are present in isotonic conditions, one may expect that they significantly activate during a single twitch.

M-PM-H7 GASTRIC SMOOTH MUSCLE CELLS HAVE ONLY Ca^{2+} and Ca^{2+} -ACTIVATED K^+ CHANNELS. R.L. Mitra & M. Morad, Dept. of Physiology, University of Pennsylvania, Philadelphia, Pa. 19104

Single gastric smooth muscle cells isolated from guinea pigs or rabbits using protease and collagenase were studied with the whole cell gigaseal technique (Hamill et al. Pflugers Arch. 391:85, 1981). Cells were bathed in 5mM Ca^{2+} Tyrode at 22 C. Depolarizing clamp steps from -80 or -40 mV to potentials positive to -20 mV activated a TTX insensitive inward current that peaked within 6ms and reached a maximum value at +20mV. This current was blocked by 0.5mM Cd^{2+} or 5mM Co^{2+}, but was not significantly altered by either luM diltiazem or D600. When the internal pipette solution (aCa^{2+}=10nM,Ca-EGTA buffer) contained primarily K^+, a large time dependent outward current was activated at potentials positive to -20mV. This current was greatly reduced when $K^+_{1/2}$ was replaced by either Cs^+ or the impermeant cation N-methyl glucamine. Since Cd^{2+} also blocked this outward current it is likely that its activation is linked to activation of the Ca^{2+} channel. Clamp steps negative to -30 mV produced no evidence for an inwardly rectifying potassium channel, a finding consistent with the low resting potentials (-45 mV) in these cells. Our results show that in gastric myocytes the excitatory inward current is carried primarily by Ca^{2+} and that the activation of this current is linked to activation of an outwardly rectifying K^+ current. No evidence for a TTX sensitive Na^+ channel could be found.

M-PM-H8 MACROSCOPIC CALCIUM CURRENTS IN ACUTELY-EXPOSED NEURONS FROM ADULT HIPPOCAMPAL SLICES. R. Gray & D. Johnston, Neurosci. Prog. & Neurol. Dept., Baylor Col. Med., Houston, TX.

A knowledge of the properties of calcium currents in adult, mammalian central neurons may be a necessary prerequisite for the full understanding of the mechanisms of synaptic plasticity. However, the methods necessary to study calcium currents quantitatively in isolation have not been applicable to adult central neurons, although calcium currents have been identified in hippocampal neurons using the single-electrode voltage clamp (Johnston et al., Nature 286:391, 1980). We have developed a partially dissociated hippocampal slice preparation in which the measurement of isolated calcium currents is possible. 300 µm slices of adult guinea pig hippocampus were incubated in proteolytic enzymes for 30-60 min and mechanically dissociated. This caused the slices to split apart along the major cell body layers, exposing the somata. Granule cells of the dentate gyrus were chosen for the study of macroscopic calcium currents because their small size (8-15 µm) and simple geometry enhanced the possibility of obtaining an adequate space clamp. The giga-seal whole-cell clamp technique was used with the internal solution containing EGTA, Cs^+, tetraethylammonium$^+$ (TEA), and 3,4-diaminopyridine (3,4-DAP) to block K^+ currents. The bath solution also contained TEA and 3,4-DAP as well as TTX and normal Ca^{++} (2 mM). Under these conditions robust calcium currents were obtained. Voltage-dependent activation of the current was found to be consistent with m^2 kinetics and slow inactivation occurred during the step depolarizations. Washout of the calcium current usually occurred within 30 min of recording, even with 10 mM EGTA and 5 mM Mg-ATP added to the internal solution. The possible effects of β-adrenergic agonists on these Ca^{++} currents are also being investigated. (Supported by NS15772, NS11535, USAMRDC DAMD17-82-C-2254, and a McKnight Found. Neurosci. Devel. Award)

M-PM-H9 PERMEABILITY OF THE FROG SKELETAL MUSCLE CA++ CHANNEL TO ORGANIC CATIONS

E.W. McCleskey, W. Almers. Intr. by C. Stirling. Physiology, U.Washington, Seattle,WA. 98102

The Ca++ channel of frog skeletal muscle becomes permeant to monovalent cations in the absence of extracellular Ca++ (ref.1,2). The permeability to organic cations has been measured by observing reversal potentials when the organic is the only extracellular current carrier and Na+ is inside the cell. Nitrendipine block was used to prove that current passed through Ca++ channels.

Permeability decreases with increasing ion size in the methylated ammonium series. Methyl-ammonium is about as permeable as Na+ whereas tetramethylammonium is about 0.05x as permeable. Tetramethylammonium is the largest ion shown to be permeable suggesting a 5-6 Å. pore size for the Ca++ channel, somewhat similar to the ACh receptor channel (ref. 3).

Hydrazinium($NH_3N^+H_3$) is 1.4x as permeable as methylammonium($CH_3N^+H_3$) and aminoguanidine is 1.7x as permeable as methylguanidine. The channel seems to prefer to pass amino over methyl groups.

N-butylammonium($CH_3(CH_2)_3 N^+H_3$) is not detectably permeable whereas 1,4 diaminobutane ($H_3N^+(CH_2)_4 N^+H_3$) gives clear inward current. This result along with the above distinction between methyl and amino groups may indicate a region within the pore to which hydrophobic compounds bind. The second amino group on diaminobutane would protect the channel from sensing the hydrophobic butane.

1) Almers et.al. (1984) J. Physiology v.353 pp.565-583
2) ibid. pp.585-608
3) Dwyer et.al. (1980) J.Gen. Physiology v.75 pp.469-492

M-PM-H10 DIRECT MEASUREMENT OF ENTRY AND EXIT RATES FOR CALCIUM IONS IN SINGLE CALCIUM CHANNELS. J.B. Lansman, P. Hess and R.W. Tsien, Dept. of Physiology, Yale University, New Haven, CT 06510

Ca channels are highly permeable to monovalent cations in the absence of divalent cations. We observed large unitary Ca channel currents carried by Na (~80 pS) or Li (~40 pS, left panel) in recordings from cell-attached patches on guinea pig ventricular cells exposed to Bay K 8644 to promote long channel openings. Addition of micromolar Ca to the pipette solution converted long-lasting unitary Li currents to bursts of brief openings and closings (right panel). Analysis of open and closed times within bursts gave histograms well-fit by single exponentials, as expected if the dominant process were block and unblock of the pore associated with Ca entry and exit. The rate of block was voltage-independent, and increased linearly with $[Ca]_o$ with a high rate coefficient (4.5×10^8 $M^{-1}s^{-1}$), suggesting that extracellular diffusion is the rate-limiting step for Ca entry. The exit rate (1200 s^{-1} at -30 mV) was independent of $[Ca]_o$ but increased e-fold with hyperpolarization from -20 to -60 mV, consistent with Ca exit into the cell.
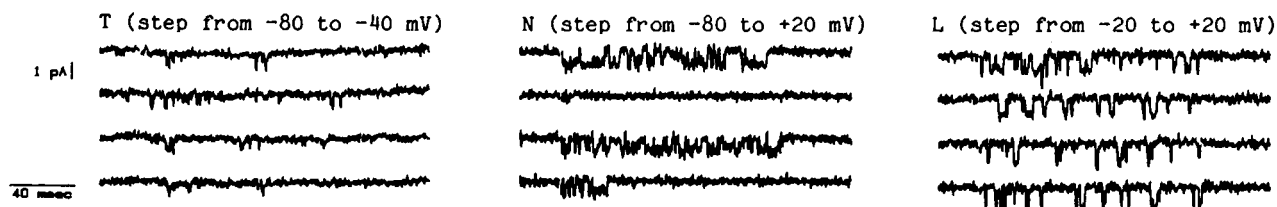
150 mM Li$^+$ + 0 Ca^{2+} 150 mM Li$^+$ + 1.63 uM Ca^{2+}

2 pA
20 ms
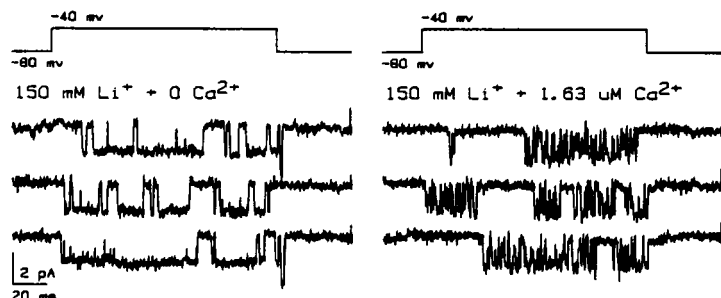
M-PM-H11 DIVALENT CATION INTERACTIONS WITH SINGLE CALCIUM CHANNELS FROM RAT BRAIN: EVIDENCE FOR TWO SITES. Mark T. Nelson, Dept. Physiology, University of Maryland, Baltimore, MD & Dept. Pharmacology, University of Miami, Miami, FL

Currents through single calcium channels from rat brain synaptosomes in planar lipid bilayers were measured. These channels are voltage-dependent, select for Ca,Ba, and Sr over monovalent ions, and are blocked by cadmium and lanthanum (Nelson et al., <u>Nature 308</u> 1984). Figure 1A shows that cadmium can reduce the single channel current when added to either side of the bilayer, but it produces a greater reduction when added to the cis side. Fig. 1B shows that when cadmium is added to the cis side of a channel the single channel current is reduced in a manner consistent both with Cd ions being impermeant and interacting with a single site. Not all "blockers" are impermeant. In the absence of divalent cations, manganese can pass through these channels. However, when Mn is added to solutions of other permeant ions (e.g. Sr), a reduction of the single channel conductance results. This reduction of current is voltage-dependent with lower voltages favoring block. At less positive voltages, the single channel conductance in this ion mixture (Sr+Mn) was less than that in manganese alone. Such "anomalous mole fraction" effects appear similar to those see in other Ca-channels (cf. Hess & Tsien, <u>Nature 309</u> 1984; Almers & McCleskey, <u>J. Physiol. 353</u> 1984). All of these results are consistent with the channel having two divalent cation binding sites that are involved in the permeation process.

A
0.5pA   0 Cd^{2+}
0.5pA   Trans Cd^{2+}
0.5pA   Cis Cd^{2+}
2sec
B
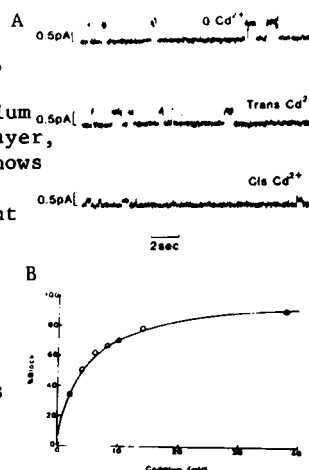
M-PM-H12 THREE TYPES OF CALCIUM CHANNELS IN CHICK DORSAL ROOT GANGLION CELLS. M. C. Nowycky~, A. P. Fox and R. W. Tsien. Neuroanatomy and of Physiology, Yale Univ. Sch. Med., New Haven CT.

We and others have previously distinguished two components of Ca channel current in chick DRG neurons, "T" and "L". In 10 Ca_o, whole-cell T current is transient and needs only weak depolarizations for activation (beyond -60 mV) and inactivation (midpoint ~-80 mV). L current is long-lasting and requires strong depolarizations for activation (beyond -10 mV) and inactivation (midpoint ~-40 mV). 20 μM Cd completely blocks L current but largely spares T current. In cell-attached patches (pipette: 110 mM $BaCl_2$, bath: 140 mM K-aspartate), unitary T currents are tiny (left), while L channels (right) have a large conductance (~25 pS). We now report a third component ("N") that is neither T nor L. Near 0 mV, N-type Ca current decays somewhat more slowly than T but much faster than L. It requires relatively negative holding potentials for removal of inactivation, strongly depolarized test potentials for activation, and is blocked by 20 μM Cd. Unitary currents with N-type kinetics (middle) are medium-sized.

T (step from -80 to -40 mV)   N (step from -80 to +20 mV)   L (step from -20 to +20 mV)

1 pA

40 msec

M-Pos1   SECONDARY AND TERTIARY STRUCTURES IN THE S8/S15 PROTEIN BINDING DOMAIN OF *E. COLI* 16S RIBOSOMAL RNA. David E. Draper, Joanne M. Kean, and Susan A. White, Department of Chemistry, The Johns Hopkins University, Baltimore, MD 21218.

To undertake detailed studies of the structure of the *E. coli* 16S ribosomal RNA, we have used a hybridization selection technique to isolate a specific 345 base fragment covering a region known to interact with two proteins, S8 and S15. Extensive structure mapping experiments, using single and double strand specific ribonucleases, show that the fragment retains the secondary structure deduced for intact 16S rRNA on the basis of phylogenetic comparisons [Woese *et al*, Microbiol. Rev. <u>47</u>, 621]. Protein binding experiments show that the fragment also retains specific recognition for S8 and S15, with nearly the same affinity as intact 16S RNA. We conclude that this region comprises a structural domain which, to a first approximation, folds independently of the rest of the 16S RNA.

Several unusual structural features have been located in this RNA fragment. The affinity cleavage reagent (methidiumpropyl-EDTA)-Fe(II)[Hertzberg & Dervan, Biochemistry <u>23</u>, 3934] intercalates at two or three sites with affinity more than an order of magnitude greater than to tRNA or synthetic helices; the affinity of ethidium bromide for the same sites is $\approx 10^7$ M^{-1} at 0.1 M Na^+ and 37°C. A bulge loop with extensive tertiary structure is intimately involved in the formation of the sites, which are all clustered in a region recognized by S15 protein. In another region, two different long range base pairing schemes exist in equilibrium. These two structures comprise a 'conformational switch' of possible functional significance for the ribosomal RNA.

M-Pos2   THE INTERACTION OF DRUGS WITH LEFT-HANDED (Z) DNA
G. Terrance Walker, Michael P. Stone, and Thomas R. Krugh
Department of Chemistry University of Rochester, Rochester New York 14627

Spectrophotometric and phase partition techniques have been used in conjunction with circular dichroism spectroscopy to characterize the equilibrium binding of ethidium, actinomycin D and actinomine to poly(dG-dC)·poly(dG-dC) and poly(dG-m^{5}dC)·poly(dG-m^{5}dC) under Z-form conditions. These studies support the following interpretations: (1) the drugs bind cooperatively under Z-form conditions, inducing a "step-by-step" conversion of the Z-helix to a right-handed drug-bound form; (2) the interface between Z-DNA and the drug-bound region of the helix is a highly favorable binding site; (3) ethidium intercalates in clusters under high salt Z-form conditions; (4) the drugs exhibit a binding treshold under Z-form conditions, the magnitude of which is dependent upon the counter-ion concentration used to stabilize Z-DNA. Ethidium converts 2-4 base pairs of left-handed poly(dG-dC)·poly(dG-dC) in 4.4 M NaCl to a right-handed form per bound drug; actinomycin D converts 4-5 base pairs. When 40 μM cobalt hexamine is used to stabilize left-handed poly(dG-dC)·poly(dG-dC), all three drugs reverse ~20 left-handed base pairs per bound drug. Approximately 7 base pairs of left-handed poly(dG-m^{5}dC)·poly(dG-m^{5}dC) in 2 mM magnesium are converted per bound drug by either ethidium or actinomine. These differences reflect the factors which stabilize the two left-handed polynucleotides under the various Z-form conditions. The concentration threshold for binding actinomycin D, ethidium, and actinomine to poly(dG-dC)·poly(dG-dC) in 4.4 M NaCl are ~0.3 μM, 20 μM, and >100 μM, respectively . An ethidium threshold of ~0.2 μM for binding to poly(dG-m^{5}dC)·poly(dG-m^{5}dC) in 2 mM magnesium increases tenfold when the magnesium concentration is raised to 25 mM.

M-Pos3   REPULSION AND ATTRACTION BETWEEN DNA HELICES: CONTROLLED HYDRATION OF THE MOLECULAR SURFACE BY ION BINDING. Donald C. Rau and V. Adrian Parsegian. National Institutes of Health, Bethesda, MD 20205

As part of a systematic effort to identify interactions responsible for macromolecular assembly, we are measuring attractive and repulsive forces between DNA helices associated with different counterions. We have already reported (PNAS 81:2621, 1984) repulsive forces with univalent and most divalent counterions, forces that increase exponentially with an approximate 3 Å decay length, for surface-to-surface separations less than about 15 Å. By analogy with forces measured between neutral bilayers in distilled water (e.g., Rand, 1981, Ann. Rev. Biophys. 10:224), we concluded that this force is due to molecular hydration.

DNA will spontaneously precipitate in a sufficient concentration of trivalent or oligovalent cations. The double helices are stably separated by surface-to-surface distances of 7-12 Å, depending on the counterion used. We find the force necessary to move the helices closer increases exponentially with an approximate decay length of only 1.5 Å, independent of the nature of the cation that caused precipitation and the ionic strength. These results are consistent with competing attractive and repulsive hydration forces.

If ion concentration is less than that necessary for precipitation, applied osmotic pressure and/or increased temperature can induce additional ion binding to strengthen the attractive hydration force. The transition pressure is well defined and readily observed by x-ray diffraction. Applying variants of the Clausius-Clapeyron equation, we determine the energetics of binding the additional $Co(NH_9)_6^{3+}$ or Mn^{2+} ions necessary to induce a net attraction between DNA helices. The energetics of the induced Mn^{2+} collapse suggest two different modes of binding to DNA.

M-Pos4   **ULTRAVIOLET RESONANCE RAMAN EXCITATION PROFILES OF NUCLEIC ACID BASES WITH EXCITATION FROM 200 TO 300 NANOMETERS** W. L. Kubasek, Department of Biology and Institute of Molecular Biology, University of Oregon, Eugene, Oregon 97403 USA

Raman spectra are presented for dilute aqueous solutions of the mononucleotides obtained with laser excitation at 299, 266, 253, 240, 229, 218, 209 and 200 nm. Distinct evidence of strong, selective resonance enhancement is obtained. Excitation profiles have been constructed for the strongest bands using the phosphate band at 994 cm^{-1} as an internal reference. The excitation spectra for many of the vibrational bands are dominated by a peak corresponding to the lowest energy electronic transition near 260 nm. Smaller peaks are seen for higher energy electronic transitions. For some modes, the resonance enhancement is dominated by the higher energy transitions. It is clear from this new data that a full description of the resonance Raman profiles of the nucleic acids will have to include several excited electronic states. Two examples are given of cases where distinct species can be easily distinguished using far UV (218 nm) excitation but where these species are not easily distinguishable with 266 nm excitation. This demonstrates the utility of far UV resonance Raman spectroscopy.
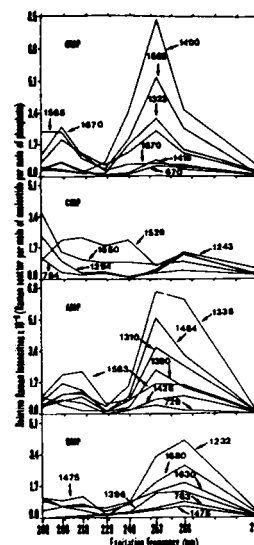
M-Pos5   SALT AND LENGTH DEPENDENCE OF OLIOGONUCLEOTIDE HELIX TO COIL TRANSITIONS
Dorothy Erie and M. Thomas Record, Jr., (Intr. by M. Sundaralingam) Department of Chemistry, University of Wisconsin, Madison, WI 53706

The effects of salt on the helix coil transition temperature (T_m) of polymeric DNA have been reasonably well described using polyelectrolyte theory. Oligomers, however, do not adhere to this theory. A semiempirical extension of polyelectrolyte theory introduced and end effect parameter to account for the reduced ion association at the ends of the oligonucleotide (Record and Lohman, Biopolymers 17, 159 (1978)). We are investigating the oligoelectrolyte-electrolyte interactions by measuring T_m as a function of salt and length. The transitions are monitored at 260nm and 280nm by UV-spectroscopy. By measuring the salt dependence of T_m, we can determine the extent of release of thermodynamically bound counterions upon denaturation. Thus we can obtain a data base for developing or testing the thermodynamic predictions of oligoelectrolyte theory. Experimental results for the dependence of T_m on counterion concentration, chain length and strand concentration for oligomers of base composition $dGG(AA)_nGG \cdot dCC(TT)_nCC$, $2 \leq n \geq 6$, will be presented.

M-Pos6   A MONTE CARLO APPROACH TO THE THERMODYNAMICS OF POLYELECTROLYTE SOLUTIONS.
Pamela Mills, M. Thomas Record, Jr., (Intr. by J. Anderegg) Department of Chemistry, University of Wisconsin, Madison, WI 53706

The melting of double stranded DNA and the binding of ligands to DNA is highly sensitive to the concentration of salt in the solution. These salt effects can be considered as primarily electrostatic and theoretical models of these effects treat the DNA and salt ions as idealized charged cylinders and spheres. Using this electrostatic model we have applied the grand canonical Monte Carlo method of such polyelectrolyte solutions in order to obtain thermodynamics (activity coefficients and preferential interaction parameter) relevant to interpret the salt dependence of melting of DNA and ligand binding to DNA. We present results to the computer simulations and compare these with the prevalent analytical polyelectrolyte theories. The application of this method to melting and ligand binding experiments is discussed.

M-Pos7   STEREOCHEMICALLY DEFINED DNA CROSSLINKING BY CONFORMATIONALLY RIGID NITROGEN MUSTARDS. Christian G. Reinhardt, Harry Robbins and Nancy Cabral, Department of Chemistry, Rochester Institute of Technology, Rochester, N.Y. 14623 and James G. Henkel, School of Pharmacy, U-92 University of Connecticut, Storrs, C.T. 06268.

     A series of disubstituted 2-azaadamantanes representing conformationally defined nitrogen mustards incorporated into an adamantyl framework with fixed separation distances between alkylating centers of 3.6 Å (1) and 2.5 Å (2,3), have been synthesized (Henkel et.al,(1981) J. Org. Chem., 46, 3483 and unpublished results) as rigid probes of DNA alkylation and crosslinking processes leading to cytotoxicity. The extent of intermolecular DNA crosslinking by the N-methyl isomer series has been measured by two complementary ethidium bromide fluorescence assay methods. Results indicate that isomers 1 and 2 form intermolecular DNA crosslinks, while 3 does not. Analysis of the kinetics of the reaction isotherms of 1 and 2 indicate significant differences in their rates and stability of crosslink formation. Crosslink reactions using DNA's of different base composition have established that the extent of crosslinking increases with increasing (G+C) content; however, the (G+C) dependence on crosslinking varies substantially between 1 and 2, and between the isomers and nitrogen mustard itself. A relationship also appears to exist between the cytotoxic activity and stereochemistry of the isomers, which may indeed reflect differences in the crosslinking behavior at the molecular level, and which may lead to further elucidation of the molecular mechanism of action of both the chloroethylnitrosoureas and the nitrogen mustards. (Supported by NCI grant CA 25436)
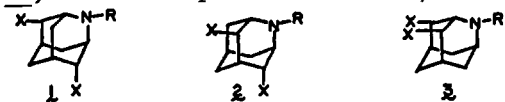
M-Pos8   EFFECTS OF O^6 GUANINE METHYLATION ON THE STABILITY, ENERGETICS AND CONFORMATIONAL FLEXIBILITY OF OLIGOMERIC DUPLEXES. Luis A. Marky, Barbara L. Gaffney, Roger A. Jones and Kenneth J. Breslauer, Department of Chemistry, Rutgers, The State University of New Jersey, New Brunswick, New Jersey 08903.

     We have synthesized a set of four self-complementary dodecanucleotides with the sequence d[CGNGAATTC(O^6Me)GCG], (N=C, T, A or G) using a phosphoramidite procedure [Biochemistry 23, 000 (1984)]. The thermally-induced helix-to-coil transitions of the duplexes formed by this family of self-complementary oligomeric sequences were monitored and characterized using differential scanning calorimetry (DSC), temperature-dependent uv absorption spectroscopy, and circular dichroism (CD). The CD spectra of all four oligomers indicate that each sequence forms a duplex in the "B" conformation. Optical and calorimetric melting curves of these duplexes reveal that, replacement of a Watson-Crick GC base pair in the parent sequence [d(CGCGAATTCGCG)] by a (O^6Me)G-N base pair reduces both the thermal stability and transition enthalpies of each modified duplex. Specifically, each modification causes a t_m reduction between 20-25°C. This decrease in thermal stability is paralleled by a decrease in transition enthalpy between 20 and 40 kcal/duplex. Comparison of the model-dependent van't Hoff enthalpies with the model-independent calorimetric enthalpies reveals that all the oligomers melt in a two state manner. These results reveal that O^6 methylation of guanine introduces an "imperfection" that reduces the thermal stability and the transition enthalpy of the modified duplex compared with the Watson-Crick parent duplex. The magnitude of these reductions in t_m and ΔH depend only partly on the identity of the nucleotide opposite the methylated base. The O^6 methylation appears to create local regions of instability which are enthalpic in origin. Significantly, however, these destabilizing "imperfections" do not change melting cooperativity.

M-Pos9   ETHIDIUM ION INTERCALATION INTO DNA AND RNA OLIGONUCLEOTIDES
     Jeffrey W. Nelson[†] and Ignacio Tinoco, Jr.
     Dept. of Chemistry, Univ. of California, Berkeley, Berkeley, CA   94720
     [†]Present address: Dept. of Biology, Univ. of Pennsylvania, Philadelphia, PA   19104

     The thermodynamics of ethidium ion binding to the double strands formed by the ribo-oligonucleotides $rCA_5G + rCU_5G$ and the analogous deoxyribo-oligonucleotides $dCA_5G + dCT_5G$ were determined by monitoring the absorbance vs. temperature at 260 and 283 nm at several concentrations of oligonucleotides and ethidium bromide. A statistical model is described which takes into account sequence-dependent and cooperative effects. For the ribo-oligonucleotides, two models fit equally well. Either two sites (assumed to be the intercalation sites at the two ends of the oligonucleotide) bind more strongly by a factor of 140 than the third site, or all sites are identical, but there is strong anti-cooperativity on binding (cooperativity parameter of 0.1). In sharp contrast, the binding to the deoxyribo-oligonucleotide of the same sequence (with thymine replacing uracil) showed all sites equivalent and no cooperativity. The binding to the ribo-oligonucleotides was approximately 10-fold stronger than to the deoxyribo-oligonucleotides. New results on the preferential binding of ethidium ion into bulged sites will be discussed, utilizing the bulge-forming deoxyribo-oligonucleotides $dCA_3CA_3G + dCT_6G$.

M-Pos10   THERMODYNAMICS FOR THE INTERCALATION OF SUBSTITUTED NAPHTHALENE MONOIMIDES TO DNA: RESULTS DERIVED FROM SPECTROSCOPIC AND CALORIMETRIC DATA. Harry P. Hopkins, Karen Stevenson, and W. David Wilson, Department of Chemistry, Georgia State University, Atlanta, Georgia 30303

Naphthalene monoimides with nitro (NO_2) and amino (NH_2) groups at the three and four positions on the naphthalene ring and the unsubstituted compound have been shown to form intercalated complexes with sonicated calf thymus DNA. Each of the substituted compounds also dimerizes in the MES buffer (pH = 6.2 and I = 0.11), in which the binding studies were performed. In the spectroscopic studies, the concentrations of the compounds were kept low enough so that the concentrations of the dimers were negligible. This could not be done in the calorimetric studies, which were performed in a Tronac titration unit, equipped with a 2 mL Dewar and interfaced to a microcomputer. Consequently, the derived enthalpy parameters depend to some extent on how one corrects for the dilution and dimerization effects. For both the unsubstituted and 3-nitro derivative, the calorimetric and van't Hoff values for ΔH^o are near 4.0 kcal mol^{-1}. The ΔH^o value derived from the calorimetric data for the 4-nitro derivative is also near 4.0 kcal mol^{-1}, but the values determined from the calorimetric data for the 3- and 4- amino derivatives are much more negative, i.e., 6.7 and 7.4 kcal mol^{-1}. These are considerably smaller than the 5.3 kcal mol^{-1} value derived from the van't Hoff plot for the 3-amino derivative. The ΔG^o value for the binding process range from 5388 (unsubstituted) to 5960 (3-nitro) cal mol^{-1}; thus the changes in the ΔH^o are compensated by changes in ΔS^o. For the amino derivatives the ΔS^o values for the binding process are negative; whereas these values are positive for the nitro derivatives.

M-Pos11   ACTIVATION OF THE INTERFERON-INDUCING AND ANTI-VIRAL ACTIVITIES OF POLYRIBONUCLEOTIDES BY INTERCALATING DRUGS. James M. Jamison, Pedro J. Bonilla, Peter H. Koo, and Chun-che Tsai, Department of Chemistry, Kent State University, Kent, Ohio 44242 and Program in Microbiology and Immunology, Northeastern Ohio Universities College of Medicine, Rootstown, Ohio 44272

We have studied the interferon-inducing and anti-viral activities of poly r(A-U) or poly r(G-C) in combination with ethidium bromide, 9-aminoacridine, or daunomycin using the human foreskin fibroblast-vesicular stomatitis virus (HSF-VSV) assay system. The interferon titers were based on the activity of NIH human fibroblast interferon reference standard and poly(rI)·poly(rC) reference standard. The role of ethidium bromide, 9-aminoacridine, or daunomycin in modulating the interferon-inducing and anti-viral activities of poly r(A-U) and poly r(G-C) was examined by experiments in which the concentrations of both polyribonucleotides were fixed at 0.05 mM, 0.1 mM or 0.2 mM while the drug (ethidium bromide, 9-aminoacridine, or daunomycin) concentration was varied to produce variable drug/ribonucleotide ratios ranging from 1:16 to 2:1. Our preliminary results demonstrated that the ethidium bromide/ribonucleotide ratio of 0.25 and the daunomycin/ribonucleotide ratio of 0.167 produced an adjuvant effect on the interferon-inducing and anti-viral activities of both poly r(A-U) and poly r(G-C). The interferon titers of the polyribonucleotide-ethidium bromide (or daunomycin) combinations were consistently greater than the sum of the interferon titers of the individual constituents. These results suggested a synergism between poly r(A-U) (or poly r(G-C)) and ethidium bromide (or daunomycin). The interferon titers of the polyribonucleotide:9-amino-acridine combinations did not display this synergism. (Supported by NIH Grant GM-31257)

M-Pos12   PHYSICAL STUDIES ON OLIGODEOXYRIBONUCLEOTIDES WITH AN ALKYL LESION OR AN UNCOMMON BASE. S. Chandrasegaran and L.-S. Kan, Division of Biophysics, The Johns Hopkins University, Baltimore, Maryland 21205

The DNA with lesions are of great importance in the study of mutagenesis and carcinogenesis. We'like to introduce a systematic method to study the implication of these alterations to DNA's structure and function by a synthesized series of decadeoxyribonucleotides with the following sequence:
d-CCAAGATTGG(a).
One and only one lesion will be inserted in the central GA region. The lesions that have been studied are mGA (mG:O^6-methylguanosine)(b), IA (I:inosine)(c), and GpA(p:ethylphosphotriester, there are two isomers, R- (d) and S-form (e)). The possible complementary decamers, d-CCAATCTTGG(f) and d-CCAATTTTGG (g), to the normal and modified oligomers were also synthesized. The UV melting experiment revealed the T_m of d·f (41°C) is very similar to that of a·f (42°C) at the same condit.-ion. This indicates that a minimal perturbation of R-form of ethyl phosphotriester to the helix. On the contrary, the T_m of e·f (38°C) is somewhat lower than that of the normal one (a·f).This indicates that the direction of the ethyl group from the backbone may interrupt the base-base stacking mode of the helix. The T_m of c·f is much lower (32°C) which may cause alternation of the hydrogen-bonding scheme of the base pairs. We found the T_m of b·f(26°C) is not only lower than that of a·f, but also lower than that of b·g (31°C). This indicates that mG prefers to base pair to T rather than C. CD and NMR studies have also confirmed these observations and will be reported in detail. (supported by NIH)

M-Pos13   DETERMINATION OF PROTON-PROTON DISTANCES IN NUCLEIC ACIDS BY NMR. Jila Honarbakhsh, L.-S. Kan, D. M. Cheng, D. Frechet, and P. O. P. Ts'o, Division of Biophysics, The Johns Hopkins University, Baltimore, Maryland 21205

The measurements of spin-lattice relaxation time (T_1) and nuclear Overhauser enhancement (NOE) can lead to the determination of the distances of two interacting magnetic spins (such as ^1H-^1H). A library of these ^1H-^1H distances in nucleic acids can be used to construct the three-dimensional structure in aqueous solution. Due to sizable variations in T_1 and NOE measurements, the distance, which depends on the reciprocal 6th power of these values, therefore cannot be determined accurately. In addition, it is a time consuming process. Two-dimensional NOE may provide a solution. However, there exists no dependable method to determine the NOE quantitatively in 2D-NMR. We are systematically studying a series of compounds, dCMP, CpG^o, G^opC, and dCGCGCG (all CG compounds were supplied by Drs. S. Uesugi and M. Ikehara, Osaka University)(where G^o is 8,2'anhydro-1-β-D-arabino-furosyl-8-hydroxyguanosine), of which at least one internal distance of ^1H-^1H is known, so that an empirical correlation between NOE and distance can be established. From preliminary results of dCMP, we can calculate the distance between H_5-H_6 as 2.4 and 2.6 A by T_1 and NOE measurements, respectively. This result is in good agreement with x-ray crystallography data (2.43 Å). However, the H_6-H_1' distance is determined as 4.1 and 3.5 Å by T_1 and comparative NOE using 2.6 A as internal reference. The 3.5 Å value is closer to the x-ray crystallography data (3.7 Å). The % of NOE from conventional methods will now be compared with the results of 2D NOE for a given molecule at the same condition. This study will be extended to that of G^opC, CpG^o and dCGCGCG. (Supported by NIH and Albert Szent-Gyorgyi Fund.)

M-Pos14   ELECTRIC BIREFRINGENCE OF DNA IN AGAROSE GELS. Nancy C. Stellwagen, Department of Biochemistry, University of Iowa, Iowa City, IA 52242.

The electric birefringence of two fairly large DNA restriction fragments, 1426 bp and 2936 bp, was studied as a function of electric field strength, pulse length, and agarose concentration. The observed relaxation times of the DNA molecule are little affected by the presence of the gel, if the mean pore size of the gel is larger than the root mean square end-to-end length of the DNA molecule. However, if the mean pore size of the gel is smaller, much longer birefringence decay times are observed, consistent with a large fraction of the oriented DNA molecules being fully stretched. The presence of the gel seems to inhibit the fast relaxation mechanisms normally associated with the birefringence decay of large DNA molecules.

M-Pos15   TRACER MOBILITY OF LABELED SPERMINE IN SOLUTIONS OF NUCLEIC ACIDS. James W. Klein, Karl Zero, and Bennie R. Ware, Department of Chemistry, Syracuse University, Syracuse, New York 13210

We have synthesized a fluorescence-labeled spermine and have studied its association with the synthetic polynucleotides poly-(dG)·poly-(dC) and poly-(dA)·poly-(dT). The association was detected both by measuring the electrophoretic mobilities of the nucleic acids using electrophoretic light scattering (ELS) and by measuring the tracer diffusion coefficient of the labeled spermine using fluorescence photobleaching recovery (FPR). In order to interpret the diffusion coefficients measured by FPR it was necessary to correct for the fact that the fluorescence yield of the fluoro-phore, NBD (7-nitrobenz-2-oxa-1,3-diazole), was reduced upon binding to nucleic acid and that this effect was much greater when the nucleic acid was poly-(dG)·poly-(dC). The results are interpreted in terms of a model that takes into account the condensation of spermine onto the nucleic acids, the Langmuir-type equilibrium between bound spermine and free spermine, and the reduced mobility of spermine ions which are not bound in a chemical sense, but which are sufficiently close to a charged polyion to experience an electrostatic attraction. (Supported by Grant No. PCM-8306006 from NSF, Grant No. 14736-AC7-C from ACS-PRF and by a fellowship to JWK from the IBM Corporation.)

M-Pos16 HYDROXYL RADICAL CAUSES MOST OF THE LETHAL EVENTS TO MAMMALIAN FIBROBLASTS EXPOSED TO ACTIVE OXYGEN SPECIES. Rogério Meneghini & Alberto C.Mello Filho - Depto Bioquímica, Instituto de Química - University of São Paulo.

Exposure of fibroblasts to xanthine oxidase-generated oxygen species produced DNA strand breaks and cellular death; o-phenanthroline completely abolished the two effects. This compound complexes with iron and prevents this metal from participating of the Fenton reaction: $Fe^{2+} + H_2O_2 \longrightarrow Fe^{3+} + OH^- + OH^·$ (A). Therefore it is proposed that most of the cell death is brought about by OH radical produced from other species by an iron mediated reaction. The iron involved in this process must be very close to the target because OH radical has a very shorth range of action. When cell were incubated with $^{55}FeCl_3$, the metal became very strongly associated to a nuclear structure from which it was not separated during the process of nuclei preparation even by treatment with 2 M NaCl. Superoxide ion might be participating in the process as a reducing agent: $O_2^- + Fe^{3+} \longrightarrow Fe^{2+} + O_2$ (B) and thus the reaction that ultimately explains the damaging effect is the sum of (A) and (B), namely the Haber-Weiss reaction catalyzed by iron bound to a nuclear structure: $O_2^- + H_2O_2 \longrightarrow OH^- + OH^· + O_2$. This is likely to be the reaction that explains the damaging action in vivo as well because the superoxide dismutase inhibitor diethyldithiocarbamate greatly enhanced the production of DNA strand breaks when cells were exposed to H_2O_2. The general conclusion is that OH radical is the species that causes the lethal event at the DNA level, when cells are exposed to oxygen species, and that this OH radical is produced by a Haber-Weiss reaction. Furthermore o-phenanthroline seems to constitute an excelent probe for Fenton or Haber-Weiss reactions in vivo.

M-Pos17   NMR STUDIES ON THE INTERMEDIATE SPECIES OF HEMOGLOBIN WITH TWO LIGANDS BY Fe—Co HYBRID HEMOGLOBINS. Toshiro Inubushi, Masao Ikeda—Saito and Takashi Yonetani. Department of Biochemistry and Biophysics, University of Pennsylvania, Philadelphia, PA 19104.

   Proton NMR spectra have been measured at various sites of intermediate hemoglobin species with two ligands and compared with those for completely deoxy species. The advantage to use Fe—Co hybrid Hb's is that the Co—porphyrin subunits stay in deoxy state under CO atmosphere, although the Fe—porphyrin subunits are converted to liganded state, and intermediate species can be selectively prepared. ^{1}H NMR spectra of inter— and intra—hydrogen bonded protons showed that both di—liganded Hb's, $\alpha(Fe.CO)_2\beta(Co)_2$ and $\alpha(Co)_2\beta(Fe.CO)_2$ are essentially in the R—state at pH 7.0 and 23 C. However, an addition of IHP induced full recovery of T—quaternary structure in the former, but very small portion of the T—structure (ca. 10%) was rewound in the latter. On the other hand, as reported previously, the proximal histidin coordination in the α—subunits is substantially strengthened by the ligation of two ligands onto the β—subunits in $\alpha(Co)_2\beta(Fe)_2$. By contrast, the ligation in the β—subunits was unchanged in the complementary hybrid. No further shifts were detected in the proximal His N_δH peaks in the di—liganded Hb's upon the addtion of IHP. The methyl resonances of E11 Val, whose chemical shifts are useful measure to monitor the structural change of protein in the distal side of prosthetic group, showed substantial change in $\alpha(Fe.CO)_2\beta(Co)_2$ by the addtion of IHP, but slight change in the complement. These results suggest that the quaternary structural change is not necessarily linked with the coordination of histidin to the heme metal ion. Such structural information is discussed in relation of ligand binding properties of these hybrid hemoglobins. (Partly supported by BRSG RR—07083 and RR—05415 from NIH.)

M-Pos18   SOLVENT STUDIES OF RAMAN ELECTRON SPIN RELAXATION RATES IN MYOGLOBIN AZIDE.
J. T. COLVIN AND H. J. STAPLETON, Dept. of Physics, University of Illinois, Urbana, IL   61801
   The fractal model of electron spin relaxation in paramagnetic proteins (1-5) predicts the temperature dependence of the Raman relaxation rate to be a simple power law in T with an exponent of $(3+2\bar{d})$, where $\bar{d}$ is the spectral dimension, having an upper bound of $\bar{d}_c$ (the chain fractal dimension computed from protein x-ray crystallographic data). Values of $\bar{d}$, previously obtained (3) from Raman rate temperature exponents in Cytochrome C551 and putidaredoxin from P. putida, were reasonable for frozen protein solutions with high salt content, but anomalously low in salt-free solvents. To study such solvent effects, 11 relaxation experiments were performed on frozen aqueous solutions of MbN_3. Concentrations of the protein, NaCl, NaN_3, and glycerol were varied. Spectral dimensions equal, within experimental error, to the chain fractal dimension were obtained for 50% glycerol-50% water, salt-free solvents and for a vacuum dried sample. The results are explained in terms of a variation in the protein-solvent coupling. A sharp transition in the temperature dependence of the Raman relaxation rate at T=6 K is interpreted as reflecting a crossover from vibrational modes of the solvent to those of the protein. Supported in part by NIH Grant GM24488.
   (1)   H. J. Stapleton et al., Phys. Rev. Lett. <u>45</u>, 1456 (1980).
   (2)   J. P. Allen et al., Biophys. J. <u>38</u>, 299 (1982).
   (3)   J. T. Colvin et al., J. Biol. Chem. (sumbitted to).
   (4)   J. T. Colvin et al., Phys. Rev. B (submitted to).
   (5)   H. J. Stapleton, comments Mol. Cell. Biophys. (to be published).

M-Pos19   FLUORESCENCE LIFETIMES OF HUMAN HEMOGLOBIN SUBUNITS AND TRYPTOPHAN MOBILITIES. J. ALBANI*, D. Krajcarski, A.G. Szabo and B. Alpert, Laboratoire de Biologie physico-chimique, Universite de Paris VII, 75251 Paris, France, and Division of Biological Sciences, National Research Council of Canada, Ottawa, Canada K1A OR6.
   The fluorescence lifetimes of tryptophenyl residues in isolated α (monomer) and β (tetramer) chains of human adult hemoglobin were determined using a sync-pumped dye laser system with time-correlated single photon counting detection. The excitation wavelength was 295 nm with a FWHM of 20 ps. The emission wavelength was 340 nm. The data were analyzed using a non-linear least squares procedure developed by one of us (A.G.S.). Liganded (with O_2 or CO) and unliganded (deoxy) forms of the isolated subunits were investigated. The results on the α chain (1 tryptophan) indicated a two component decay with τ_1 and τ_2 values near 80 ps and 2.0 ns, respectively; these values are similar to those observed for the two shorter components in the intact hemoglobin. The fractional contributions of each component depend upon the state of ligation. The two components suggest that there are two conformations in which the tryptophan-heme dispositions are different. The results on the β chain (2 tryptophan/monomer) were best fit with a three component decay with τ values near 90 ps, 2.5 ns and 6.4 ns. These results did not originate from oxidized proteins, because upon oxidation of the thiol group different results were obtained. Spectroscopic and other analytical methods support these latter observations.
*Present address: Department of Pharmacology, University of Texas Health Science Center at Dallas, Dallas, TX 75235.

M-Pos20   DYNAMICS OF THE F-HELIX IN CYANOMETMYOGLOBIN FROM HYDROGEN EXCHANGE
N. Vasant Kumar and N.R. Kallenbach
Department of Biology, University of Pennsylvania,
Philadelphia, PA 19104.

The F-helix in sperm whale myoglobin plays an essential role in the
structure and function of this molecule. This α-helical segment includes
residues 86 to 94, enclosing a large area of heme as well as providing the
essential proximal histidine side chain that ligands heme iron. We have
investigated the hydrogen isotope exchange rate of a set of four consecutive
amide NH protons in this helix using ^{1}H NMR at 360 MHz. The amide resonances
of Ala90, Gln91 and Ser92 have been assigned by use of selective nuclear
Overhauser effect. The temperature dependence of the chemical shifts of these
protons is consistent with the presence of hyperfine interaction from the heme
iron in MbCN. Some implications of these measurements for proton exchange
mechanisms in proteins will be discussed.

M-Pos21   UNFOLDING THERMODYNAMICS OF CHICKEN CARDIAC AQUO METMYOGLOBIN. Leslie A. Holladay,
          Department of Chemistry, Louisiana Tech University, Ruston, LA 71272
    The guanidinium chloride unfolding at pH 8, 25°C, of metmyoglobin isolated from chicken hearts
(Deconinck et al. Biochimie 54:969, 1972) was analyzed using the two-state model. Reversibility of
unfolding exceeded 95%. Tanford's transfer model gave an estimate of 8.3 ± .3 Kcal·mol^{-1} for the
conformational free energy (ΔG_D^o) with $\Delta\alpha$ = 0.20 ± .01. Aune's binding model with a binding con-
stant of 0.6 (Pace and Vanderburg, Biochem. 18:288, 1979) gave an estimate of 8.2 ± .3 Kcal·mol^{-1}
for the conformational free energy with Δn = 36 ± 1. The decrease in ΔG_D^o relative to that of sperm
whale metmyoglobin was 5.3 ± .6 Kcal·mol^{-1}. The temperature dependence of unfolding was obtained
at six guanidinium chloride concentrations from 18°C to 50°C. Plots of $\Delta H_T{}^{app}$ vs. T were linear
($r \geq$ .96) and gave values of ΔH_{313}^{app} markedly dependent on denaturant concentration. Assuming that
the heat of preferential binding is a linear function of denaturant concentration gave an estimate
of ΔH_{313}^o of 48 ± 6 Kcal·mol^{-1}, close to previous estimates for sperm whale metmyoglobin. Two
lysine for arginine replacements in the chicken protein could be responsible for a decrease in
ΔG_D^o from that of sperm whale of up to 2.8 Kcal·mol^{-1} (Puett, J. Biol. Chem. 248:4623, 1973). A
significant change occurs at position 52 within the D helix with the replacement of glutamate by
proline. The resulting shorter possible helix segment has a $<P\alpha>$ value of .94 and has lost a
stabilizing salt bond. The observed decreases, relative to sperm whale, of the unfolding para-
meters Δn and $\Delta\alpha$ of 20%, along with the sequence changes, suggest the D helix may not form in
chicken myoglobin.

M-Pos22   PROTON NUCLEAR MAGNETIC RESONANCE STUDIES OF PORCINE INTESTINAL CALCIUM BINDING PROTEIN.
Judith G. Shelling, Theo Hofmann[+], and Brian D. Sykes. MRC Group in Protein Structure and Function,
Department of Biochemistry, The University of Alberta, Edmonton, Alberta, Canada. [+]From the
Department of Biochemistry, The University of Toronto, Toronto, Ontario, Canada.
    Porcine intestinal calcium binding protein binds two mole equivalents of calcium, with each of
the two binding sites displaying approximately equal affinities for calcium. The data obtained
from the titration of this protein with calcium, in the presence of the competing chelator EDTA,
has been analyzed to determine if the protein binds calcium cooperatively. The protein also binds
two mole equivalents of the lanthanide ions ytterbium and lutetium but, unlike calcium, these ions
bind sequentially, indicating that each of the two binding sites have different affinities for the
lanthanides. The addition of one equivalent of the diamagnetic lanthanide lutetium induced spec-
tral perturbations which were very similar to those induced by the addition of two equivalents of
calcium. The addition of a second equivalent of lutetium had little effect on the protein spec-
trum, while the presence of excess lutetium resulted in protein aggregation. The addition of the
paramagnetic lanthanide ytterbium resulted in lanthanide-induced shifts which were fairly broad at
room temperature. The effect of increasing KCl concentration and increasing temperature upon
these resonances suggested that this broadening arose from the close proximity of protein residues
to the ytterbium ion in the ytterbium-substituted metal binding site of the protein. Although the
apoprotein bound two equivalents of ytterbium, only one equivalent was bound by the calcium-
saturated protein, indicating that one of the sites had a higher affinity for calcium than for the
lanthanide. In the latter case, the protein did not aggregate in the presence of excess ytterbium.

M-Pos23 BINDING OF Ca^{++} AND ITS ANALOGUES ONTO CALMODULIN : A FOURIER-TRANSFORM INFRA-RED STUDY D. Rainteau, F. Lavialle, S. Weinman and A. Alfsen

Calmodulin (CaM) is an ubiquitous Ca^{++}-dependent protein among the living cells. It is involved in regulation of many cellular processes such as cell motility, cyclic nucleotide metabolism, intermediary metabolism, Ca^{++}-transport systems... Calmodulin becomes activated by Ca^{++} binding through conformational changes. The specificity of CaM for Ca^{++} is challenged by different cations like Cd^{++} Zn^{++} and lanthanides. With the aim to compare the effect of Ca^{++} and these analogues on the protein conformation we have performed FT-IR experiments on lyophilized samples. CaM (Ca^{++} depleted), CaM $2Ca^{++}$, CaM 4 Ca^{++}, CaM $CaCl_2$, CaM $CdCl_2$, CaM $ZnCl_2$, CaM $GdCl_3$ and CaM $LaCl_3$ were investigated. In the Amide I region the same features are revealed for CaM^-, CaM $CaCl_2$ and whatever the analogue bound to the protein. In contrast Ca^{++} binding induces significant perturbations in the 1550-1500, 1450-1400 and 1300-1240 cm^{-1} regions. The modifications arise in two steps. The first two Ca^{++} slightly increase the Amide II band width; the second two Ca^{++} produce a large increase of this parameter, accompagnied by an increase in I_{1400}/I_{1440} peak height intensity ratio. This is in agreement with fluorescence and NMR data which detected conformational changes via a two step process. Modifications of the Amide II band width, I_{1400}/I_{1440} and I_{1300}/I_{1200} ratios were found different for each analogue and different from Ca^{++} even if they are known to occupy the same binding sites.
Results will be discussed in terms of biological activity of the protein.

M-Pos24 CALCIUM-BINDING PROTEINS: ^1H NMR STUDIES OF THE α-PARVALBUMIN FROM RAT MUSCLE. T.C. Williams, D.C. Corson, and B.D. Sykes. Department of Biochemistry and the MRC Group on Protein Structure and Function, University of Alberta, Edmonton, Canada T6G 2H7.

As a model for the four-site proteins such as troponin C and calmodulin, parvalbumin's two high-affinity Ca(II)/Mg(II) binding sites have provided significant details of the metal-ion exchange characteristics of these biochemical chelators. Using high-resolution ^1H NMR techniques, we have shown that the *apo*-α-parvalbumin from rat muscle exists as a preformed double-domain chelator at 26°C, its compact tertiary structure differing little from the Ca(II), Mg(II), or Ln(III)-bound forms. Mg(II) titration of the *apo* form induces relatively minor conformational adjustments, ^1H NMR spectral changes being comparable to those observed for the Mg(II)/Ca(II) and Ca(II)/Ln(III) exchange reactions. Whether or not Mg(II) binding is cooperative remains unanswered; however, Mg(II)/Ca(II) exchange appears to slightly favor one site. Laser photo-CIDNP, homonuclear NOE determinations, and pH titrations have been used to assign the ^1H NMR resonances of HIS-26, HIS-48, and PHE-47 and thereby assist in the tentative identification of the more labile Mg(II). Whereas Ca(II)/Lu(III) and Ca(II)/Yb(III) exchange selectively displace the EF-site Ca(II) first (analogous to the exchange characteristics of the β-parvalbumins from carp), Ca(II) has a slight tendency to displace the CD-site Mg(II). This is consistent with the proposal that the CD-site is rigid (compared to the more flexible EF site), allowing easier exchange of metal ions not optimally fitted to its cavity size.

M-Pos25 IDENTIFICATION OF THE CALMODULIN-BINDING DOMAIN OF SKELETAL MUSCLE MYOSIN LIGHT CHAIN KINASE. D.K. Blumenthal, K. Takio, A.M. Edelman, H. Charbonneau, K. Walsh, K. Titani, E.G. Krebs. Howard Hughes Medical Institute and Department of Biochemistry, University of Washington, Seattle, WA 98195

Myosin light chain kinase is a well-characterized Ca^{2+}/calmodulin-dependent enzyme which exists in tissue- and species-specific forms. In the course of determining the amino acid sequence of the enzyme from rabbit skeletal muscle we have identified a peptide fragment which binds to calmodulin with high affinity. The peptide binds to calmodulin with a dissociation constant of approximately 5nM as determined by its ability to inhibit MLCK activity in an assay which is limiting in calmodulin concentration. The peptide is not present in digests of MLCK which have been rendered calmodulin-independent by proteolytic digestion. Thus, the catalytic and calmodulin-binding domains of MLCK represent distinct and seperable regions of the molecule. The calmodulin-binding peptide represents the C-terminus of MLCK and contains a high percentage of basic residues, no acidic residues, and no proline. The sequence shows no significant homology with any protein in the current protein sequence database (>2500 protein sequences). In order to study the interactions of calmodulin and MLCK we have prepared a synthetic peptide corresponding to the calmodulin-binding sequence of MLCK. The peptide binds to calmodulin with a dissociation constant of 0.9nM. The higher affinity of this peptide relative to the peptide obtained by digestion of MLCK may reflect alterations in the latter resulting from the harsh conditions used in digestion and/or purification.

The work described here represents the first structural information regarding the calmodulin-binding domain of a calmodulin-dependent enzyme.

M-Pos26   CHANGE IN SULFHYDRYL GROUP MICROENVIRONMENT AND TERTIARY STRUCTURE OF αCRYSTALLIN IN PHO-
          TOSENSITIZED REACTIONS. S.K.Bose, K.Mandal and B.Chakrabarti(intr. by A.Adler), Eye Res-
earch Institute and Harvard Medical School, Boston, Mass 02114.

Investigations to date suggest that light is a factor causing various changes in lens protein dur-
ing aging and cataratogenesis. We have irradiated bovineα-crystallin with white light in the pres-
ence of methylene blue(MB) or riboflavin(RF) as photosensitizers and measured changes in fluorescen-
ce of Trp, photoproducts of Trp, and of MIANS(Maleimidylanilino-naphthalene sulfonate)-labeled SH
groups. Circular dichroism(CD) of the irradiated samples was also monitored. Photolyzed samples show
decreased Trp emission, increase in fluorescence of Trp-photoproducts such as N-formylkynurenine
(NFK) and a red shift(420 to 433nm) in λ_{em} of the MIANS-labeled SH groups. The red shift could not
be prevented significantly by using inhibitors specific for active oxygen species($^1O_2,O_2^-,\cdot OH,H_2O_2$)
in the photolytic solutions, indicating that the photosensitizer by itself plays a major role in
this process. In contast,α-crystallin irradiated with 340nm light in the presence of the sensitizer
NFK(added exogeneously or generated endogeneously by irradiating with 300nm light) shows no such red
shift. In the presence of MB or RF, the far-UV CD(secondary structure) of the protein remains uncha-
nged even after 6 hrs of irradiation, but distinct changes are observed in the near-UV CD(tertiary
structure) after 25 mins of photolysis; after 6 hrs, the spectrum is completely disrupted. We sugg-
est that in MB or RF-photosensitized reactions, the tertiary structure changes followed by an un-
folding of the protein, thereby causing SH groups to change from nonpolar to polar environments as
manifested in flurescence and CD. Since RF is present in the lens, the phenomena could be signifi-
cant in terms of changes seen in cataractous and older lenses.

M-Pos27   **TEMPERATURE AND IONIC STRENGTH EFFECTS IN THE IONIZATION OF INDIVIDUAL AMINO
          GROUPS IN METHYLATED LYSOZYME.** Mark Payne, Thomas Gerken, Robert Waller and Dorr
Dearborn, Depts. of Pediatrics and Biochemistry, Case Western Reserve University, Cleveland, Ohio.

The reductive methylation of protein amino groups with ^{13}C enriched formaldehyde and NaCNBH$_3$ and
subsequent carbon-13 NMR studies offers an ideal approach for the study of the microenvironments
and ionization states of protein amino groups. This probe has been used to study the titration
behavior (pK$_a$ and chemical shift limits) of the 7 individual amino groups in hen eggwhite lysozyme
(HEWL). Based on chemical perturbation methods four of the seven dimethylamino group resonances
have been assigned to specific residues, while the remaining resonances have been tentatively
assigned. Two assigned resonances are involved in ion pair interactions showing the existence in
solution of interactions proposed by X-ray crystallographers [see JBC 257 2894 (1982)]. The pK$_a$
values for each dimethylamino group have been obtained as a function of temperature and ionic
strength for the native protein and several covalently modified derivatives. Increasing the temper-
ature between 0 and 49°C results in a decrease in pK$_a$ values of over one pH unit which is
accompanied by a decrease in stability of the protein at elevated pH. No major differences in the
temperature dependencies of the pK$_a$ values are found between amino groups involved in ion pair
interactions compared to the amino groups in other types of interactions. Plots of pK$_a$ vs. 1/T are
biphasic, possibly reflecting this protein's reported temperature dependent conformational change
[PNAS 72,2095(1975), Biochemistry 23,3522(1984)]. Increasing ionic strength results in large in-
creases in pK$_a$ values which also parallel an apparent increase in the stability of the protein at
high pH. The effect of the inhibitor, GlcNAc, on the amino group titrations will also be
discussed. (Supported by NIH grant GM 25930).

M-Pos28   FLUORESCENCE DECAY STUDIES OF ENZYME I OF THE PHOSPHOTRANSFERASE SYSTEM. Paolo Neyroz,
Bonnie Bassler, Joseph M. Beechem, Norman D. Meadow and Ludwig Brand. The Johns Hopkins
University, Baltimore, MD., 21218. (Intr. by Saul Roseman).

Enzyme I catalyzes the first step of the reaction that allows phosphorylation and concomitant
translocation of sugars across the bacterial membrane. Previous studies (Kukuruzinska et al, J.
Biol. Chem., 259, 11679 (1984)) have shown that the enzyme exists in a temperature-dependent
monomer-dimer equilibrium. The intrinsic fluorescence decay can be described in terms of a
biexponential. At 2°C (monomer) the decay constants are $\tau_1=2.7$ns, $\alpha_1=0.18$, $\tau_2=7.5$ns, $\alpha_2=0.82$. The
short decay constant is associated with a fluorescence emission maximum at 335nm while the long
decay constant is associated with a fluorescence emission maximum at 340nm. At 24°C (dimer) the
decay constants are $\tau_1=4.4$ns, $\alpha_1=0.50$, $\tau_2=7.7$ns, $\alpha_2=0.50$. In addition to the change in α_1/α_2, the
monomer-dimer conversion can be measured by nanosecond time-resolved emission anisotropy. We were
able to measure a correlation time of 71 ns at 2°C (monomer) and one of 102 ns at 24°C (dimer).
Iodide quenching studies indicate that the emitting species with the short decay time is more
accessible to the quencher. Since each EI subunit contains two tryptophan residues, this
preferential quenching may reflect the specific locations of the tryptophans in the protein. The
results we have obtained on EI will be presented and discussed in detail. (Supported by NIH grant
No. CA21901).

M-Pos29   CATALYSIS IN METALLOENZYMES: CARBOXYPEPTIDASE A, by Kim Ferris and Leland C. Allen, Princeton University, Department of Chemistry, Princeton, NJ 08544. Intro. by Professor Thomas G. Spiro, Princeton University.

Carboxypeptidase A is a zinc metalloenzyme which hydrolyses the C-terminal amino acid of a polypeptide. The currently proposed reaction pathways are: 1) anhydride formation, 2) nucleophilic attack on the substrate carbonyl carbon by a zinc-bound hydroxyl, and 3) general base catalysis. We have employed electronic structure calculations and the recently determined 1.7 Å resolution X-ray structure to evaluate these three mechanistic hypotheses. All activity linked active site amino acid residues plus formamide as substrate were included in ab initio molecular orbital calculations. Zinc and its three fixed ligands were represented by an 18 electron pseudopotential. Two striking conclusions have come from our computations: (a) the preferred reaction pathway indicates a transition state that is approximately midway between that of the hypothesized zinc hydroxyl and general base mechanisms, (b) the transfer of a proton from a substrate oxygen to its amide nitrogen, long believed to be accomplished by Tyr 248, seems instead to be carried out by a water molecule. Site specific mutagenesis recently carried out by Rutter et al at UCSF has found that enzyme activity is not diminished by replacement of Try 248 by a phenylalanine.

M-Pos30   GUANINE NUCLEOTIDE EXCHANGE BY TUBULIN. L.T. Baty, J.J. Correia, H.B. Croom, and R.C. Williams, Jr., Dept. of Molecular Biology, Vanderbilt Univ., Nashville, TN   37235

Phosphocellulose-purified tubulin (Tb), after gel filtration into a nucleotide free buffer containing 1 mM Mg^{2+}, has 1.8 to 2.0 moles of guanine nucleotide (less than 10% of which is GDP) bound per mole of Tb. As reported [Baty et al., J. Cell Biol. 99, 38a (1984)], substoichiometric exchange of GTP is observed when this Tb is incubated with [^{3}H]GTP. This exchange of < 1 mol GTP/mol Tb does not depend on time of incubation (> 5 min), temperature (0-35°C), concentration of GTP (> 0.1 mM), capacity of Tb to assemble, or composition of buffers (PIPES, MES, phosphate). Partial exchange is not a result of radiochemical impurity of the [^{3}H]-nucleotide, as shown by thin-layer chromatography and HPLC. Removal of a contaminating nucleotide diphosphokinase activity by DEAE-cellulose chromatography or by $(NH_4)_2SO_4$ precipitation also has no effect. The concentration dependence of [^{3}H]GTP exchange is approximately hyperbolic with a plateau at a value < 1 mol GTP/mol Tb. [^{3}H]GDP exchanges more readily for bound guanine nucleotide than does [^{3}H]GTP, although the concentration-dependence of the fraction of nucleotide exchanged is non-hyperbolic, indicating that there may be at least two populations of exchangable binding sites. The nature of these two kinds of "exchangable" sites may be partially dependent upon the initial nucleotide content of the Tb. The ratio of GTP to GDP bound to Tb decreases as the Mg^{2+} concentration in the buffer decreases. These results may explain variability in the ratio of GTP to GDP bound to Tb and the variation of reported nucleotide exchange behavior of Tb prepared by different methods. (Supported by NIH Grants GM 25638 and T32 GM 07319.)

M-Pos31   MN(II) BINDING BY AEQUORIN, M. D. Kemple, B. D. Ray, B. D. Nageswara Rao, IUPUI, Indpls., IN 46223, G. K. Jarori, Ca. Inst. of Tech., Pasadena, CA   91125, and F. G. Prendergast, Mayo Med. School, Rochester, MN   55901

Aequorin is a bioluminescent protein from the jellyfish Aequorea forskalea. Light emission occurs as a consequence of the oxidation of a chromophore which is noncovalently bound by the protein. The bioluminescent reaction is triggered by the binding of Ca(II) and Ln(III) ions, and is inhibited by Mn(II) and Mg(II). The Ca(II) concentration effect curves for bioluminescence of aequorin indicate that there are at least three Ca(II) binding sites on aequorin. EPR measurements show that the stoichiometry of Mn(II) binding to aequorin, however, is 1:1 with a dissocia-constant of $\sim$ 30 µM. Mn(II) inhibition of aequorin may be based upon the fact that Mn(II) has only one binding site. Competition of other ions for the Mn(II) site will be described. (Supported in part by grants NSF PCM-8022075, and NIH GM 30178. Acknowledgment is made to the donors of the Petroleum Research Fund, administered by the American Chemical Society.)

M-Pos32   NMR STUDIES OF THE SUBMAXILLARY MUCINS FROM SHEEP AND PIG. Thomas A. Gerken, Departments of Pediatrics and Biochemistry, Case Western Reserve University, Cleveland, Ohio 44106.

Both carbon-13 and proton NMR spectroscopy are being used to determine the detailed solution structure and dynamics of mucous glycoproteins. Carbon-13 NMR studies of pig submaxillary mucin (PSM) will be compared to the previously reported carbon-13 studies of the relatively simple ovine submaxillary mucin (OSM) [Biochemistry 23, 1485 (1984)] and the results of an initial proton NMR study of both OSM and PSM will be discussed. Well-resolved natural abundance carbon-13 spectra are obtained from the highly viscous PSM samples indicating the presence of substantial internal segmental mobility , similar to OSM. Most resonances have been assigned to specific carbohydrate and peptide carbons. The anomeric carbon resonances have chemical shifts that are sensitive to carbohydrate structure, thus allowing the determination of the oligosaccharide side chain distribution. On the basis of the ^{13}C relaxation times no significant differences are detected between the petide core mobilities of PSM and OSM (at 67.9 MHz). The mobilities of the carbohydrate side chains in PSM appear to be slightly more restricted compared to OSM. The removal of sialic acid from PSM produces no detectable long range inter-residue perturbations in its carbon-13 NMR spectra, although the proton spectra of asialo PSM (and asialo OSM) show the removal of sialic acid causes a small shift in the threonine methyl resonance. These results suggest the sialic acid residue may be folded back towards the GalNAc residue to which it is attached and may interact with the peptide core. Such a conformation for the sialic acid residue is suggested from our ^{13}C NMR studies on OSM and Berman's NMR studies on oligosaccharides [Biochemistry 23, 3754 (1984)]. (supported by the Cystic Fibrosis Foundation)

M-Pos33   IS YEAST ALCOHOL DEHYDROGENASE A GOOD CONTROL FOR RADIATION INACTIVATION ANALYSIS?
M.D. Suarez, E.S. Kempner and S. Ferguson-Miller. Biochemistry Dept. Michigan State University, E. Lansing, MI., and NIH-NIADDKD, Bethesda, MD.

Yeast alcohol dehydrogenase is commonly used as a standard for target analysis of enzymes. Our radiation studies on purified YADH reveal that after irradiation at -135°C in the frozen state, the decay in activity with increasing dose can be described by a simple exponential that extrapolates to 30% rather than 100% of the initial activity. The large drop in activity observed after low doses suggests that more damage than that caused by the direct effect of radiation is occurring. In fact, addition of water irradiated at low temperature results in considerable inactivation of the enzyme.

The high susceptibility to radiation of this cysteine-rich enzyme is probably due to the large number of sulfhydryl groups, which are extremely labile to radiolytic products. The presence of an excess of small sulfhydryl-containing molecules during irradiation and thawing decreases inactivation at low doses and changes the slope of the inactivation curve in the direction of a smaller molecular weight. The extent of protection varies depending on specific experimental conditions, but at the highest level of protection observed the inactivation curve extrapolated back to 100% of the initial activity and gave a molecular weight estimate (67,000) that is consistent with the functional unit of YADH being a dimer (76,000), rather than a tetramer, as is often assumed. These results indicate that unusual care may be necessary when applying radiation inactivation analysis to some sulfhydryl-containing enzymes. Supported by NIH Grant GM 26916.

M-Pos34   NMR STUDIES OF THE EXCHANGE RATES OF THE AMIDE PROTONS OF d-BIOTIN AND ITS DERIVATIVES.
D. C. Fry, T. Fox, M. D. Lane & A. S. Mildvan, Johns Hopkins Medical School, Baltimore, MD 21205

The enzymatic carboxylation of d-biotin involves the replacement of the 1'-NH amide proton by $-COO^-$. Transfer of saturation and T_1 measurements were used to determine the 1'- and 3'-NH proton exchange rates with water of free d-biotin (B), its methyl ester (BE), O-heterobiotin (OB), des-thiobiotin (DB), and imidazolidone (IM). At pH 7.5 and 25° the exchange rate of the 1'-NH of B (58 s^{-1}) is similar to the carboxylation rates of enzyme-bound B (15 to 74 s^{-1}), indicating that deprotonation can precede carboxylation. Both H^+- and OH^--catalyzed exchange were faster at 1'-NH than at 3'-NH in B, BE, and OB but not in DB or IM, implying steric inhibition of exchange at 3'-NH by the side chain. At 3'-NH both H^+- and OH^--catalyzed exchange rates followed the order: DB>IM>B>BE>OB, while at 1'-NH the order was: B>BE>DB>IM>OB. While all other exchange rates were first order in [H^+] or [OH^-], that at 1'-NH of B and BE displayed an unprecedented 2nd order dependence on [H^+]^2, suggesting the protonation of both the carbonyl O and the 1'-N but not the 3'-N in the rate limiting step. Simple first order H^+-catalyzed exchange with OB indicates that sulfur stabilizes the H_2B^{2+} and H_2BE^{2+} species, possibly by transannular bonding to the carbonyl carbon. H^+-catalyzed exchange at the 1'-NH of B had a lower enthalpy of activation (6 Kcal/mol) than did the 3'-NH of B and the 1'- and 3'-NH of OB (9 Kcal/mol). The rapid exchange of the 1'-NH and facile protonation of the amide carbonyl of B under mild conditions strongly support biotin carboxylation mechanisms involving enolization of the ureido system.

M-Pos35   INTERACTION OF LYSINE RESIDUES WITH THE METAL-THIOLATE CLUSTERS IN METAL-LOTHIONEIN. J. Pande*, M. Vašák, D. Gilg, and J.H R. Kägi, Biochemisches Institut der Universität Zürich, Winterthurerstrasse 190, CH-8057 Zürich, Switzerland.

Metallothioneins are unique diamagnetic metal-thiolate cluster proteins. Both the vertebrate and invertebrate forms contain, besides their large cysteine content (>30%), up to 14% lysine plus arginine. In the amino acid sequences, the basic residues are juxtaposed to cysteine and have been suggested to play a role in neutralizing the excess negative charge of the metal-thiolate complexes (Kojima et al., PNAS 73, 3413, 1976). To document such a function, we compared the susceptibility of the lysine residues in native metallothionein and in the metal-free S-carboxamidomethyl derivative towards alkylation by trinitrophenylsulfonate (TNPS). The results show a more than 20fold lower initial rate of reaction with the metal-containing as opposed to that with the metal-free form, indicating a protective effect of metal complex formation on the lysine residues, the degree of protection being dependent on the nature of the metal. The eventual modification of the lysines by TNPS leads to loss of metal from the protein and to changes in the spectropolarimetric properties of the latter. The lowered chemical reactivity of the lysines is associated with an upward shift of their average pK_a from 10.3 in the metal-free to 10.9 in the metal-containing form as measured by ^{1}H NMR and potentiometric pH titration studies (Vašák et al., Experientia, in press). The results imply a mutual intramolecular electrostatic stabilization of the seven to eight positively charged basic residues and the two threefold negatively charged metal-thiolate clusters.

M-Pos36   C.D. STOPPED FLOW KINETICS OF ACID DENATURATION OF THE HEMOGLOBIN SYSTEM. By C.
Fronticelli, E. Bucci, Dept. of Biological Chemistry, Univ. of Md., School of Medicine,
Baltimore, MD 21212

Human hemoglobin and its isolated β subunits were denatured by addition of HCl so to reach a
final pH value ranging from 1.9 to 2.4. The β subunits were alkylated in both the $\beta93$ and $\beta112$
cysteines, this treatment makes the β subunits monomeric ($\beta1AA$). The kinetic of acid
denaturation of the two proteins was followed spectropolarimetrically in the millisecond time
range measuring the changes in circular dichroism at 225 nm. Computer simulation were performed
assuming a pseudo first order reaction. At all pH values, in both systems, the decay of
ellipticity could be simulated by two exponentials. The initial ellipticity of the solutions,
obtained by extrapolation at zero time, were those expected for the native proteins. The half
times of the decay were longer in the hemoglobin system than in the $\beta1AA$. The data suggest that
in the tertiary structure of hemoglobin there are at least two sets of different domains which
unfold at different rates upon exposure to acid.

Protein	Final pH	$k1$ (sec-1)	% Amplitude of $k1$	$k2$ (sec-1)	$t1/2$ (sec)
Hemoglobin	1.9	2.67 ± 0.22	68 ± 06	0.14 ± 0.11	0.16
	2.4	1.03 ± 0.13	59 ± 10	0.15 ± 0.03	0.53
$\beta1AA$	2.0	5.86 ± 0.70	73 ± 10	0.22 ± 0.12	0.08
	2.4	2.51 ± 0.26	63 ± 04	0.04 ± 0.02	0.28

M-Pos37   A MOLECULAR MECHANISM FOR THE ALLOSTERIC EFFECT OF INORGANIC PHOSPHATE IONS ON HUMAN
NORMAL ADULT HEMOGLOBIN, by A. K.-L. C. Lin, I. M. Russu, and C. Ho, Department of Bio-
logical Sciences, Carnegie-Mellon University, Pittsburgh, PA 15213, U.S.A.

High-resolution ^{1}H nuclear magnetic resonance (NMR) spectroscopy has been used to investigate
the contributions of individual sites in human normal adult hemoglobin (Hb A) to the allosteric
effect of inorganic phosphate ions. The individual pH-titration curves for twenty-two surface
histidyl (His) residues have been measured by ^{1}H NMR for 1.5 mM deoxy Hb A and HbCO A solutions at
29°C in the absence and in the presence of 100 mM inorganic phosphate ions. The results indicate
that the inorganic phosphate ions alter the electrostatic environment and the ionization properties
of sixteen of the surface His residues in deoxy Hb A and four to six of the surface His residues in
HbCO A. For some of these His residues, such as $\beta2$ His and $\beta143$ His, the changes in the individual
titration curves are consistent with direct binding of the inorganic phosphate ions to these sites.
For the remaining His residues, we have found that inorganic phosphate ions lower their pK_a values
and/or increase the Hill coefficient for cooperativity in hydrogen ion titration. These findings
suggest that inorganic phosphate ions could also affect Hb function by perturbing the intramole-
cular electrostatic interactions, both tertiary and quaternary, within the charge matrix of the Hb
molecule. The implications of these results for the allosteric effect of inorganic phosphate ions
and the molecular mechanism of the Bohr effect will be discussed. [This work is supported by a
research grant from the NIH (HL-24525)].

M-Pos38   RESONANCE RAMAN SPECTRA OF DEOXY AND CARBONMONOXY HEMOGLOBINS OF THE BLOODWORM, GLYCERA
DIBRANCHIATA, S. D. Carson, J. D. Satterlee, I. Constantinidis, and M. R. Ondrias,
Department of Chemistry, University of New Mexico, Albuquerque, NM 87131.

In recent years, the dynamics of ligand binding in heme proteins has been the subject of a
great deal of investigation. It has been shown that changes in both tertiary and quaternary
structure play major roles in this process. Distal heme pocket perturbations result in signifi-
cant changes in ligand binding kinetics. The hemoglobin of the bloodworm Glycera dibranchiata is
of interest because it exhibits both quaternary and tertiary differences from mammalian hemo-
globins. The protein consists of multiple monomeric and polymeric components, with the distal
histidine being replaced by leucine in at least one constituent of the monomeric form. Recent
experimental data have shown hemoglobin Glycera has an extremely high ligand association and
dissociation rate constants.

Resonance Raman spectra is particularly suited to the evaluation of the structural effects of
the unique protein environment of Glycera hemoglobin on the kinetics and thermodynamics of the
ligand binding process. Resonance-enhanced vibrational modes of the porphyrin macrocycle are
sensitive to changes in heme electron density, Fe spin state and porphyrin core size. Any effort
to correlate observed spectral differences with ligand binding kinetics must consider both steady-
state and time-resolved data. Resonance Raman spectra are presented for deoxy and carbonmonoxy
Glycera hemoglobins and the photolytic deoxy transient species generated within 10 ns of CO
photolysis. The relationship between the known structural perturbations at the heme active site
in Glycera hemoglobin and its ligand binding kinetics will be discussed.

M-Pos39   A RESONANCE RAMAN STUDY OF LIGAND BINDING GEOMETRY IN GLYCERA DIBRANCHIATA CARBON-
MONOXY HEMOGLOBIN. S. D. Carson, J. D. Satterlee, and M. R. Ondrias, Department of
Chemistry, University of New Mexico, Albuquerque, NM 87131.

The hemoglobin of the bloodworm, Glycera dibranchiata has been the object of considerable
investigation in recent years due to its unique features: 1) the protein consists of both
monomeric and polymeric forms, with the number of components in the former being a subject of
some controversy, 2) both amino acid sequencing and X-ray crystallographic data have shown that
the distal histidine is replaced by leucine in at least one of the monomeric components, thus
precluding any type of distal bonding interaction with the heme binding site, and 3) monomeric
Glycera hemoglobin exhibits extremely rapid ligand kinetics.

Using ^{12}CO and ^{13}CO liganded protein and 406 nm laser excitation to minimize ligand
photolysis, we have identified multiple $\nu(Fe-CO)$, $\nu(C-O)$ and $\delta(Fe-C-O)$ bands in the
resonance Raman spectra of monomeric and polymeric Glycera hemoglobins. These data were then
employed in an isolated three-body oscillator calculation to obtain approximate values for the
Fe-C-O bond angle. Evidence for heme heterogeneity and distortion from a linear Fe-C-O bond will
be discussed.

M-Pos40   RESONANCE RAMAN STUDIES OF STEADY-STATE AND DYNAMIC HEME-PROTEIN INTERACTIONS IN
PEROXIDASES. R. G. Alden[a], J. A. Shelnutt[b], and M. R. Ondrias[a], [a]Department
of Chemistry, University of New Mexico, Albuquerque, NM 87131 and [b]Division 1154,
Sandia National Labs, Albuquerque, NM 87117.

Resonance Raman scattering has proven to be a powerful probe of the interactions between the
heme active site and protein matrix in a wide variety of heme proteins. Recently time-resolved
techniques have been employed to probe the dynamics of those interactions in hemoglobins and
oxidases. Here we present the initial results of a steady-state and transient Raman study of
heme peroxidases. Specifically, we have examined the liganded (CO and NO) and unliganded
steady-state ferrous forms as well as the transient heme species generated within 10 nsec. of
ligand photolysis of a variety of peroxidases (horseradish peroxidase, lactoperoxidase,
catalase). The dependence of the electron density marker band (ν_4) of ferrous horseradish
peroxidase upon pH has also been determined. It correlates with shifts in the Fe-His mode but
the correlation is qualitatively different from that observed for hemoglobins and myoglobins.
The transient behavior of the peroxidases will be compared and contrasted to that of hemoglobin
and cytochrome oxidases.

M-Pos41   IRON LIGATION AND ELECTRONIC STRUCTURE OF THE HEMES IN HUMAN AND CANINE MYELOPEROXIDASE
BY RAMAM DIFFERENCE SPECTROSCOPY* R. Stump, J. Oliver, University of New Mexico,
Albuquerque, NM 87131, J. A. Shelnutt, Sandia National Laboratories, Albuquerque, NM 87185.

Myeloperoxidase from dog and human in the native and dithionite-reduced form have been compared
by by resonance Raman difference spectroscopy. The protein contains two heme-like chromophores
thought to be iron chlorins. Our data are consistent with this interpretation based on "extra"
lines appearing in the otherwise porphyrin-like spectrum. For the reduced form, frequencies of
core-size and oxidation-state marker lines indicate significant differences in the canine and human
myeloperoxidases with the canine protein having the higher frequency Raman lines. The finding is
consistent with higher charge in the antibonding orbitals for the human peroxidase. The marker line
frequencies for both proteins compare favorably with those of 5-coordinate, high-spin-hemes. For
the native Fe(III) forms differences of up to 5 cm^{-1} are found for the marker lines; again, the
canine protein exhibits the higher frequencies of the two. The marker line frequencies are in the
range of the high spin, 6-coordinate hemes, although marker line frequencies for canine myeloper-
oxidase are shifted toward 5-coordinate, high spin heme frequencies. In neither protein is the
vinyl stretching mode, expected in the 1620-1630-cm^{-1} region, observed. The mode at 244 cm^{-1}
between pH5 and pH7 in the reduced form is assigned to an Fe-histidine stretch in analogy with the
pH-dependent mode in horseradish peroxidase appearing at 244 cm^{-1} below pH 6.0.

M-Pos42   PICOSECOND TIME RESOLVED RESONANCE RAMAN STUDIES OF PHOTODISSOCIATED COHb AND COMb

E. W. Findsen,* J. M. Friedman,** M. R. Ondrias,* and S. R. Simon,*** *Dept. of Chem.,
U. of N.M., Albuquerque, N.M. 87106, **AT&T Bell Laboratories, Murray Hill, N.J. 07974,
***Dept. of Biochem., SUNY at Stony Brook, Stony Brook, N.Y. 11794

We report the first picosecond time resolved Raman spectra of hemoglobin (Hb) and myoglobin (Mb)
generated with blue picosecond pulses (25 ps) of sufficient intensity to completely photo-
dissociate the starting ligated sample. It is observed that for both R and T state ligated Hb's,
the peak frequencies in the spectrum of the deoxy transient are the same as 25 ps as those
observed at 10 ns subsequent to photodissociation. In particular the large R-T differences in
the frequency of the stretching motion of the iron-proximal (ν_{Fe-His}) histidine mode detected in
previously reported ns resolved spectra are also evident in the ps spectra. These values reflect
not only the effect of the quaternary structure but also the long lived (>100's of n.s.) in-
fluence on the deoxy heme of the ligend induced modifications of the R and T structures. In
contrast to Hb, the low frequency Raman spectrum of the photodissociated COMb is at 25 ps iden-
tical to that of equilibrium deoxy Mb. This indicates a vary rapid loss of protein structural
memory with respect to ligand binding. The implications of these findings with respect to both
the distribution of strain energy within the ligated protein and the origin of the time course
for geminate recombination are discussed.

M-Pos43   LOW- TO HIGH-SPIN CONVERSION OF HEME BOUND TO HISTIDINE-RICH GLYCOPROTEIN

by Mary K. Burch and William T. Morgan, Dept. of Biochemistry, Louisiana State
University Medical Center, New Orleans, LA 70112.

Rabbit serum histidine-rich glycoprotein (HRG, Mr 94000 Da; 11.2 mole % histidine) binds 20-25
equivalents of mesoheme and 15-20 equivalents of divalent Zn, Co, Ni, and Cu. Although its
physiological function is unknown, HRG interacts with a variety of macromolecules, such as
heparin, thrombospondin, and plasminogen. In particular, the interaction with heparin may be
modulated by the presence of metal ions bound to HRG. We have concentrated on a program to
identify regions within the protein which bind heme, metals and other ligands and to determine the
overlap among sites. The mesoheme bound to HRG is primarily low-spin iron(III) as determined by
absorbance and epr measurements. Addition of Cu(II) or Ni(II) causes a dramatic change in the
absorbance spectrum of the 1:1 heme:HRG complex with the appearance of a new band at 616 nm,
usually attributed to high-spin heme complexes. These absorbance changes are not seen until at
least three equivalents of metal have been added, indicating separate heme and metal binding sites
for the first several equivalents of metal added. In contrast, Zn(II) and Co(II) have only a
small effect on the 1:1 heme:HRG complex even at high stoichiometries (up to 20 equivalents) of
metal per protein. (Supported by grants to M.K.B., NIH-GM-09797 and to W.T.M., NIH-HD-14481.)

M-Pos44   EFFECTS OF DPG ON COOPERATIVITY AND REGULATION IN HUMAN HEMOGLOBIN.   Benjamin W. Turner

and Gary K. Ackers, Biology Dept., The Johns Hopkins University, Baltimore, Maryland
21218.

The thermodynamic linkage between oxygen binding and dimer-tetramer assembly has been investi-
gated as a function of DPG (2,3-diphosphoglycerate) concentration (0-4 mM DPG) at pH 7.4, 0.1 M
Tris, 0.1 M NaCl, 1.0 mM EDTA, 21.5°C. Oxygen binding curves were measured at a series of DPG and
hemoglobin concentrations. Kinetic and analytical gel chromatography experiments were carried out
over the same range of DPG concentrations to explore subunit assembly in deoxy- and fully oxygenated
hemoglobin. All these data were fit simultaneously to the model-independent thermodynamic para-
meters forbinding of DPG by dimers and tetramers in all oxygenation states. Results include deter-
minations of: (a) Free energies for the entire thermodynamic linkage. (b) The effect of DPG
upon the regulatory free energy at each stage of ligation. (c) The distribution of intermediate
ligation states and cooperativity of oxygen binding in the DPG saturated tetramer. All four of the
tetramer Adair oxygen binding constants exhibit a significant DPG dependence. While the regulatory
effects of DPG are profound, the cooperativity and distribution of intermediate ligation states are
virtually unchanged. These findings have required the resolution provided by simultaneous analysis
of data covering wide ranges of the experimental variables. Supported by a grant from the National
Science Foundation.

M-Pos45   STRUCTURAL DIFFERENCES BETWEEN R&T STATES OF CARBOXYHEMOGLOBIN COMPOUNDS Chance,M.[1], Chance,B[1], Powers,L.,[2]Parkhurst,L.[3],Kumar,C.,[3]&Chou,Y. H.[1] 1-Dept. of Biochemistry and Biophysics, University of Pennsylvania & Inst. for Structural and Functional Studies,Phila. Pa. 2-AT&T Bell Laboratories,Murray Hill N.J.3-Dept. of Chemistry,University of Nebraska,Lincoln Neb.

The two state model of hemoglobin has been popular for many years but the description of the structural differences between the two states has been established only for the oxy to deoxy transition. X-ray absorption spectroscopy provides a method of precisely determining the interatomic distances of iron and its ligands in heme proteins. We have studied the CO complexes of various hemoglobins in order to detect structural differences between the R and T states represented by the different compounds. Our results are consistent with an earlier study by Chance et. al. (Biochem.,1983,v.22,p.3820),which showed that when myoglobin-CO is photolyzed,the resultant geminate state trapped at $4^{\circ}K$ has an expanded iron-pyrrole nitrogen distance(Fe-Np) and a slightly expanded Fe-CO distance compared to the R state. Carp HbCO makes a well characterized shift from R to T states when the pH is lowered or upon the addition of organic phosphates(IHP). We found that not only is the Fe-CO bond enlarged upon the switch to the T state,but the distribution of the bond population is broader. A comparison of Uriches HbCO and Leghemoglobin CO compounds,which also represent R and T states,generally follows the same trend.

M-Pos46   EVIDENCE FOR EXCHANGEABLE PROTONS ASSOCIATED WITH THE HEME IN CYTOCHROME OXIDASE. Y.-c Ching, P. V. Argade, and D. L. Rousseau, AT&T Bell Laboratories, Murray Hill, NJ 07974

Cytochrome c oxidase, the terminal enzyme in the electron transport chain, generates a proton gradient across the inner mitochondrial membrane. To determine if the hemes may be playing a direct role in the proton translocation process, we have compared the resonance Raman spectra of cytochrome oxidase in protonated and in deuterated buffers. We analyze the data by taking advantage of assignments of modes made by full spectral separation of the hemes. For the fully reduced enzyme we find differences in many modes of the cytochrome a heme and also in a few modes of the cytochrome a_3 heme. For both hemes no changes are found in modes ascribed as carbonyl stretching frequencies of the formyl groups. No changes were detected in the iron-histidine stretching mode of cytochrome a_3. Thus, these data supply strong evidence for exchangeable protons on both cytochrome a and a_3. This is consistent with models for proton translocation in which the heme redox centers participate directly. Furthermore, labile protons at one of the hemes may be utilized in the generation of H_2O in the oxygen reduction process.

M-Pos47   AN ASSESSMENT OF HEME-HEME INTERACTION IN CYTOCHROME OXIDASE. P. V. Argade, Y.-c. Ching, and D. L. Rousseau, AT&T Bell Laboratories, Murray Hill, NJ 07974

Cytochrome c oxidase contains two heme chromophores-cytochrome a which is an electron transport element and cytochrome a_3 which is the exogenous ligand binding site. To assess the influence of changes in redox state and ligand binding at cytochrome a_3 on cytochrome a, we compared the resonance Raman spectrum of cytochrome a when CO is bound to ferrous cytochrome a_3 to the resonance Raman spectrum of cytochrome a when CN^- is bound ferric cytochrome a_3. In addition we compared the Raman spectrum of cytochrome a in the fully reduced enzyme to that immediately following (10 nsec) photodissociation of CO from cytochrome a_3. We find that the modes in cytochrome a associated with spin equilibrium and heme electron density are the same independent of the state of cytochrome a_3. However, some of the low frequency modes of cytochrome a appear to change with changes in cytochrome a_3. These changes may result from differences in the heme pocket structure of cytochrome a. Possible mechanisms of heme-heme interaction will be discussed.

M-Pos48 ISOLATION OF A FULL LENGTH cDNA CLONE FOR HUMAN MYOGLOBIN R. Varadarajan and <u>Steven G. Boxer</u>, Dept. of Chemistry, Stanford University, Stanford, CA. 94305

A full length cDNA clone for human myoglobin has been isolated from a human skeletal muscle cDNA library (1). A 2kb long EcoR1-EcoR1 restriction fragment of the seal myoglobin gene (2) was used as a probe. This fragment contained the 223 bp long central exon of the seal gene, which has substantial sequence homology with the human gene. The clone for human myoglobin as isolated has a cDNA insert approximately 1kb long. It has 5' and 3' untranslated regions of approximately 90 and 530 nucleotides, respectively. The translated region was sequenced and corresponds exactly to the sequence predicted from the human myoglobin gene (3). Efforts to express myoglobin in E. coli are now underway. We thank Professors Kedes (Stanford) and Jeffreys (Leicester) for invaluable assistance at various stages of this work.

(1) Gunning et al., Mol. Cell Biol. <u>3</u>, 787-95(1983); (2) Blanchetot et al., Nature <u>301</u>, 732-734 (1983); (3) Weller et al., EMBO J. <u>3</u>, 439-46(1984).

M-Pos49 MAGNETIC CIRCULAR DICHROISM CHARACTERIZATION OF SPLEEN GREEN HEME PROTEIN
<u>M. IKEDA-SAITO, M. SONO, and J. H. DAWSON</u> Department. of Biochemistry and Biophysics, Univ. of Pennsylvania School of Medicine, Philadelphia, PA. 19104 and Department of Chemistry, University of South Carolina, Columbia, SC. 29208
Magnetic circular dichroism (MCD) spectroscopy has been used to probe an unique, yet unidentified, prosthetic group of green heme protein (GHP) isolated from bovine spleen. All of the protein forms examined in this work, including resting ferric form (high spin), its Cl^- (high spin) and CN^- (low spin) complexes, and native ferrous (high spin) and its CO complex (low spin), exhibit MCD spectra which hardly resemble analogous oxidation states or ligand complexes of any known iron porphyrin complexes except for myeloperoxidase. MCD of GHP has several salient features: (1) Soret region (380-500 nm) MCD intensity for a high spin ferrous and low spin ferric GHP derivatives are noticeably smaller ($|\Delta\varepsilon/H| \leq 20$ $M^{-1}cm^{-1}T^{-1}$) than those of common heme proteins by factors of 4 to 10. (2) Peak to trough derivative line shapes of the MCD spectra of the ferrous low spin form of GHP are inverted from and are less symmetric than those seen for a normal porphyrin system. MCD of the ferric high spin forms also exhibit such an inverted spectral line shape in Soret region. (3) Prominent MCD spectral features of GHP derivatives are seen around 450 and 630 nm, which are considerably red-shifted in comparison to normal hemoproteins. These results indicate that GHP contains the prosthetic group with unusual strucure and that the structures of the heme and its vicinity of GHP and myeloperoxidase are similar between each other. Supproted by NIH AI-20463 and GM26730.

M-Pos50 AMINO TERMINAL SEMISYNTHESIS OF HEMOGLOBIN: PREPARATION AND CHARACTERIZATION OF DES-VAL$^{\alpha^1}$-HEMOGLOBIN. Stephen B. Lyle, Stanley A. Hefta, Mary L. Crowl-Powers, David E. Harris, Mark R. Busch, and Frank R. N. Gurd, Department of Chemistry, Indiana University, Bloomington, Indiana 47405.
The amino termini of the α-chains of human hemoglobin are known to play an important role in the alkaline Bohr effect and to be involved in the binding of chloride ion and carbon dioxide. In order to further investigate this region of the molecule, des-Val$^{\alpha^1}$-hemoglobin has been prepared by revising previous methods (Harris et al., Biophys. J. <u>45</u>, 9a, 1982) for improved yields and in preparation for semisynthetic reincorporation of ^{13}C enriched amino terminal residues. Purified A_0 hemoglobin is initially treated with a modified Edman reagent, 3-sulfophenylisothiocyanate, under conditions in which the reaction is limited to the amino terminus. Chain separation is achieved by reaction with p-hydroxymecuribenzoate (PMB) followed by ion exchange chromatography. The SPTC-PMB-α-chains are dehemed using acidic acetone, cleaved with anhydrous trifluoroacetic acid, and exposed to cyanide for removal of the PMB group. Reconstitution is accomplished by the addition of stoichiometric amounts of cyanoferri β-chains followed by heme addition and ion exchange purification. Physical and chemical characterization includes amino acid analysis, amino terminal sequencing, electrophoresis, and UV/visible spectroscopy. Functional studies, including potentiometric titration and oxygen binding studies, are designed to determine the effect of the truncation on the molecule and its interactions with known effectors. For the production of ^{13}C-enriched amino terminal variants, acetimidyl protection of lysines will direct coupling to the amino terminus, while the PMB group will provide sulfhydryl protection. (Supported by PHS Research Grants HL-05556 and HL-14680.)

M-Pos51   DIMER-TETRAMER KINETICS OF NORMAL AND ABNORMAL HUMAN HEMOGLOBINS. H. R. Halvorson and
W. R. Johnston, Henry Ford Hospital, Detroit, Michigan 48202

The communication (energy flow) responsible for cooperative oxygen binding by hemoglobin neces-
sarily crosses the $\alpha_1 \beta_2$ interface. Experiments designed to probe the interactions at this inter-
face thus have the potential of providing information on the underlying mechanism. Using 8 atm
pressure-jump relaxation kinetics, we have studied the oxygenation-linked dimer-tetramer associa-
tion for hemoglobins A_O, Hôtel Dieu (β99 Asp $\rightarrow$ Gly), British Columbia (β101 Glu $\rightarrow$ Lys), and
Bartley (α95 Pro $\rightarrow$ Thr). In general, the relaxation behavior is described by a single exponen-
tial whose rate and amplitude can be correlated with protein concentration and oxygen tension by
linked function theory. The major exception is hemoglobin Hôtel Dieu. The FG corner is so sensi-
tive to alteration that dimer and tetramer are alike in their oxygen binding properties (coopera-
tivity is abolished). The consequence of this is that there is no measurable amplitude for the
dimer-tetramer process. Despite the differences between the nature and location of the other two
mutations, their subunit association behavior is qualitatively similar. The equilibrium associa-
tion constants are reduced about 50-fold. Although the kinetic dissociation constants are
increased (relative to Hb A), the major effect is a marked reduction in the association rate con-
stants. The results can be rationalized in the context of a model in which translational and
rotational diffusion (fast) precede relatively slower docking interactions. The rate constant of
the docking step for Hb A can be estimated at 5×10^5 s^{-1}, whereas it would be about 2×10^4 s^{-1}
for hemoglobins British Columbia and Bartley.